REPORT DOCUMENTATION PAGE

Form Approved OMB NO. 0704-0188

1. REPORT DATE (DD-MM-YYYY)	2. REPORT TYPE	3. DATES COVERED (From - To)
19-12-2013	Final Report	30-Sep-2010 - 29-Sep-2013

4. TITLE AND SUBTITLE
Investigation of Aerogel/Xerogel Catalysts for Autothermal Reforming of JP-8

5a. CONTRACT NUMBER
W911NF-10-1-0514

5b. GRANT NUMBER

5c. PROGRAM ELEMENT NUMBER
611102

6. AUTHORS
Jale Akyurtlu, Ates Akyurtlu, M.V.Phanikrishna Sharma

5d. PROJECT NUMBER

5e. TASK NUMBER

5f. WORK UNIT NUMBER

7. PERFORMING ORGANIZATION NAMES AND ADDRESSES
Hampton University
100 E. Queen Street

Hampton, VA 23668 -0108

8. PERFORMING ORGANIZATION REPORT NUMBER

9. SPONSORING/MONITORING AGENCY NAME(S) AND ADDRESS (ES)
U.S. Army Research Office
P.O. Box 12211
Research Triangle Park, NC 27709-2211

10. SPONSOR/MONITOR'S ACRONYM(S)
ARO

11. SPONSOR/MONITOR'S REPORT NUMBER(S)
58359-CH-H.3

12. DISTRIBUTION AVAILIBILITY STATEMENT
Approved for Public Release; Distribution Unlimited

13. SUPPLEMENTARY NOTES
The views, opinions and/or findings contained in this report are those of the author(s) and should not contrued as an official Department of the Army position, policy or decision, unless so designated by other documentation.

14. ABSTRACT
Use of fuel cells for applications, like auxiliary power units in Abrams tanks, unmanned aerial vehicles and ground vehicles, is of importance to the Army. The primary barrier to the commercialization of fuel cells is cost-driven. This project will contribute to the solution of this problem by preparing novel reforming catalyst formulations by the sol-gel method.
The objective of this investigation was to prepare various xerogel catalysts with high resistance to coking and sulfur poisoning, and to investigate their performance in the autothermal reforming (ATR) of n-dodecane (a surrogate for

15. SUBJECT TERMS
Xerogel catalysts, autothermal reforming, hydrogen generation, sol-gel method, reforming of n-dodecane, reforming of isobutanol

16. SECURITY CLASSIFICATION OF:			17. LIMITATION OF ABSTRACT	15. NUMBER OF PAGES	19a. NAME OF RESPONSIBLE PERSON
a. REPORT	b. ABSTRACT	c. THIS PAGE			Jale Akyurtlu
UU	UU	UU	UU		19b. TELEPHONE NUMBER 757-727-5589

Report Title

Investigation of Aerogel/Xerogel Catalysts for Autothermal Reforming of JP-8

ABSTRACT

Use of fuel cells for applications, like auxiliary power units in Abrams tanks, unmanned aerial vehicles and ground vehicles, is of importance to the Army. The primary barrier to the commercialization of fuel cells is cost-driven. This project will contribute to the solution of this problem by preparing novel reforming catalyst formulations by the sol-gel method.

The objective of this investigation was to prepare various xerogel catalysts with high resistance to coking and sulfur poisoning, and to investigate their performance in the autothermal reforming (ATR) of n-dodecane (a surrogate for JP-8) and isobutanol; and to relate observed activity and selectivity to the physical and chemical properties of the catalyst. The preparation method and the catalyst composition were optimized.

All the prepared catalysts have high BET surface area and mesoporous pore size, and exhibit uniform distribution of nano-sized metal oxides in the solid matrix. Nickel catalyst supported on CeO2-Zr2O3-Al2O3 was the most active and selective catalyst for ATR of n-dodecane, exhibiting low coke formation and high stability. Nickel catalyst supported on CeO2-Zr2O3-Al2O3 and promoted by ruthenium was the best catalyst for the ATR of isobutanol. After the long runs, the morphology and features of the catalysts did not change appreciably.

Enter List of papers submitted or published that acknowledge ARO support from the start of the project to the date of this printing. List the papers, including journal references, in the following categories:

(a) Papers published in peer-reviewed journals (N/A for none)

Received Paper

TOTAL:

Number of Papers published in peer-reviewed journals:

(b) Papers published in non-peer-reviewed journals (N/A for none)

Received Paper

TOTAL:

Number of Papers published in non peer-reviewed journals:

(c) Presentations

1. Accepted for presentation at the 23rd North American Catalysis Society Meeting, 6/6-7/2013, Louisville, KY

Autothermal Reforming of n-Dodecane for Fuel-Cell Applications – Nickel Based Xerogel Catalysts for Activity, Stability and Coking Studies

Authors: Venkata Phanikrishna Sharma Mangalampalli, phani.mangalampalli@hamptonu.edu
Jale Akyurtlu jale.akyurtlu@hamptonu.edu
Ates Akyurtlu ates.akyurtlu@hamptonu.edu

Chemical Engineering, Hampton University, Hampton, VA 23668

Summary: (only 50 words)
Nickel catalysts, supported on alumina and promoted by Ru, Ce and Zr, were investigated for autothermal reforming of n-dodecane. Catalysts were prepared by sol-gel method and characterized by different spectroscopic and physical techniques. NiCeZrAl2O3 catalyst was found to be the optimum for high catalytic activity, stability, low coking and good resistance to sintering.

Extended abstract (1 page)
Fuel cells are one of the alternative solutions to evade the problems of air pollution and global warming due to emissions from transportation. Fuel cells work on clean hydrogen and air to produce electricity with lower or no emissions. The combination of an on-board reformer and a SOFC would enable commercial fuels such as jet fuel and diesel to be used as a hydrogen source because of high energy density of these fuels. The US military is the single largest petroleum consumer in the world and jet fuel represents 64% (volume basis) of all petroleum products consumed in the USA1. Hence in the present study we have chosen auto thermal reforming (ATR) of n-dodecane for the production of clean hydrogen, which is a surrogate for jet fuel. ATR is chosen as the best method in the present study because it has advantages over present technologies i.e., steam reforming (SR) and partial oxidation (POx), like compact and quick starting reactors, and better sulfur tolerance and less coking. ATR is a combination of endothermic SR and the exothermic POX process; hence it is self-sustained and evades catalyst deactivation for longer operation. This process requires less energy and helps reduce the amounts of methane and coke produced while providing a high H2 yield and a low CO yield under optimal operating conditions. Additionally, the water gas shift reaction, which proceeds simultaneously, reduces the CO content of the hydrogen-rich gas.
The present challenges in the development of ATR catalysts for higher hydrocarbons are catalyst deactivation by coking and sulfur intolerance. Even though the noble metal (Rh, Ru, Pt, Pd)-promoted catalysts are showing higher activity and stability for this reaction, catalyst cost is one of the main obstacles. Hence in our study we have tried to minimize the use of noble metals without compromising in hydrogen production. In the present experimental study, we have developed Ni-based catalysts which are resistant to carbon formation by incorporating Ce and Zr species, using a typical sol-gel method. Preparation of metal oxides by the sol-gel method results in the retention of hydroxyl-rich surfaces, which exhibit unique textural and chemical properties compared with those prepared by other conventional methods, along with high surface areas.
In the present study, with an objective to conserve noble metal usage, and, also, to improve the ATR performance, we have studied Ni-based catalysts with an alumina support along with transition metals and Ru promoter. Sol-gel method is used to prepare the catalysts. Catalysts were characterized by X-ray diffraction (XRD), temperature programmed reduction (TPR), pore size distribution, hydrogen chemisorption, XPS and BET surface area measurements. The catalysts are evaluated for ATR of n-dodecane in a microreactor setup at different reaction temperatures ranging from 650-8500C, space velocity (132000 - 660000h-1), oxygen/carbon ratio (0 - 1) and steam/carbon ratio (0 - 3.14). NiCeZrAl2O3 catalyst is optimized for high catalytic activity, low carbon deposition, good resistance to sintering and prolonged stability compared to the equal mass of other catalysts prepared in the project. Used catalysts are evaluated for carbon formation by TEM, SEM-EDAX and TPO studies. The results from these experiments will be discussed during the presentation in terms of the effect of operation variables on the hydrogen yield and product gas composition.
Acknowledgement: The authors gratefully acknowledge financial support from ARO grant (W911NF-10-1-0514).
Reference: 1. Defense Energy Support Center. Fact book 2010

---

2. Accepted for presentation at 2013 AIChE Annual Meeting, 11/3-8/2013, San Francisco, CA

OXIDATIVE STEAM REFORMING OF ISO-BUTANOL OVER PROMOTED NICKEL XEROGEL CATALYSTS

M.V. Phanikrishna Sharma phani.mangalampalli@hamptonu.edu
Jale Akyurtlu jale.akyurtlu@hamptonu.edu
Ates Akyurtlu ates.akyurtlu@hamptonu.edu

Chemical Engineering, Hampton University, Hampton, VA 23668

Rapid development of alternative energy resources is the main challenge to meet the growing energy demand in the reality of depleting fossil fuels. Hydrogen energy is one of the clean alternatives. However main drawbacks involved in this process are direct distribution and storage; hence onsite production from various feed stocks is one of the choices. In this process, current route for H2 production is the catalytic reforming of hydrocarbons and alcohols. Presently, there is a growing interest in the use of C2-C4 alcohols as the raw materials for reforming, since these compounds can be produced from biomass feedstock. However, formation of coke and other undesired by-products is the main obstacle in the process of steam reforming of these alcohols. Hence development of new catalysts for higher hydrogen production and less or no coke formation are of great interest. The oxidative steam reforming of alcohols is one of the best options to

achieve these goals. It is a combination of steam reforming and partial oxidation. The addition of oxygen into the reaction prevents coke formation and results in a comparatively high hydrogen yield; it, also, requires less energy compared to the conventional steam reforming process. But thermal sintering of active and support materials make this process more challenging.
The present experimental study has been undertaken to investigate the effect of the operation variables on the oxidative steam reforming of isobutanol. In this present study, we have prepared Ni-based catalysts by the sol-gel method, which results in the retention of hydroxyl-rich surfaces, which exhibit unique textural and chemical properties compared with those prepared by other conventional methods, like the impregnation method. Alumina is used as the support material, Ni is the main active metal, and Ce-ZrO2 and Ru are chosen as promoters. Catalysts were characterized by XRD, TPR, TPD of H2, BET surface area and porosity measurements. The oxidative steam reforming of isobutanol was performed in a microreactor setup at different reaction temperatures, space velocity, oxygen/carbon ratio and steam/carbon ratio. The Ru-Ni-Ce-Zr-Al2O3 catalyst showed high catalytic activity, low carbon deposition, good resistance to sintering and prolonged stability compared to the other catalysts prepared in the project. The results from these experiments will be discussed during the presentation in terms of the effect of operation variables on the hydrogen yield and product gas composition.

Acknowledgement
The authors acknowledge financial support from ARO grant (W911NF-10-1-0514).

---

3. Presented at the 2012 AIChE Annual Meeting, at Pittsburgh, PA, October, 16-21/2012

Autothermal Reforming of Dodecane over Ni-Based Sol-Gel Catalysts

Venkata Phanikrishna Sharma Mangalampalli phani.mangalampalli@hamptonu.edu
Jale Akyurtlu jale.akyurtlu@hamptonu.edu
Ates Akyurtlu ates.akyurtlu@hamptonu.edu

Chemical Engineering, Hampton University, Hampton, VA 23668
Increasing energy demand, due to the population growth, urges for new and more efficient technologies, which will, also, reduce the level of exhaust gas emissions into the environment. Eco-friendly energy solutions are being sought, especially for mobile applications. For example, the auxiliary power units (APUs) can increase fuel economy by displacing engine idling. The combination of an on-board reformer and a SOFC would enable commercial fuels such as jet fuel and diesel to be used as a hydrogen source because of high energy density of these fuels. More popular in transportation, military, and industrial applications, commercial fuels could be a good first step toward a hydrogen-based society. The US military is the single largest petroleum consumer in the world and jet fuel represents 64% (volume basis) of all petroleum products consumed1. Hence in the present study, we have chosen to investigate the auto thermal reforming (ATR) of dodecane, which is used as a surrogate of commercial jet fuel, for the production of clean hydrogen.
The current existing technologies for the production of hydrogen from hydrocarbon fuels are steam reforming (SR), partial oxidation (POx), combustion and autothermal reforming (ATR). Among all the above methods, ATR is regarded as the best option, because it is a combination of the endothermic SR and the exothermic POX process and exhibits better sulfur tolerance than SR. ATR reactors are smaller, quick-starting and faster-responding than SR reactors. This process requires less energy and helps reduce the amounts of methane and coke produced while providing a high H2 yield and a low CO yield under optimal operating conditions. Additionally, the water gas shift reaction, which proceeds simultaneously, reduces the CO content of the hydrogen-rich gas.
The main obstacles in the development of ATR catalysts for the reforming of higher hydrocarbons are catalyst deactivation by carbon formation and sulfur intolerance. Although supported noble metal (Rh, Ru, Pt, Pd) catalysts provide higher activity and stability compared to Ni catalysts, the price is the key factor for choosing nickel catalysts. In this experimental study, we synthesized Ni-based catalysts which are resistant to carbon formation by incorporating cerium and zirconium species into the catalyst structure by a typical sol-gel method; these catalysts do not display any compromise on hydrogen production. Preparation of metal oxides by the sol-gel method results in the retention of hydroxyl-rich surfaces, which exhibit unique textural and chemical properties compared with those prepared by other conventional methods, along with the attainment of high surface areas.

In the present study, we have prepared sol-gel derived Ni-based catalysts supported on alumina (Al2O3) for the ATR of dodecane. Catalysts were characterized by X-ray diffraction (XRD), temperature programmed reduction (TPR), pore size distribution, hydrogen chemisorption and BET surface area measurements. The autothermal reforming of dodecane was performed in a microreactor setup at different reaction temperatures, space velocity, oxygen/carbon ratio and steam/carbon ratio. The Ni-Ce-Zr-Al2O3 catalyst showed high catalytic activity, low carbon deposition, good resistance to sintering and prolonged stability compared to the other catalysts prepared in the project. The results from these experiments will be discussed during the presentation in terms of the effect of operation variables on the hydrogen yield and product gas composition.

References:
1. Defense Energy Support Center, Fact book 2010.
Acknowledgement
The authors acknowledge financial support from ARO grant (W911NF-10-1-0514).

---

4. Accepted for presentation at 2011 AIChE Annual Meeting, 10/16-21/2011, Minneapolis, MN

AUTOTHERMAL REFORMING OF N-DODECANE OVER PROMOTED NICKEL XEROGEL CATALYSTS

M.V. Phanikrishna Sharma phani.mangalampalli@hamptonu.edu
Jale Akyurtlu jale.akyurtlu@hamptonu.edu
Ates Akyurtlu ates.akyurtlu@hamptonu.edu

Chemical Engineering, Hampton University, Hampton, VA 23668

Energy demand continues to climb as the world population grows. Meanwhile petroleum reserves are diminishing. Developing new energy sources and more efficient technologies is extremely important. At the same time, the level of emissions and exhaust gases needs to be reduced to minimize their contribution to the greenhouse effect. Environmentally friendly energy solutions are being sought, especially for mobile applications. For example, the auxiliary power units (APUs) can increase fuel economy by displacing engine idling. The combination of an on-board reformer and a SOFC would enable commercial fuels such as jet fuel and diesel to be used as a hydrogen source because of the existing infrastructure and high energy density of these fuels. More popular in transportation, military, and industrial applications, commercial fuels could be a good first step toward a hydrogen-based society.

The conversion of hydrocarbon fuels to hydrogen can be carried out by several different reforming approaches including steam reforming, partial oxidation, and autothermal reforming. Autothermal reforming (ATR) is regarded as the best option since the combustion of some of the fuel supplies the energy required for the reforming reaction and better sulfur tolerance than steam reforming (SR). ATR reactors are smaller, quick-starting and faster-responding than SR reactors, and give higher hydrogen concentration. Faster startup time and better transient response can be attained by tuning the feed stoichiometry. Additionally, the water gas shift reaction, which proceeds simultaneously, reduces the CO content of the hydrogen-rich gas; also, the methane content of the gas is lower than the other methods. The operation variables have to be optimized according to the catalyst employed to minimize carbon formation and methane production.

The present experimental study has been undertaken to investigate the effect of the operation variables on the ATR of n-dodecane, which is selected as a jet fuel surrogate to simplify the reaction study and the interpretation of the test results.

Promoted nickel xerogel catalysts were prepared by sol-gel method. Catalysts were characterized by XRD, TPR, TPD of H2 & CO2, BET surface area and porosity measurements. The autothermal reforming experiments were performed in a fixed bed micro-reactor system in a temperature range of 600-800°C and space velocity of the order of 100,000 hr-1. The reaction feed containing n-dodecane, water, oxygen and carrier gas were sent through a vertical flow quartz reactor containing the catalyst. The product gases were analyzed by two online GCs. The results from these experiments will be discussed during the presentation in terms of the effect of operation variables on the hydrogen yield and product gas composition.

Acknowledgement

The authors acknowledge financial support from ARO grant (W911NF-10-1-0514).

5.presented at the NOBCChE (The National Organization for the Professional Advancement of Black Chemists and Chemical Engineers) 38th National Conference held in Houston, TX, April 19-22, 2011

Synthesis and Characterization of Nickel-Silica Aerogels Using a Sub-Critical Drying Approach

Rhonda Jack*, Brittany Henderson*, Dinah Holland*, Jale Akyurtlu*, M.V.P. Sharma*

* Department of Chemical Engineering, Hampton University, Tyler Street, Hampton VA, USA

The physical characteristics that typify aerogels including their high structural porosity, low density and large surface area to volume ratio render these solids very advantageous in number of practical applications. For instance, the high surface area to volume ratio is favored when constructing catalytic supports for reactions that depend on catalytic activity. Moreover, the ability of nickel to act as a catalyst in the reforming of higher hydrocarbons makes the nickel aerogel structure particularly attractive in such catalytic processes since the metal catalyst can be dispersed throughout a highly porous support structure. This high availability of catalytic sites would lead to high rates of reaction and thereupon, a process that exploits time and raw materials more efficiently. Aerogels have been conventionally prepared by drying sol gels under supercritical conditions, where CO2 is typically used as the supercritical fluid. This conventional approach has proven to be costly as well as time consuming, and limitations on mass production of the aerogels have resulted in a rather inconvenient synthesis approach. However, the sub-critical drying approach we developed and employed for the synthesis of the nickel aerogels allows for a simpler and more convenient drying route, resulting in structures that are transparent, monolithic, as well as porous. A 2P factorial design method was used to determine the effects of the factors such as water/TEOS ratio, alcohol/TEOS ratio and temperature of the sol gel synthesis and their influence on the transparency, monolithicity and surface area of the resulting aerogels. The results of these experiments will be discussed during the presentation.

Number of Presentations: 5.00

Non Peer-Reviewed Conference Proceeding publications (other than abstracts):

Received	Paper

TOTAL:

Number of Non Peer-Reviewed Conference Proceeding publications (other than abstracts):

Peer-Reviewed Conference Proceeding publications (other than abstracts):

Received	Paper

TOTAL:

Number of Peer-Reviewed Conference Proceeding publications (other than abstracts):

(d) Manuscripts

Received	Paper	
08/30/2012	1.00	Venkata Phanikrishna Sharma Mangalampalli, , Ates Akyurtlu, Jale F. Akyurtlu, , Vidya Sagar Guggilla,. H2 production by autothermal reforming of n-dodecane over highly active Ru-Ni-Ce-Al2O3 catalyst, Ind. Chem. Eng. Res. (08 2012)
12/19/2013	2.00	V.S. Guggilla, V.P.S.Mangalampalli, J.F. Akyurtlu, A. Akyurtlu. H2 Production by Autothermal Reforming of n-Dodecane over Highly Active Ru-Ni-Ce-Al2O3 Catalyst, Industrial and Engineering Chemistry, Research (03 2012)

TOTAL: **2**

Number of Manuscripts:

Books

Received	Paper

TOTAL:

Patents Submitted

Sol-Gel mediated Ce-Zr-Al-supported Ni catalyst for dodecane autothermal reforming for clean hydrogen production, to prevent coking; US patent, to be applied in 2014.

Patents Awarded

Awards

Graduate Students

NAME	PERCENT_SUPPORTED
FTE Equivalent:	
Total Number:	

Names of Post Doctorates

NAME	PERCENT_SUPPORTED
Dr. M.V. Phanikrishna Sharma	1.00
FTE Equivalent:	**1.00**
Total Number:	**1**

Names of Faculty Supported

NAME	PERCENT_SUPPORTED	National Academy Member
Jale Akyurtlu	0.00	
Ates Akyurtlu	0.15	
FTE Equivalent:	**0.15**	
Total Number:	**2**	

Names of Under Graduate students supported

NAME	PERCENT_SUPPORTED	Discipline
Julian Brathwaite	0.10	
Joshua Gopeesingh	0.10	
Rhonda Jack	0.00	
Brittany Henderson	0.00	
Dinah Holland	0.00	
FTE Equivalent:	**0.20**	
Total Number:	**5**	

Student Metrics

This section only applies to graduating undergraduates supported by this agreement in this reporting period

The number of undergraduates funded by this agreement who graduated during this period: 5.00

The number of undergraduates funded by this agreement who graduated during this period with a degree in science, mathematics, engineering, or technology fields:..... 5.00

The number of undergraduates funded by your agreement who graduated during this period and will continue to pursue a graduate or Ph.D. degree in science, mathematics, engineering, or technology fields:..... 3.00

Number of graduating undergraduates who achieved a 3.5 GPA to 4.0 (4.0 max scale):..... 3.00

Number of graduating undergraduates funded by a DoD funded Center of Excellence grant for Education, Research and Engineering:..... 0.00

The number of undergraduates funded by your agreement who graduated during this period and intend to work for the Department of Defense 0.00

The number of undergraduates funded by your agreement who graduated during this period and will receive scholarships or fellowships for further studies in science, mathematics, engineering or technology fields: 0.00

Names of Personnel receiving masters degrees

NAME
Total Number:

Names of personnel receiving PHDs

NAME
Total Number:

Names of other research staff

NAME	PERCENT_SUPPORTED
FTE Equivalent:	
Total Number:	

Sub Contractors (DD882)

Inventions (DD882)

Scientific Progress

Technology Transfer

FINAL REPORT

Grant # W911NF-10-1-0514

Reporting Period: 09/30/2010 – 09/29/2013

Investigation of Aerogel/Xerogel Catalysts for Autothermal Reforming of JP-8

by

Dr. Jale Akyurtlu, PI,
Dr. Ates Akyurtlu, Senior Researcher
Dr. M.V. Phanikrishna Sharma, Postdoctoral Research Associate
Chemical Engineering
Hampton University, Hampton, VA 23668

ABSTRACT

Use of fuel cells for applications like auxiliary power units in Abrams tanks, fuel cell propulsion systems for non-tactical vehicles, unmanned aerial vehicles (UAV's) and ground vehicles (UGV's), etc. is of importance to the Army. The primary barriers to the commercialization of fuel cells and to the large scale hydrogen production and delivery are cost-driven. Since the distribution system for JP-8 is in place for the military, its reforming is a feasible approach for the production of hydrogen for fuel cells. However, conversion of JP-8 to hydrogen is a process fraught with difficulties: Its hydrogen to carbon ratio is low, resulting in extensive coke formation on the catalysts. It, also, contains large amounts of sulfur since the military uses worldwide fuel sources. Reforming of isobutanol is, also, an attractive alternative, since isobutanol can be produced from biomass. This project will contribute to the solution of this problem by preparing novel catalyst formulations by the sol-gel method, resulting in catalysts with high resistance to coking and sulfur poisoning.

The objective of this investigation on hydrocarbon reforming was to prepare and perform materials characterization and kinetics measurements on various xerogel catalysts to investigate their performance in the autothermal reforming process; and to relate the observed activity and selectivity to the physical and chemical properties of the catalyst**.** Several characterization techniques were being employed on this catalyst system to collect crucial data for this goal. The reasons for the use of xerogels are the advantages of nanoscale for increased catalyst activity and selectivity, ability to tailor support properties, and the ability to increase the stability of the catalyst by incorporating the active metal into the support structure during the preparation of the support. The main catalysts were Ni supported on CeO_2-Al_2O_3, and CeO_2-Zr_2O_3-Al_2O_3, promoted by Ru, prepared as xerogels. The preparation method and the catalyst composition were optimized; and the effect of addition of zirconia to the catalysts on the autothermal reforming of dodecane was investigated extensively. Based on the recommendation of Dr. Ivan Lee of the US Army Research Laboratory, these catalysts were also employed for the ATR of isobutanol, which is regarded as a promising raw material for hydrogen production for fuel cells. The stability of the Ni-based catalysts was investigated by long-time tests. Additionally, catalysts were prepared by replacing nickel with cobalt in the ceria-zirconia-alumina matrix; and their activity was investigated in the autothermal reforming process. Autothermal reforming of JP8 was studied using the Ni-based catalysts. This project also supported the integration of research into education, by hiring minority undergraduate engineering students to work on the project. Since there is no graduate program in chemical engineering, five undergraduate students in the chemical engineering program were hired and were taught to prepare catalysts by the sol-gel process and operate instruments.

All the catalysts prepared in this project have high BET surface area and mesoporous pore size. XRD patterns indicate an amorphous nature of the fresh catalysts. Addition of metal oxides in the catalyst matrix reduced the reduction temperature of the catalyst appreciably. SEM and TEM images exhibit the uniform distribution of the metal oxides in the solid matrix and their nano-size nature. Active metal (Ni) dispersion and metal area increased with the addition of metal oxides in the matrix, increasing the availability of active Ni atoms for the reaction. Among the prepared Ni-based catalysts, NCZA catalyst produced higher hydrogen yield and less methanation products for the ATR of n-Dodecane, a surrogate of JP8 fuel. NCZA catalyst was active during a 50h run, and low coke formation indicated that this catalyst is highly stable and has a long life under the optimized operating conditions, namely, a temperature of $750^{O}C$, a space velocity of $220000h^{-1}$, an O/C ratio of 0.35 and a H_2O/C ratio of 2. Used catalysts are characterized extensively to support the results from the ATR, SR and POx reactions. The results from

characterization confirm that coke formation is appreciable in SR and POx of n-dodecane, while it is very low in the case of ATR of n-dodecane. XRD, SEM and TEM patterns of the used catalysts indicate that the morphological features of the catalysts have not changed appreciably, supporting the previous observation that the catalysts are very stable and remained active during 50 hours of operation.

RNCZA catalyst was found to be the best compared to the other Ni-based catalysts for the ATR of isobutanol. The optimum conditions for the autothermal reforming of isobutanol are a temperature of 700 ^{O}C, a space velocity of 217000h^{-1}, an O/C ratio of 0.35 and a H_2O/C ratio of 2. The catalyst was stable during a 25h run with low coke formation. After the long run, the morphology and features of the catalyst did not change appreciably.

Co-based catalysts were also prepared by the sol-gel method. They were found to be very hard to reduce, mainly, since the sol-gel method used for preparation results in cobalt being dispersed very homogeneously within the support matrix. However, Co catalysts exhibited very high BET surface areas. RNCZA and NCZA catalysts were tested for the ATR of JP-8, but due to the high sulfur content of JP-8, the catalysts deactivated within 3 hours. Overall, among the developed catalysts, NCZA catalyst was proven to undergo less coking and to exhibit high stability for the ATR of n-Dodecane and JP-8.

Table of Contents

List of Tables

List of Figures

A. OBJECTIVE

The primary barriers to the commercialization of fuel cells and to the large scale hydrogen production and delivery are essentially cost-driven. Therefore, either new onboard hydrogen storage methods need to be developed, or hydrogen needs to be generated onboard as needed. This research project addresses the latter of these efforts by developing highly active and stable fuel reforming catalysts for hydrogen production. Conversion of hydrocarbon fuels, such as gasoline, methanol, diesel, JP-8 and isobutanol by reforming is an attractive method for onboard production of hydrogen to reduce vehicular emissions. Autothermal Reforming (ATR) emerges to be the best option since the combustion of some of the fuel supplies the energy required for the endothermic reforming reaction. Additionally, the methane content of the gas is lower than the other reforming methods. Faster startup time and better transient response are the other advantages of ATR, attained by tuning the feed composition. ATR reactors are smaller, quick-starting and faster-responding than Steam Reforming (SR) reactors, and give higher hydrogen concentrations. The temperature control in the ATR reactor is improved, thus, reducing the formation of the hot spots, and consequently sintering and coke formation. The cited advantages of the ATR make it the technology of choice for the small or medium-scale hydrogen/syngas generators for providing fuel for fuel cells, especially for solid oxide fuel cells (SOFCs). The most important operating variables for ATR are temperature, pressure, oxygen/carbon ratio, steam/carbon ratio, the catalyst, and the space velocity. The values of these variables are selected to minimize the carbon formation on the catalyst, and methane production. The reforming catalysts are required to have high activity, high hydrogen selectivity, a wide temperature range of operation, high WGS activity and strong resistance to coking, sintering, sulfur poisoning and oxygen shock. The catalysts should be able to be exposed to oxidizing-reducing atmospheres without loss in activity. It is crucial to develop highly effective catalysts for ATR, especially for the fast commercialization of fuel cells. Therefore, t**he objective of this project is to prepare, and perform materials characterization and kinetics measurements on various xerogel catalysts to investigate their performance in the autothermal reforming of the jet fuel surrogate n-Dodecane and isobutanol; and to relate the observed activity and selectivity to the physical and chemical properties of the catalyst.** This information is essential for the design of optimum catalysts for the ATR process.

B. RELEVANCE TO THE ARMY

The fuel infrastructure for US military is in place for jet fuel (JP-8). US Army adopted JP-8 for all ground and aircraft systems following the 'one fuel forward' concept, simplifying fuel transport and distribution operations. JP-8 is a kerosene-based fuel consisting of aliphatic and aromatic hydrocarbons and it is used by US military in aircraft engines, ground vehicles and all kinds of diesel engine-powered systems and furnaces. The annual worldwide use of JP-8 is more than 60 billion gallons per year, almost 5% of which is used by the US Air Force. This fuel also powers the aircraft used by the US Navy; the ships are powered by lower grade fuel. JP-8 is approximately 99.8% kerosene by weight (mainly naphthenes, paraffins, aromatics-mostly toluene but also benzene) and additives. The aliphatic range observed is from C_{10} through C_{18}, the average being at about C_{13}. JP-8+100 is a version of JP-8 that includes supplementary additives to enhance its thermal stability. Use of fuel cells for various applications, like auxiliary power units (APU's) in Abrams tanks, fuel cell propulsion systems for non-tactical vehicles, unmanned aerial vehicles (UAV's) and unmanned ground vehicles (UGV's), portable power systems, etc. is of importance to the Army, which represents 19% of DOD energy consumption. This approach helps to reduce fuel usage, thus, also, reducing green house gas emissions. Since the

distribution system for JP-8 is in place for the military, its reforming is a feasible approach for the production of hydrogen for fuel cells. However, conversion of JP-8 to hydrogen is a process fraught with difficulties: The hydrogen to carbon ratio in JP-8 is low, resulting in extensive coke formation on the reforming catalysts. It, also, contains large amounts of sulfur, up to 3000 ppm by wt, since the military uses worldwide fuel sources. Therefore, designing novel reforming catalysts with high resistance to coking and sulfur poisoning is of utmost importance for hydrogen production by reforming of JP-8. This project will contribute to the solution of this problem by preparing novel catalyst formulations by the sol-gel method, resulting in catalysts with high resistance to coking and sulfur poisoning. Since, even for the reforming of natural gas, there still is extensive research on the preparation of catalysts with high sulfur and coke-resistance, the catalysts prepared and tested in this project will be relevant to the commercial and civilian use of reforming processes, too.

C. WORK DONE

Codes used in this report:

CA	- 3wt% Ce/Al_2O_3
CZA	- 3wt% $Ce/Zr/Al_2O_3$
NA	- 10wt% Ni/Al_2O_3
NCA	- 10wt% $Ni/3wt\% Ce/Al_2O_3$
NZA	-10wt% $Ni/Zr/Al_2O_3$(Zr amount equivalent to atomic Ce in NCZA catalyst)
NCZA	- 10wt% $Ni/3wt\% Ce/Zr/Al_2O_3$ (Ce/Zr = 1:1 atomic ratio)
RNCZA	- 0.3wt%Ru/10wt% $Ni/3wt\% Ce/Zr/Al_2O_3$
CoA	- 10wt% Co/Al_2O_3
CoCA	- 10wt% $Co/3wt\% Ce/Al_2O_3$
CoZA	- 10wt% $Co/Zr/Al_2O_3$ (Zr amount equivalent to atomic Ce in CoCZA catalyst)
CoCZA	- 10wt% $Co/3wt\% Ce/Zr/Al_2O_3$ (Ce/Zr = 1:1 atomic ratio)
RCoCA	- 0.3 wt% $Ru/10wt\% Co/3wt\% Ce/Zr/Al_2O_3$
SR	- Steam Reforming
PO	- Partial Oxidation
ATR	- Autothermal Reforming
GHSV	- Gas Hourly Space Velocity
TPR	- Temperature Programmed Reduction
TPD	- Temperature Programmed Desorption
TPO	- Temperature Programmed Oxidation

A surrogate of JP-8, n-Dodecane, was used to optimize the composition of and operating conditions for the reforming catalysts. Two types of catalysts were prepared, namely, Ni-based and Co-based xerogel catalysts. Once the catalysts were optimized for n-Dodecane, they were tested for the autothermal reforming of isobutanol and JP-8 fuel. The catalysts were also investigated for their activity and selectivity in the autothermal reforming of isobutanol.

I. Nickel-Based catalysts

I.A. Catalyst preparation

The xerogel catalysts were prepared by the sol−gel method. Aluminum trisec-butoxide (ATSB), nickel acetate, cerium ammonium nitrate, zirconium (IV) butoxide and ruthenium chloride were used as precursors for aluminum, nickel, cerium, zirconium and ruthenium, respectively. Ni-based sol gel catalyst preparation was optimized by varying conditions like amount of solvent, addition of ingredients, gelation time and calcination conditions. The final optimized catalyst preparation is presented below:

a) 10wt% Ni/Al_2O_3: A known amount of ATSB was dissolved in warm ethanol at 70 ^{0}C with vigorous stirring. For the partial hydrolysis of the aluminum precursor, small amounts of nitric acid and distilled water (40% nitric acid) solution, which had been mixed with ethanol, were slowly added to the solution containing the aluminum precursor, and stirred for 10 min at room temperature; the mixture was, then, transferred to a flat bottom 250 mL flask. Then, the desired amount of nickel acetate was added slowly into the solution containing the aluminum precursor, and stirred for 30 min at room temperature. Subsequently, the temperature was raised to 80 ^{0}C and kept there for 2 h under vigorous stirring. The resulting clear solution was then cooled to room temperature with vigorous stirring. A transparent gel was formed after a few minutes by adding a few drops of water diluted with ethanol to the solution. After aging the gel for 2 days with covering and 2 days as exposed to air, it was dried in an oven at 50 ^{0}C by mixing it at regular intervals to form a powder. The resulting xerogel was calcined step by step, i.e. at 150 ^{0}C for 30 min, at 300 ^{0}C for 30 min, and finally at 500 ^{0}C for 5 hours in air.

b) 10wt% Ni/3wt% CeO_2/Al_2O_3: A known amount of ATSB was dissolved in warm ethanol at 70 ^{0}C with vigorous stirring. For the partial hydrolysis of the aluminum precursor, small amounts of nitric acid and distilled water (40% nitric acid) solution, which had been mixed with ethanol, were slowly added to the solution containing the aluminum precursor, and stirred for 10 min at room temperature; the mixture was, then, transferred to a flat bottom 250 mL flask. Then, the desired amounts of cerium ammonium nitrate and nickel acetate were added sequentially into the solution containing the aluminum precursor, and stirred for 30 min at room temperature. Subsequently, the temperature was raised to 80 ^{0}C and kept there for 2 h under vigorous stirring. The resulting clear solution was then cooled to room temperature with vigorous stirring. A transparent gel was formed after a few minutes by adding a few drops of water diluted with ethanol to the solution. After aging the gel for 2 days with covering and 2 days as exposed to air, it was dried in an oven at 50 ^{0}C by mixing it at regular intervals to form a powder. The resulting xerogel was calcined step by step, i.e. at 150 ^{0}C for 30 min, at 300 ^{0}C for 30 min, and finally at 500 ^{0}C for 5 hours in air.

c) 10wt% $Ni/ZrO_2/Al_2O_3$: A known amount of ATSB was dissolved in warm ethanol at 70 ^{0}C with vigorous stirring. For the partial hydrolysis of the aluminum precursor, small amounts of nitric acid

and distilled water (40% nitric acid) solution, which had been mixed with ethanol, were slowly added to the solution containing the aluminum precursor, and stirred for 10 min at room temperature Then, the desired amounts of zirconium (IV) butoxide (atomic ratio equivalent to cerium in NCZA catalyst) and nickel acetate were added into the solution containing the aluminum precursor, and stirred for 30 min at room temperature. Subsequently, the temperature was raised to 80 ^{0}C and kept there for 2 h under vigorous stirring. The resulting clear solution was then cooled to room temperature with vigorous stirring. A transparent gel was formed after a few minutes by adding a few drops of water diluted with ethanol to the solution. After aging the gel for 2 days with covering and 2 days as exposed to air, it was dried in an oven at 50 ^{0}C by mixing it at regular intervals to form a powder. The resulting xerogel was calcined step by step, i.e. at 150 ^{0}C for 30 min, at 300 ^{0}C for 30 min, and finally at 500 ^{0}C for 5 hours in air.

d) 10wt% Ni/Ce(3wt%)O_2/ZrO_2/Al_2O_3: The NCZA catalysts were prepared by varying Ce and Zr atomic ratios as 1:3, 1:1 and 3:1 using the same procedure presented below to study the effect of stabilizer/support composition on the ATR reaction. A known amount of ATSB was dissolved in warm ethanol at 70 ^{0}C with vigorous stirring. For the partial hydrolysis of the aluminum precursor, small amounts of nitric acid and distilled water (40% nitric acid) solution, which had been mixed with ethanol, were slowly added to the solution containing the aluminum precursor, and stirred for 10 min at room temperature; the mixture was, then, transferred to a flat bottom 250 mL flask. Then, the desired amounts of zirconium (IV) butoxide (atomic ratio of cerium to zirconium), cerium ammonium nitrate and nickel acetate were added sequentially into the solution containing the aluminum precursor and stirred for 30 min at room temperature. Subsequently, the temperature was raised to 80 ^{0}C and kept there for 2 h under vigorous stirring. The resulting clear solution was then cooled to room temperature with vigorous stirring. A transparent gel was formed after a few minutes by adding a few drops of water diluted with ethanol to the solution. After aging the gel for 2 days with covering and 2 days as exposed to air, it was dried in an oven at 50 ^{0}C by mixing it at regular intervals to form a powder. The resulting xerogel was calcined step by step, i.e. at 150 ^{0}C for 30 min, at 300 ^{0}C for 30 min, and finally at 500 ^{0}C for 5 hours in air.

e) 0.3wt% Ru/10wt% Ni/Ce(3wt%)O_2/ZrO_2/Al_2O_3: A known amount of ATSB was dissolved in warm ethanol at 70 ^{0}C with vigorous stirring. For the partial hydrolysis of the aluminum precursor, small amounts of nitric acid and distilled water (40% nitric acid) solution, which had been mixed with ethanol, were slowly added to the solution containing the aluminum precursor, and stirred for 10 min at room temperature; the mixture was, then, transferred to a flat bottom 250 mL flask. Then, the desired amounts of zirconium (IV) butoxide (atomic ratio of cerium to zirconium is kept at 1), cerium ammonium nitrate, nickel acetate and ruthenium chloride were added sequentially into the solution containing the aluminum precursor and stirred for 30 min at room temperature. Subsequently, the temperature was raised to 80 ^{0}C and kept there for 2 h under vigorous stirring. The resulting clear solution was then cooled to room temperature with vigorous stirring. A transparent gel was formed after a few minutes by adding a few drops of water diluted with ethanol to the solution. After aging the gel for 2 days with covering and 2 days as exposed to air, it was dried in an oven at 50 ^{0}C by mixing it at regular intervals to form a powder. The resulting xerogel was calcined step by step, i.e. at 150 ^{0}C for 30 min, at 300 ^{0}C for 30 min, and finally at 500 ^{0}C for 5 hours in air.

f) 3wt% CeO_2/Al_2O_3: A known amount of ATSB was dissolved in warm ethanol at 70 ^{0}C with vigorous stirring. For the partial hydrolysis of the aluminum precursor, small amounts of nitric acid and distilled water (40% nitric acid) solution, which had been mixed with ethanol, were slowly added to the solution containing the aluminum precursor, and stirred for 10 min at room temperature; the mixture was, then, transferred to a flat bottom 250 mL flask. Then, the desired amount of cerium ammonium nitrate was added into the solution containing the aluminum precursor, and stirred for 30 min at room temperature. Subsequently, the temperature was raised to 80 ^{0}C and kept there for 2 h under vigorous stirring. The resulting clear solution was then cooled to room temperature with vigorous stirring. A transparent gel was formed after a few minutes by adding a few drops of water diluted with ethanol to the solution. After aging the gel for 2 days with covering and 2 days as exposed to air, it was dried in an oven at 50 ^{0}C by mixing it at regular intervals to form a powder. The resulting xerogel was calcined step by step, i.e. at 150 ^{0}C for 30 min, at 300 ^{0}C for 30 min, and finally at 500 ^{0}C for 5 hours in air.

g) 3wt% $CeO_2/ZrO_2/Al_2O_3$: A known amount of ATSB was dissolved in warm ethanol at 70 ^{0}C with vigorous stirring. For the partial hydrolysis of the aluminum precursor, small amounts of nitric acid and distilled water (40% nitric acid) solution, which had been mixed with ethanol, were slowly added to the solution containing the aluminum precursor, and stirred for 10 min at room temperature; the mixture was, then, transferred to a flat bottom 250 mL flask. Then, the desired amounts of zirconium (IV) butoxide (atomic ratio of cerium to zirconium is kept at 1) and cerium ammonium nitrate were added sequentially into the solution containing the aluminum precursor, and stirred for 30 min at room temperature. Subsequently, the temperature was raised to 80 ^{0}C and kept there for 2 h under vigorous stirring. The resulting clear solution was then cooled to room temperature with vigorous stirring. A transparent gel was formed after a few minutes by adding a few drops of water diluted with ethanol to the solution. After aging the gel for 2 days with covering and 2 days as exposed to air, it was dried in an oven at 50 ^{0}C by mixing it at regular intervals to form a powder. The resulting xerogel was calcined step by step, i.e. at 150 ^{0}C for 30 min, at 300 ^{0}C for 30 min, and finally at 500 ^{0}C for 5 hours in air.

I.B. Catalyst Characterization

After calcining the prepared catalysts, they are ground finely in a mortar and pestle, and characterized for structural, chemical and morphological features. X-ray powder diffraction patterns were obtained with a XPERT diffractometer (Phillips), using Cu Kα radiation (1.5406 Å) at a scanning rate of 5.4°/min. The BET surface area and pore size of catalysts were measured by ASAP 2020 (Micromeritics, USA) instrument at liquid nitrogen temperature. The powders were first degassed at 300 ^{0}C under high vacuum to ensure a clean surface prior to construction of the adsorption isotherm. H_2-TPR for the fresh catalysts was conducted in 10% H_2/Ar using Chembet Pulsar (Quantachrome instruments, USA) instrument to study the metal dispersion and reducibility. The sample (100 mg) was pre-treated at 150 ^{0}C for 30 min in Ar flow to remove water. At room temperature, Ar was replaced with 10% H_2/Ar (50 ml/min) and the cell temperature was raised from 30 to 1000 ^{0}C at a rate of 10 ^{0}C /min. TPD of H_2 was carried out in the same system as described for TPR. After reduction at 600 ^{0}C for 2 h, the sample was heated up to 800 ^{0}C under argon flow, then cooled down to room temperature in the same argon flow. The adsorption of H_2 took place for 45 min at room temperature. Subsequently the flow was switched from H_2 to argon and the cell temperature was raised from 30 to 1000 ^{0}C at a rate of 10 ^{0}C /min. The desorbed H_2

(uptake) was detected using a TCD. TPO was carried out in the same system as described for TPR. In a typical experiment, ca. 20 mg of used sample was mounted on a quartz wool plug and placed in a U-shaped quartz sample tube. The sample was heated up to 1000 ^{0}C at 10 ^{0}C/min under 3%O_2/He flow with a flow rate of 50 ml/min. The desorbed CO_2 was detected using a TCD detector. Amount of carbon deposited on the surface of the catalyst was calculated by assuming that each atom of carbon reacts to form CO_2. XPS spectra were recorded on a Kratos Axis Ultra DLD X-ray Photoelectron Spectrometer equipped with Mg Ka radiation (1253.6 eV) at 75W apparatus using Mg Ka anode and a hemispherical analyzer, connected to a five-channel detector. The C 1s line at 284.6 eV was used as an internal standard for the correction of binding energies. SEM-EDAX analysis was carried out at FEI Helios 600 Nanolab Dual Beam System. TEM analyses were carried out on JEOL 2010F-FasTEM operated at 80 kV with a filament current of 27 mA.

I.C. Experimental setup

The autothermal reforming experiments were carried out in a quartz vertical flow microreactor system. The schematic diagram of the experimental setup is illustrated in Figure 1. The reactor consisted of a 43 cm long quartz tube with 1.2 cm O.D. and 0.9 cm I.D. Powder catalyst samples were diluted with quartz chips to avoid preferential gas flow paths and hot spots, and packed between two plugs of quartz wool inside the reactor tube. Inconel sheathed K-type thermocouples were placed at upstream and downstream sides of the catalyst bed in quartz thermowells. The reactor was then placed inside a thermostat-controlled vertical tube furnace whose temperature was maintained constant within ±5 ^{0}C. The flows of nitrogen (carrier gas) and argon (internal standard) were metered into the system by AALBORG AFC 3600 mass flow controllers. Flows of fuel and water were both metered into the system by KD Scientific 200 series syringe pumps. All three components (feed gases, water, fuel) were mixed in a heated cross which exited into a 2 m long section of heat-traced 6 mm O.D. stainless steel tubing that served as a vaporizer with its surface at a temperature of approximately 230 ^{0}C. In order to determine whether the fuel was fully vaporized, the mass balance on the fuel through a blank reactor tube held at 250 ^{0}C was performed. The blank run showed complete vaporization of the fuel with better than 99% closure of the mass balance. Prior to reaction, the temperature in the reactor was raised to 600 ^{0}C with a ramp of 10 ^{0}C/min for the reduction of the catalyst in a flow of 50 sccm of 9.7% H_2/Ar for 2 hours. The system was, then, flushed with nitrogen for 30 minutes to remove the physisorbed hydrogen on the catalyst. The steam, prepared on the by-pass line, was subsequently introduced into the reactor, followed by the fuel after stabilization at the desired temperature. The temperature of the feed stream was 600 ^{0}C prior to reaching the catalyst bed. The total gas flow rate was kept at 300 sccm and the n-Dodecane concentration in the feed gas mixture was fixed at 1 vol%. The reactor effluent passed through a condenser to knock out any condensable liquids before entering the gas analysis train.

The gaseous reactor effluent was analyzed by two online Varian 3800 gas chromatographs periodically (every hour), one equipped with a TCD which was used for the analysis of carbon dioxide, carbon monoxide, argon, methane and C_2 hydrocarbons (Hayesep, Molsieve 5A PLOT fused silica column), and an FID for heavier hydrocarbon analysis (C_1-C_{16}) separated by a capillary column (100 m CPSil Pona CB); and the second GC with a TCD for H_2 and Ar analysis (Carboxen 1000). The fractional conversion of n-Dodecane resulting from reforming (X_{ref}) and the product yields of H_2, CO, CO_2, and C_1-C_4 hydrocarbons (CH_4, C_2H_4, C_2H_6, C_3H_6, C_3H_8, C_4H_8 and C_4H_{10}) were calculated as follows:

$$Y_{H_2} = \frac{F_{H_2,\ out}}{13.F_{C_{12}H_{26},in}} \qquad (1)$$

$$Y_{CO_2} = \frac{F_{CO_2,\ Out}}{12.F_{C_{12}H_{26},in}} \quad (2)$$

$$Y_{CO} = \frac{F_{CO,Out}}{12.\ F_{C_{12}H_{26},\ in}} \quad (3)$$

$$Y_{C_1-C_4} = \frac{F_{C_1-C_4,\ Out}}{13.F_{C_{12}H_{26},in}} \quad (4)$$

$$X_{REF} = \frac{F_{CO,Out} + F_{CO_2,Out}}{12.F_{C_{12}H_{26},\ in}} \quad (5)$$

The extent of reforming (equation 5) is the conversion of carbon in n-Dodecane to reforming products, which is quantified by carbon monoxide and carbon dioxide formation due to reforming and WGS/RWGS reactions. In all the equations, *F* is the molar flow rate of the subscripted species in mol s^{-1}. The molar flow rate of n-Dodecane was calculated from the volumetric flow rate through the pump. The flow rate of the individual product species was determined from the species effluent concentration and the total effluent flow rate on the dry basis. X_{ref} is defined based on the assumption that the extent of the combustion reactions of the hydrocarbon is negligible.

Figure 1. Experimental Setup

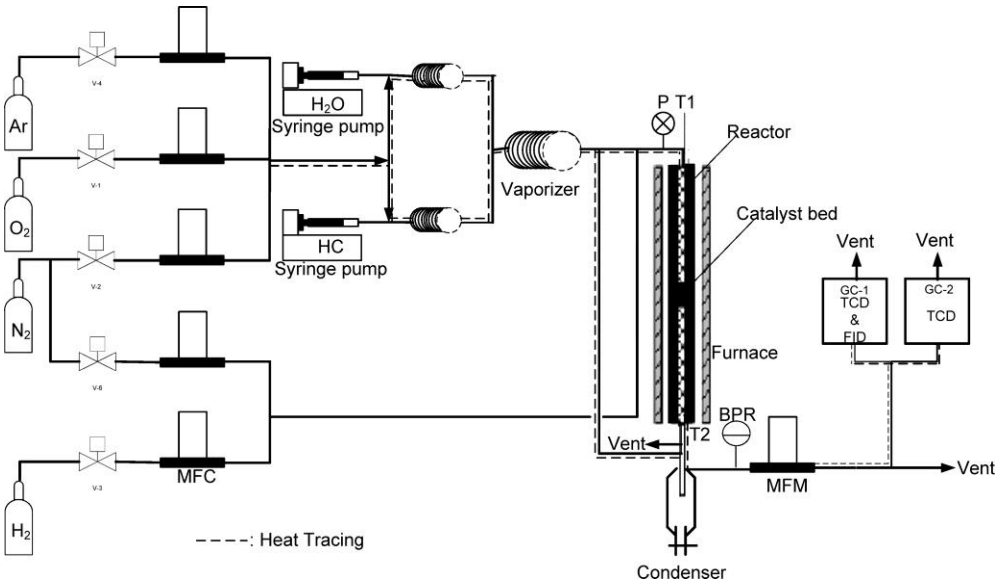

II. Catalyst Characterization - Results and Discussion

II.A. Surface area & Pore size

The specific BET surface area and pore size distribution of the catalyst samples were calculated from N_2 adsorption-desorption data at liquid nitrogen temperature and the results are presented in table 1. The NA catalyst has the highest BET surface area; with the incorporation of metal precursors into the

catalyst matrix, the surface area decreased. The results suggested that the addition of metal precursors caused a decrease in the surface areas of the catalysts. This might be due to the fact that the crystallite growth process was accelerated by the incorporation of Ce, Zr, and Ru ions into the mixed oxide catalysts; but this hypothesis has not been verified by the XRD measurements. Another explanation may be that the larger particle size of cerium atoms instigated a rearrangement in the distribution of the atoms of nickel, zirconium, and ruthenium, affecting the BET surface area of the catalysts.

Figure 2. N_2 adsorption-desorption isotherms of Ni-based catalysts; inset: Pore size distribution curves

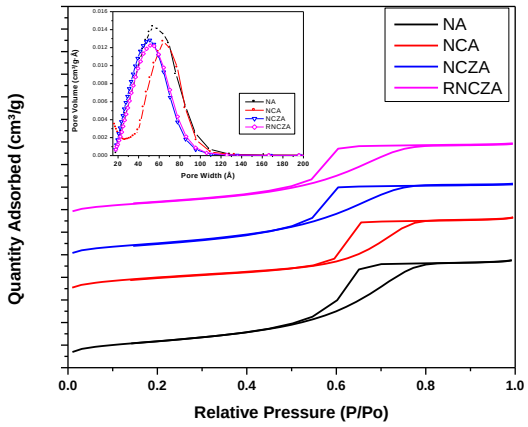

Table 1. Surface area, average pore diameter, cumulative pore volume, T_{max} of TPR peak, metal dispersion and active metal area of catalysts

Catalyst	**BET Surface area (m^2/g)**	**Average Diameter (Å)**	**Cumulative pore volume (cm^3/g)**	**TPR-peak T_{max} (^0C)**	**H_2 desorbed (µmol/g)**	**Metal dispersion (Ni - %)**	**Active metal area (Ni-m^2/g)**
NA	417.44	54.43	0.749	826.1	180.66	10.6	7.1
NCA	380.25	58.33	0.598	750.2	210.98	12.4	8.3
NZA	395.12	-	-	709.2	213.89	12.6	8.4
NCZA	375.06	47.15	0.583	695.8	226.12	13.3	8.8
RNCZA	364.94	49.79	0.567	574	236.94*	13.9*	9.3

*- cumulative Ni and Ru

N_2 adsorption-desorption isotherms and pore size distribution of the catalysts are presented in Figure 2 and Table 1. All the N_2 adsorption/desorption isotherms show type-IV isotherm pattern and have a steep increase in hysteresis loop at relatively high pressures. These are the main characteristic of mesoporous materials with a lagging loop as a result of capillary condensation of N_2 inside the pores occurring at different pressures[1,2]. In the NA catalyst (Fig. 2 inset), the pore diameter distribution is in the range from 16 to 150 Å with an average diameter of 54.43 Å with 0.749 cm^3/g cumulative pore volume. This indicates a mesoporous pore distribution in the NA catalyst framework. In the NCA catalyst, the bimodal pore diameter distribution is observed from 16 to 25 and 25-120 Å with maximum pore size distribution in the mesoporous range. The NCA catalyst has an average diameter of 58.33 Å with 0.598 cm^3/g cumulative pore volume. This clearly indicates more mesoporous pores in the catalyst framework with a minor microporous range. With the incorporation of Ce in the framework, the mesoporous range is lower compared to NA catalyst. In NCZA catalyst, the pore diameter distribution is from 16-110 Å range. The NCZA catalyst has an average diameter of 47.15 Å with 0.583 cm^3/g of cumulative pore volume. This indicates that with the incorporation of Ce and Zr in the framework, the mesoporous range is lower

than that of the NA catalyst. In the RNCZA catalyst, the broad pore diameter distribution is from 16 to 110 Å with a single distribution range. It has an average diameter of 49.79 Å with 0.567 cm^3/g of cumulative pore volume. In this catalyst, after the addition of ruthenium to NCZA catalyst, microporous range pores are not apparent as in the NCA catalyst. During the optimization of the catalyst preparation process, addition of metal precursors and volume of ethanol were varied during the sol-gel procedure; drying process was carried out with no ethanol on the surface and calcination was carried out directly at 500 ^{0}C. In all these cases, surface area and pore size distributions were low compared to the optimized preparation conditions. The main inferences from these results are that a large mesopore volume and high surface area in the catalysts resulted due to the limited alcohol usage during the sol-gel preparation process; and optimized drying, and calcination processes.

II.B. XRD

To investigate the crystallinity/phase identification, X-ray analysis was performed on the prepared samples; they are presented in figure 3, which shows that all the catalysts are amorphous in nature, and no clear sign of any crystallinity is evidenced as by the broader peaks[1]. This result is supported by the high surface area and pore size of the catalysts. The XRD results do not exhibit any clear Ru, Ni and Ce crystalline phases; these results suggest that the metal oxides are dispersed well in the catalyst network.

Figure 3. XRD patterns of Ni-based catalysts

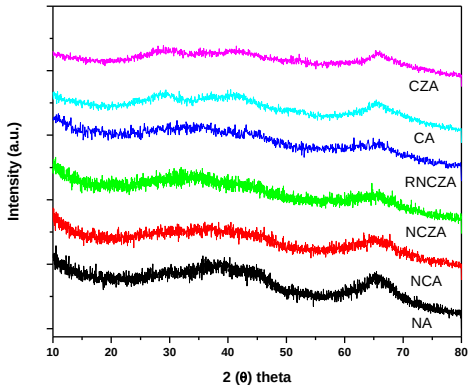

II.C. SEM

Figure 4. SEM photographs of a) NA b) NCA C) NZA d) NCZA and d) RNCZA

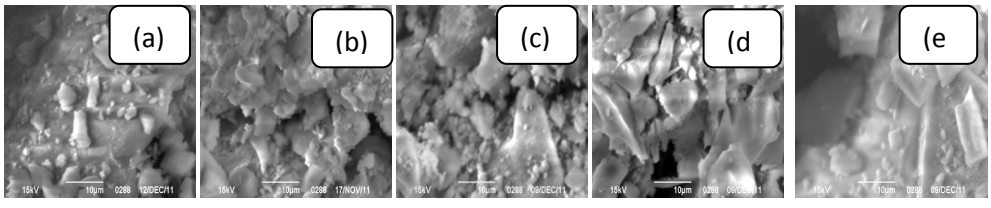

Scanning Electron Microscopy (SEM) was performed over the prepared catalysts to investigate the surface morphology and particle size; the results are presented in figure 4. All the catalysts exhibit the same type of rough morphology with the formation of irregular clusters and no sign of a clear phase development. It is difficult to determine the particle size from these types of clusters. This behavior

resulted from the Sol-Gel preparation technique through which all the components are mixed at the molecular level. The origin of the clusters is the coalescence of several nanometric single-crystals, or crystallites[3].

II.D. TPR

Figure 5. TPR profiles of Ni-based catalysts

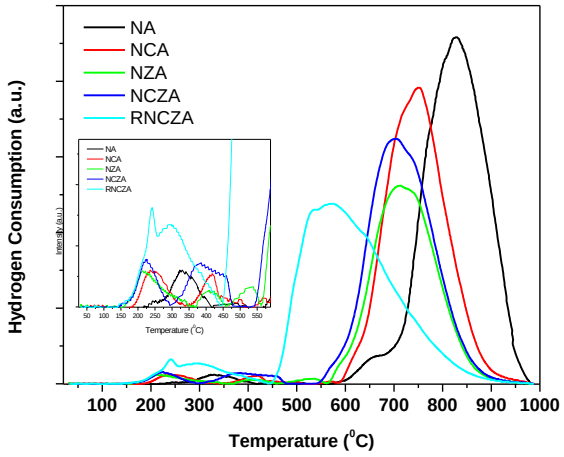

Temperature-programmed reduction (TPR) has been extensively applied in recent years for characterizing reducible catalysts including metal and metal oxide systems. This technique allows the visualization of a profile of catalyst reduction. This is very suitable for studying low loading and highly dispersed systems. TPR studies were carried out on a ChembetPulsar instrument (Quantachrome, USA) to study the metal dispersion and reducibility. In a typical experiment, ca. 100 mg of oven-dried sample (dried at 80 ^{0}C overnight) was mounted on a quartz wool plug and placed in a U-shaped quartz sample tube. Prior to TPR studies, argon gas was passed with a flow of 50 mL/min at 120 ^{0}C for 2 h to pretreat the catalyst sample. After pretreatment, the sample was cooled to ambient temperature and TPR analysis was carried out in a flow of 9.7% H_2/Ar. The TPR profiles of calcined catalysts are presented in Figure 5, and the corresponding data are summarized in Table 1.

The TPR of pure NiO powder exhibits a strong reduction peak at 420 ^{0}C followed by a small hump[4]. Figure 5 indicates that all the catalysts have different reduction sites, demonstrated by the small low-temperature and large high-temperature peaks. In the NA catalyst, two reduction peaks at 331 ^{0}C and 826.1 ^{0}C are observed. The small peak can be attributed to the freely available NiO on the surface of the catalyst, and the high temperature peak indicates strong interaction between highly dispersed and amorphous NiO with Al_2O_3[5]. With the incorporation of Ce into the matrix of NA catalyst, the high temperature reduction peak moved to 750.2 ^{0}C, which denotes lesser interaction of NiO with Al_2O_3, resulting in greater availability or higher reducibility of NiO for the reaction. The low-temperature peaks at 239.3 and 417 ^{0}C of the NCA catalyst are due to the reduction of free NiO clusters and of NiO interacting physically with the other oxides, respectively[6]. In the NZA catalyst, three low temperature reduction peaks at 213, 410 and 535 ^{0}C are observed and they can be attributed to NiO species weakly interacting with Zr and Al_2O_3 support[7]. The high-temperature reduction peak at 709.2 ^{0}C is attributed to a strong interaction between alumina and NiO. In NCZA catalyst, two low-temperature reduction peaks,

observed at 223 and 387 ^{0}C, are due to the NiO species weakly interacting with the support metal oxides; and the high temperature peak at 695.8 ^{0}C indicates strong interaction of NiO species with Al_2O_3. With the incorporation of Ru along with Ni, Ce, Zr and Al_2O_3, the high-temperature reduction peak shifted to 574 ^{0}C and low-temperature reduction peak shifted to 240.6 ^{0}C along with a shoulder peak at 296^{0}C. This suggests the promoting effect of Ru on the reduction of NiO particles, probably by the spillover of hydrogen dissociated on Ru to NiO. In all the catalysts, with the increasing incorporation of metal oxides into the catalyst matrix, reducibility of Ni increased due to the weakening interaction between Ni and Al_2O_3. Also in the presence of interaction between two metal oxides, the reduction of easily reducible metal oxide may enhance the reduction of the other metal oxide, depending on the degree of interaction between them[8]. This is in agreement with the earlier results[9].

II.E. TPD

Temperature Programmed Desorption (TPD) experiments were performed to study the metal dispersion and the active metal area present on the surface of the catalysts. TPD of H_2 was carried out in the same system as described for TPR. In a typical experiment, ca. 100 mg of oven-dried sample (dried at 80 ^{0}C overnight) was mounted on a quartz wool plug and placed in a U-shaped quartz sample tube. Prior to TPD studies, argon gas was passed with a flow of 50 mL/min at 120 ^{0}C for 2 h to pretreat the catalyst (surface cleaned) sample. After pretreatment, the sample was cooled to ambient temperature and was reduced at 600 ^{0}C for 2h. The sample was then heated up to 800 ^{0}C under argon flow, and cooled down to room temperature in the same argon flow. Subsequently, the adsorption of H_2 took place for 60 min at room temperature. The flow was switched from H_2 to argon and the cell temperature was raised from 30 to 1000 ^{0}C at 10 ^{0}C/min rate. The desorbed H_2 (uptake) was detected using a TCD. TPD results of Ni dispersion and active nickel surface area were calculated by assuming hydrogen uptakes at monolayer coverage of the Ni atoms and each surface Ni atom chemisorbs one hydrogen atom ($H/Ni_{surface} = 1$)[10,11]. H_2 uptake, percentage of Ni dispersion and active metal area results are reported in Table 1.

Pure Al_2O_3 support did not show any measurable hydrogen uptake. Ni dispersion increased from 10.6 to 13.9 and active metal area from 7.1 to 9.3 m^2/g catalyst, respectively from NA to RNCZA catalyst. Ni dispersion increased with the addition of metal oxides into the matrix leading to a positive effect in the reaction. This also indicates more availability of active metal on the surface of the catalyst. Additionally, it reiterates the TPR results that indicated a weak interaction between Ni and Al_2O_3 matrix. In the RNCZA catalyst, we are not able to distinguish between the active metal dispersion of Ru and Ni because the result does not have the degree of freedom to distinguish between the extent of hydrogen uptake on ruthenium, nickel, ceria and zirconia (spillover of H_2 on Ce and Zr from Ru) individually. Since the loading of ruthenium is very low compared to that of nickel, the metal dispersion on this catalyst was evaluated as if all the hydrogen was adsorbed on nickel.

III. Autothermal Reforming of n-Dodecane on Nickel Catalysts -Results and Discussion

For the ATR of dodecane reaction, the catalyst bed was to be designed for optimum flow conditions since powder catalysts were used in the reactor. Therefore, the catalyst bed was diluted with quartz beads in a ratio of one to three to prevent channeling and realize optimum heat and mass transfer conditions. Generally in ATR, two primary catalytic processes, namely PO_x and SR, transform n-dodecane into mainly carbon monoxide and hydrogen. The presence of reforming products makes the water-gas shift reaction possible during reforming and is often considered equilibrated at reforming

temperatures. Other reactions like combustion, methanation and coking are, also, probable and the equations are given below:

$C_{12}H_{26} + 6\,O_2 \rightarrow 12\,CO + 13\,H_2$	PO_x	(6)
$C_{12}H_{26} + 12H_2O \rightarrow 12\,CO + 25\,H_2$	SR	(7)
$CO + H_2O \leftrightarrow H_2 + CO_2$	WGS/RWGS	(8)
$C_{12}H_{26} + 18.5\,O_2 \rightarrow 12\,CO_2 + 13\,H_2O$	complete combustion	(9)
$C_{12}H_{26} + 12.5\,O_2 \rightarrow 12\,CO + 13\,H_2O$	incomplete combustion	(10)
$CO + 3\,H_2 \rightarrow CH_4 + H_2O$	methanation	(11)
$CO_2 + 4\,H_2 \rightarrow CH_4 + 2\,H_2O$	methanation	(12)
$CO + H_2 \rightarrow C + H_2O$	coking	(13)
$2CO \leftrightarrow C + CO_2$	Boudouard reaction	(14)
$CH_4 \rightarrow C + 2H_2$	coking	(15)

III.A. Primary Screening

Figure 6. Extent of reforming and product yields during the autothermal reforming of n- dodecane over catalysts. (Catalyst reduction at 600 ^{0}C for 2 h; reaction conditions: temp: 800 ^{0}C; GHSV: 220000 h^{-1}; H_2O/C: 2.0; O/C: 0.35)

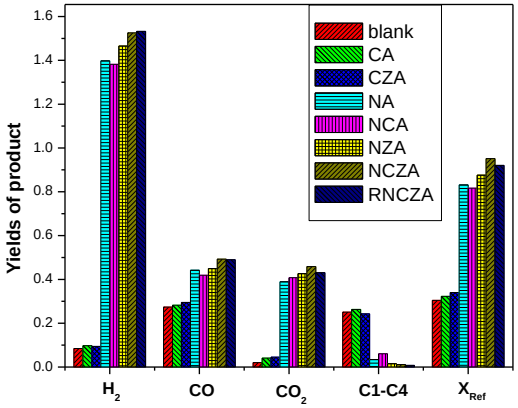

In primary screening, all prepared catalysts were evaluated at a standard condition, i.e. at 800 ^{0}C, catalyst amount of 75 mg, O/C=0.35 and H_2O/C=2 for Autothermal Reforming (ATR) of dodecane. Additionally, a blank test was run at the same conditions to check the extent of reactions in the absence of a catalyst. The results are presented in Figure 6. The reaction products were H_2, CO, CO_2, CH_4 and other hydrocarbons (C2-C4). There were very low methane levels, and no C2-C4 by-products were detected on NCZA and RNCZA catalysts; however, they were detected in the other catalysts. Higher production of H_2

on NCZA and RNCZA catalysts may be due to higher water gas shift activity and lower methanation activity as evidenced by fig. 6. The ATR activity of CA and CZA catalysts (supports) was measured to determine their effect on the reaction; they exhibited poor or no ATR activity as in the case of the blank test; but CO and CO_2 levels increased compared to the blank test, exhibiting the presence of oxygen mobility on these supports. Complete conversion of n-Dodecane was observed in all the Ni-loaded catalysts. Fractional conversion of n-Dodecane resulting from reforming and hydrogen yield over the NA catalyst is 0.83 and 1.39, respectively. After incorporation of Ce along with nickel and alumina in NCA catalyst, these variables changed to 0.81 and 1.38 (calculated as an average of several replicate experiments performed after the last report), respectively. This may be due to Ce being caged in the network of alumina and Ni, resulting in insufficient free Ni atoms available for the reaction and also, the inability of Ce to mobilize oxygen freely, causing the extent of methanation to increase. In the NZA catalyst, Zr has a positive effect on the reaction by increasing the extent of reforming and hydrogen yield to 0.88 and 1.45, respectively. This positive effect may be due to Zr attached to the support freeing Ni for the reaction and also, due to its oxygen mobility effect[12]. In NCZA catalyst, Ce and Zr are rearranged in the network by preventing the interaction of Ce with alumina to form $CeAlO_3$ and thus, making the nickel and cerium species available for the reaction[13]; hence, the extent of reforming and hydrogen yield increased to 0.93 and 1.52, respectively. Literature also shows evidence to the positive effects of Ce and Zr as supports for reforming catalysts by forming a CeZr solid solution in the structure of the catalyst and providing abundant oxygen storage and mobility to the surface[12,14-15]. This helps in reducing coke formation on the surface during the ATR reaction and increases the life of the catalyst. To study the effect of Ru on the NCZA catalyst, 0.3 wt% Ru was loaded on to it. The performance of this catalyst was similar to the NCZA catalyst for the hydrogen yield, i.e., 1.53, however, the extent of reforming decreased to 0.88. Thus, the positive effect of Ru as a promoter was not observed, because the addition of Ru favors the C-H bond formation leading to the production of CH_4[16]. Therefore, the effect of Ru addition to Ni on the NCZA catalyst was not noteworthy. Hence, NCZA catalyst was chosen for further experimentation to determine the optimum operating conditions to get the best ATR activity for n-Dodecane.

III.B. Effect of Temperature

NCZA catalyst was tested for ATR activity in the temperature range of 650 to 850 ^{0}C and the results are presented in figure 7. It was observed that 750 ^{0}C was the optimum temperature for this reaction. Above 700 ^{0}C, complete conversion of n-Dodecane was observed, but below 700 ^{0}C, unconverted dodecane/organic liquids were observed in the condenser, corresponding to a dodecane conversion of 92%. Increasing the temperature from 650 to 850 ^{0}C resulted first in an increase and then a decrease in the yield of H_2. This is due to the enhancement of reforming rate with increasing temperature; however, at a higher temperature, it causes the unfavorable equilibrium for the WGS reaction and the methanation reaction[17]. Our data on CO and CO_2 production support this explanation. Reduced activity of the catalysts at lower temperatures is due to insufficient energy supply, which was not enough to activate all the available active species and therefore, resulting in a low rate for steam reforming.

Figure 7. Extent of reforming and product yields during the autothermal reforming of n- dodecane on NCZA catalyst at different temperatures. (Catalyst reduction at 600 ^{0}C for 2 h; reaction conditions: GHSV: 220000 h^{-1}; H_2O/C: 2.0; O/C: 0.35)

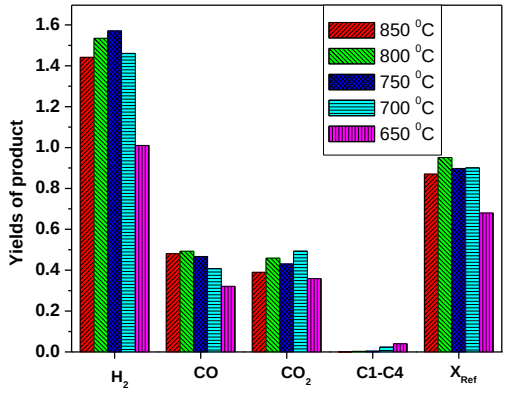

III.C. Effect of Space velocity

Figure 8. Extent of reforming and product yields during the autothermal reforming of n- dodecane on NCZA catalyst at different GHSVs. (Catalyst reduction at 600 ^{0}C for 2 h; reaction conditions: Temp: 750 ^{0}C; H_2O/C: 2.0; O/C: 0.35)

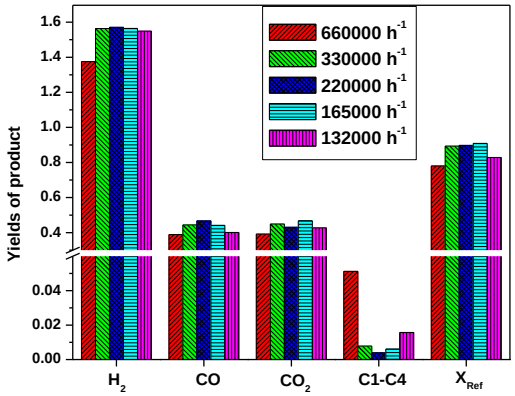

The effect of space velocity on the ATR of n-Dodecane, was studied over NCZA catalyst at a GHSV range of 132000-660000 h^{-1} and the results are presented in figure 8. At the highest space velocity of 660000 h^{-1}, the yield of H_2 as well as X_{Ref} are low compared to those at lower space velocities. This is mainly due to insufficient space time in the catalyst bed to convert all of the dodecane into end products; and is evidenced by the reaction products which contain a larger amount of lower hydrocarbons (C1-C4) at this space velocity. With space velocities ranging from 330000 to 132000 h^{-1}, the hydrogen yield did not change much due to the availability of sufficient number of active sites and space time. When we decreased the space velocity from 330000 to 132000 h^{-1}, the extent of reforming first increased and later decreased; this is because of the progress of the methanation reaction. It was observed in the graph that an increase in the yield of lower hydrocarbons was accompanied by a reduction in the hydrogen yield. Maximum hydrogen yield was reached at GHSV of 220000 h^{-1} with very low methane production. At

165000 h^{-1}, methane formation is higher and hydrogen yield was lower compared to those at 220000 h^{-1}. At 330000 h^{-1}, there are still some unconverted lower hydrocarbons present. Yield of CO increased from 660000 to 220000 h^{-1} and then decreased indicating that methanation reaction is occurring at lower space velocities. The CO and CO_2 yields are dependent on the equilibrium between the water gas shift and reverse water gas shift reactions. Thus, space velocity of 220000 h^{-1} is the optimum for the reforming reactions on NCZA catalysts for higher hydrogen production and lower hydrocarbon and coke formation.

III.D. Effect of H_2O/C

Figure 9. Extent of reforming and product yields during the autothermal reforming of n- dodecane on NCZA catalyst at different H_2O/C ratios. (Catalyst reduction at 600 ^{0}C for 2 h; reaction conditions: Temp: 750 ^{0}C; GHSV: 220000 h^{-1}; O/C: 0.35)

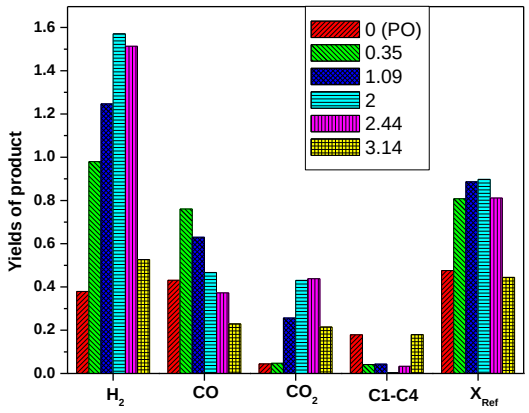

The effect of H_2O/C mole ratio on the ATR of n-Dodecane over NCZA catalyst was investigated in the range of 0-3.14 and the results are depicted in figure 9. With no water, i.e. partial oxidation, complete conversion of dodecane and a low yield of hydrogen were observed. Also, CO yield was higher compared to the yield of CO_2, and the production of lower hydrocarbons was more pronounced. These observations suggest the enhancement of cracking and oxidation reactions. At water to carbon ratio of 0.35, the extent of reforming and hydrogen yield drastically increased compared to those when no water was present. Appreciably higher CO yield compared to the yield of CO_2 is due to the dominance of the reverse water gas shift reaction. The formation of lower hydrocarbons (C1-C4) decreased due to the increased rate of the steam reforming reaction. With increasing H_2O/C ratio from 0.35 to 2, the extent of reforming increased; with a further increase in the ratio, the extent of reforming decreased. At higher water to carbon ratio (3.14), even though the initial H_2 yield was high, the time-on-stream catalyst activity decreased significantly. This may be due to the fact that the high dilution of hydrocarbon with steam causes oxidation of the active metal with prolonged reaction times. We studied the oxidized catalyst visually after the reaction. Above the H_2O/C ratio of 2, there was no visible carbon formation on the catalyst or on the walls of the reactor, but in partial oxidation, appreciable amounts of coke formed on the downstream walls of the reactor and on the catalyst. There was coke formation on the catalyst surface only in the case of H_2O/C ratios of 0.35 and 1.09. These results clearly indicate that for water-to-carbon ratios of less than 2, partial oxidation and cracking reactions are more dominating than steam reforming. Thus, water to carbon ratio of 2 is accepted as the optimum for obtaining a high hydrogen yield and low coke formation.

III.E. Effect of Oxygen to carbon ratio

Figure 10. Extent of reforming and product yields during the autothermal reforming of n- dodecane on NCZA catalyst at different O/C ratios. (Catalyst reduction at 600 ^{0}C for 2 h; reaction conditions: Temp: 750 ^{0}C; GHSV: 220000 h^{-1}; H_2O/C: 2)

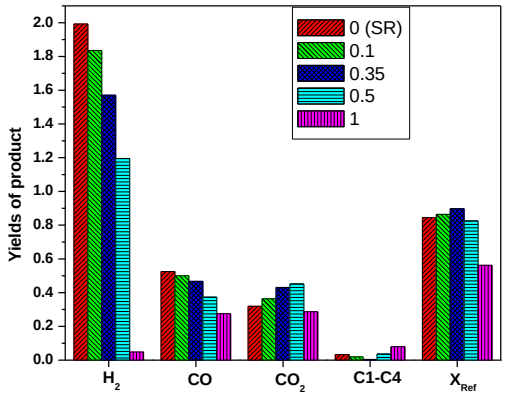

The effect of oxygen to carbon mole ratio on the ATR of n-Dodecane over the NCZA catalyst was investigated in the range of 0-1, and the results are presented in figure 10. As the O/C ratio was increased from 0 to 1, hydrogen and CO yields decreased. The CO_2 yield increased from 0 to 0.5 and then decreased. From 0.35 to 1, methanation products also increased, the extent of reforming decreased, and more water was produced by the reactions than that introduced to the reactor with the reactants. These results indicate the possibility of thermal cracking, combustion, methanation, and hydrogen oxidation reactions prevailing at higher O/C ratios. At a ratio of 1, we found that nearly 60% additional water was produced in the reaction over that in the reactor feed and more coke formation was visible on the catalyst bed. This gives the inference that at this ratio, incomplete and complete combustion reactions are more dominating compared to the reforming reactions. Also growing methanation products and carbon on the surface of the catalyst reveals coking and methanation processes are progressing. These are the main reasons for the lower hydrogen production at this ratio. Therefore, X_{ref} in this case does not represent the extent of reforming, but mainly, the extent of combustion reactions (page 15).

III.F. Effect of Ce/Zr ratio

To investigate the effect of Ce/Zr in NCZA catalyst with respect to hydrogen production from ATR of dodecane, we prepared NCZA catalysts at three Ce/Zr atomic ratios; and the results are presented in figure 11. We found that NCZA with Ce/Zr atomic ratio 1:1 is optimum for the reaction. At Ce/Zr ratio 3:1, with a high level of Ce, the extent of reforming, and the production of H_2, CO and CO_2 decreased, and C1-C4 products increased along with carbon formation. This is due to the inability of Ce to mobilize oxygen on the catalyst surface due to its strong interaction with alumina and Ni. This also results in insufficient free Ni atoms available for the reaction. At Ce/Zr ratio 1:3, with high Zr, the extent of reforming, and CO, CO_2 and C1-C4 production increased and H_2 production and carbon formation decreased. This may be due to the higher water gas shift reaction dominance and the excess Zr in Ce and Zr solid solution increasing the hydrogenation of products due to its acidic nature. At the Ce/Zr ratio of 1:1, higher H_2 production, less C1-C4 products, and no coke formation on the catalyst surface were observed, because Ce and Zr, forming a solid solution, act synergistically towards carbon oxidation and

make Ni atoms available for the ATR of dodecane, thus, enabling higher H_2 production. These results give us a glimpse on how the Ce and Zr ratios affect the activity and selectivity of the reforming catalysts. Walker et al.,[18] also observed in their recent investigation that addition of Zr at an equal atomic ratio to Ce improves oxygen storage capacity and redox properties, which enhances the catalytic activity of the mixed oxides at the elevated temperatures used in reforming reactions.

Figure 11. Extent of reforming and product yields during the auto thermal reforming of n- dodecane on NCZA catalyst at different Ce/Zr ratios. (Catalyst reduction at 600 ^{0}C for 2 h; reaction conditions: Temp: 750 ^{0}C; GHSV: 220000 h^{-1}; H_2O/C: 2; O/C : 0.35)

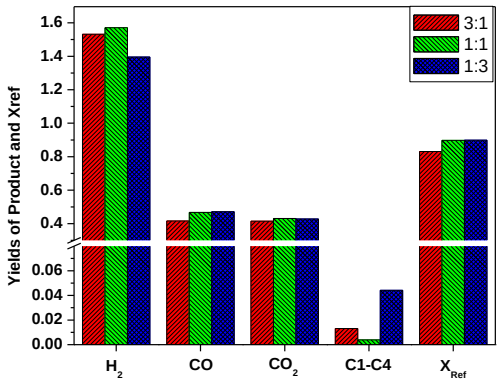

III.G. Stability test

To test the stability of the catalyst, we chose two reaction conditions, one with more hydrogen yield and the second with no visible carbon formation, i.e. O/C ratio of 0.1 and 0.35, respectively. Even though all these catalyst runs were conducted by stopping and restarting at regular intervals every day, and also, for refilling the feed pumps, the catalyst retained its activity in both of these conditions. The reformer was operated for 26 hours using the NCZA catalyst at O/C ratio of 0.1, and the results are presented in figure 12, which shows that the hydrogen yield decreased from 1.94 to 1.8 and the yield of methane and the extent of reforming were almost stable until the end of the reaction. With time-on-stream, the yield of lower hydrocarbons did not change appreciably. Carbon formation was visible on the catalyst.

NCZA catalyst, with an O/C ratio of 0.35, was run for 50 hours, and the results are presented in Figure 13. Even after 50 hours of reaction, the decrease in the hydrogen yield was not appreciable, namely, the initial hydrogen yield of 1.6 decreased to 1.43 at the 50th hour, and the yield of lower hydrocarbons (C_1-C_4) stayed below 0.05. The extent of reforming was almost stable until the end of the reaction and very small carbon formation was visible compared to the previous condition of the O/C ratio of 0.1. Coke formation will be discussed in the next section of the report. Overall, the NCZA catalyst exhibited high stability towards the autothermal reforming of n-Dodecane under both conditions.

Figure 12. Extent of reforming and product yields during the autothermal reforming of n-dodecane on NCZA catalyst for the extended run. (Catalyst reduction at 600 ^{0}C for 2 h; reaction conditions: Temp: 750 ^{0}C; GHSV: 220000 h^{-1}; H_2O/C: 2; O/C: 0.1)

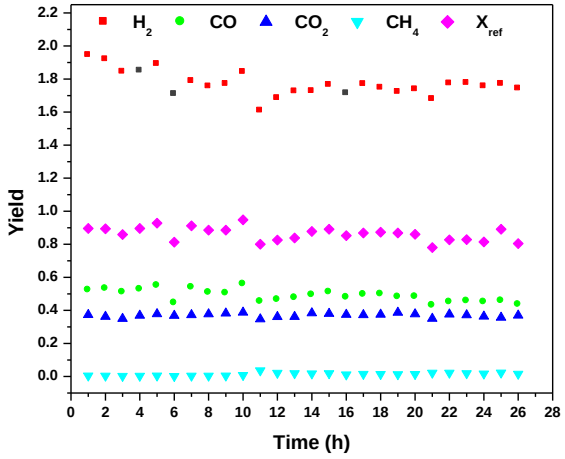

Figure 13. Extent of reforming and product yields during the autothermal reforming of n- dodecane on NCZA catalyst for the extended run. (Catalyst reduction at 600 ^{0}C for 2 h; reaction conditions: Temp: 750 ^{0}C; GHSV: 220000 h^{-1}; H_2O/C: 2; O/C: 0.35)

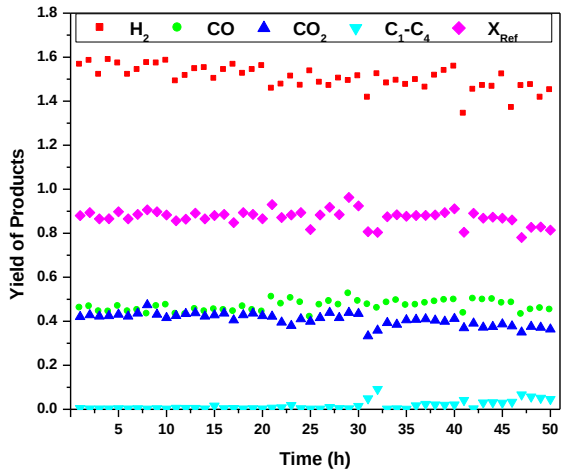

III.H. Post- reaction analysis of NCZA catalysts for ATR of n-Dodecane

III.H.1. Visible Carbon analysis

In figure 14, the photographs of ATR of n-Dodecane post-reaction reactors, quartz beads and catalysts are presented to make deductions on the carbon formation by visible examination. In SR post-reaction reactor (Fig. 14a), there is visible coke formation on the walls, beads and catalyst bed at the feed inlet side. In PO post-reaction reactor (Fig. 14b), there is visible coke formation on the walls as well as catalyst bed at the reactor outlet side; and we can observe coke formation on the catalyst powder during both SR and PO. But in the ATR post-reaction reactor (Fig. 14c), there is no visible coke formation neither on the walls, the beads and the catalyst bed, nor in visual examination of the catalyst powder. After 50h-long run under the same ATR conditions (Fig. 14d), carbon formation was observed but it is more or less the same as in fig. 14c. We can observe more coke formation on the catalyst bed for the O/C

ratio at 0.1 (Fig. 14e) compared to fig. 14d, and also, the extent of coke formation increased after the long run for 26 hours, but it is not as appreciable as the coke formation after the 5h-SR reaction. These results clearly indicate that the NCZA catalyst performs well under ATR conditions with respect to coke formation.

Figure 14. Post reaction profiles of NCZA (C/Z=1:1) catalysts, reactor and beads a) SR after 5h (Catalyst reduction at 600 ^{0}C for 2 h; reaction conditions: Temp: 750 ^{0}C; GHSV: 220000 h^{-1}; H_2O/C: 2); b) PO after 5h (Catalyst reduction at 600 ^{0}C for 2 h; reaction conditions: Temp: 750 ^{0}C; GHSV: 220000 h^{-1}; O/C: 0.35); c) ATR after 5h (Catalyst reduction at 600 ^{0}C for 2 h; reaction conditions: Temp: 750 ^{0}C; GHSV: 220000 h^{-1}; H_2O/C: 2; O/C: 0.35); d) ATR at O/C of 0.35 after 50h (Catalyst reduction at 600 ^{0}C for 2 h; reaction conditions: Temp: 750 ^{0}C; GHSV: 220000 h^{-1}; H_2O/C: 2; O/C: 0.35); e) ATR at O/C of 0.1 after 26h (Catalyst reduction at 600 ^{0}C for 2 h; reaction conditions: Temp: 750 ^{0}C; GHSV: 220000 h^{-1}; H_2O/C: 2; O/C: 0.1) and f) fresh NCZA catalyst

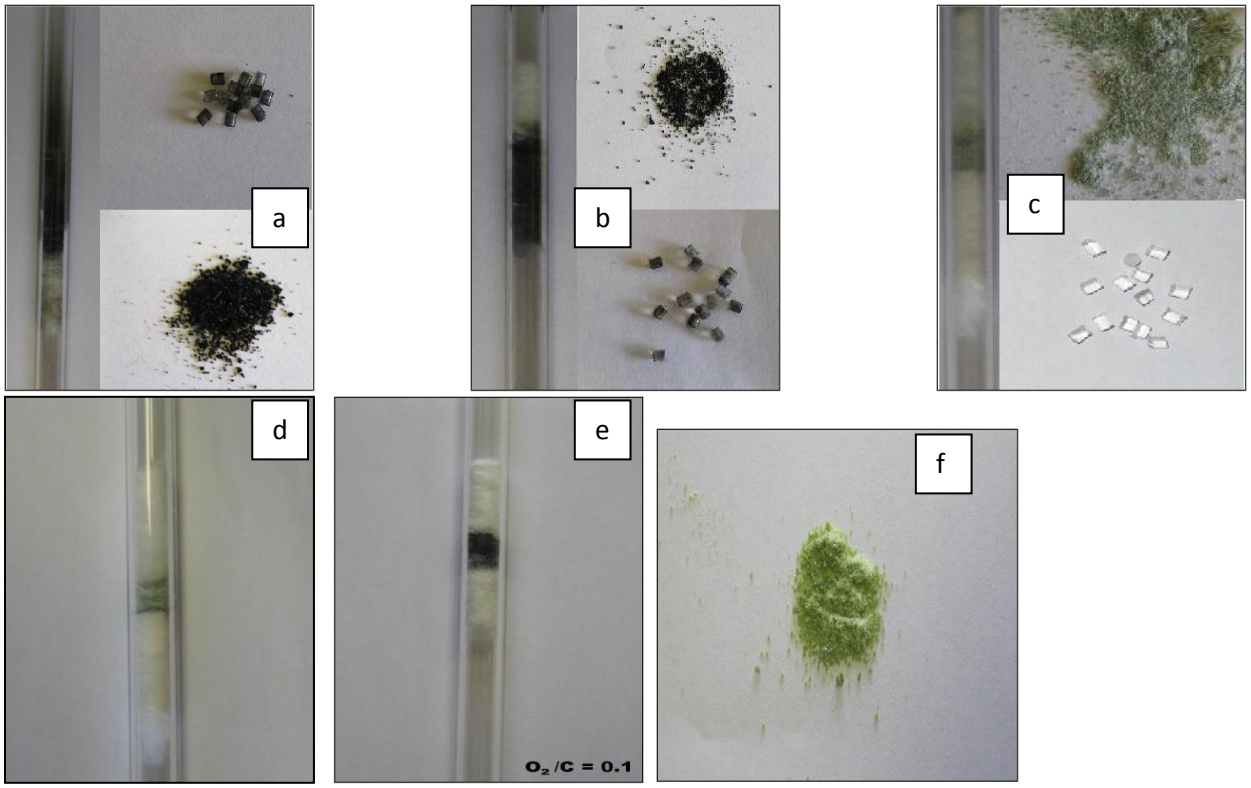

III.H.2. Results from SEM-EDAX and TEM studies

High resolution SEM photographs of fresh and used NCZA catalysts are presented in figure 15. These figures indicate that there was no carbon formation, and appreciable textural changes did not occur during the 5h- and 50h-runs on the NCZA catalysts with an O/C ratio of 0.35. In the case of ATR with O/C ratio of 0.1, on the catalyst surface, there are evolving carbon filaments, which have not yet completely covered the surface of the catalyst; also, a slight change occurred in the texture of the catalyst surface. To investigate these changes, TEM of fresh and used catalysts was performed, and the corresponding photographs are presented in figure 16. The TEM photographs show that the particle size of the fresh catalyst and the catalyst used in the 5h-run (O/C:0.35) did not change, remaining in a range of around 5-6 nm. In the catalyst used in the 50h-reaction with an O/C ratio of 0.35, the particle size

increased to 7-9 nm, with no evidence of carbon filaments. In the catalyst used for 26 hours (O/C= 0.1), the particle size increased to 7-8 nm; and carbon nanotubes formed in the range of 25-35nm width.

To study the changes in surface composition as well as the carbon content on the catalyst surface, SEM-EDAX analysis was performed on these fresh and used catalysts. The results from these analyses are presented in table 2. It is observed from the table that Ce/Zr atomic ratio remained the same in all the catalysts. There is no carbon formation on the surface of the catalyst used for 5 hours while about 2.29% carbon was found on the catalyst used for 50 hours (carbon was found only on 2 out of 6 spots; spot with the high carbon content is presented here). This indicates that the catalyst surface composition remained intact after the reforming reaction and that carbon was not dispersed uniformly on the surface.

Figure 15. SEM photographs of NCZA catalysts a) fresh, b) used for 5h (Catalyst reduction at 600 ^{0}C for 2 h; reaction conditions: Temp: 750 ^{0}C; GHSV: 220000 h^{-1}; H_2O/C: 2; O/C: 0.35), c) used for 50h (Catalyst reduction at 600 ^{0}C for 2 h; reaction conditions: Temp: 750 ^{0}C; GHSV: 220000 h^{-1}; H_2O/C: 2; O/C: 0.35) and d) used for 26h (Catalyst reduction at 600 ^{0}C for 2 h; reaction conditions: Temp: 750 ^{0}C; GHSV: 220000 h^{-1}; H_2O/C: 2; O/C: 0.1)

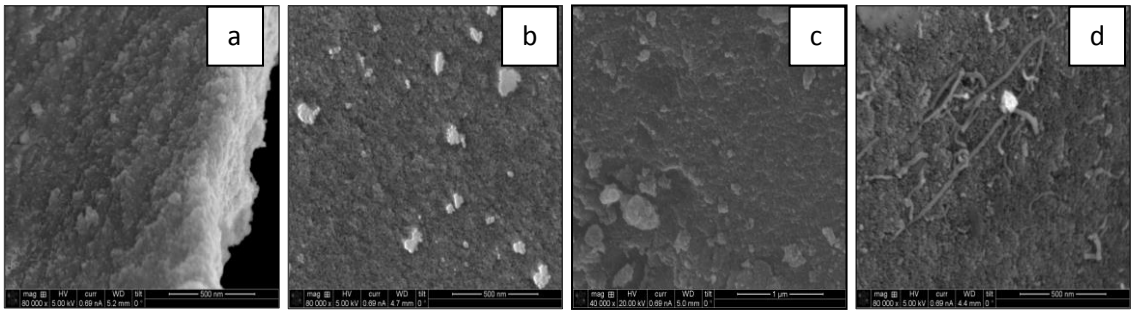

Figure 16. TEM photographs of NCZA catalysts a) fresh, b) used for 5h (Catalyst reduction at 600 ^{0}C for 2 h; reaction conditions: Temp: 750 ^{0}C; GHSV: 220000 h^{-1}; H_2O/C: 2; O/C: 0.35), c) used for 50h (Catalyst reduction at 600 ^{0}C for 2 h; reaction conditions: Temp: 750 ^{0}C; GHSV: 220000 h^{-1}; H_2O/C: 2; O/C: 0.35), d) used for 26h (Catalyst reduction at 600 ^{0}C for 2 h; reaction conditions: Temp: 750 ^{0}C; GHSV: 220000 h^{-1}; H_2O/C: 2; O/C: 0.1) and e) Carbon nanotubes formed in 26h run.

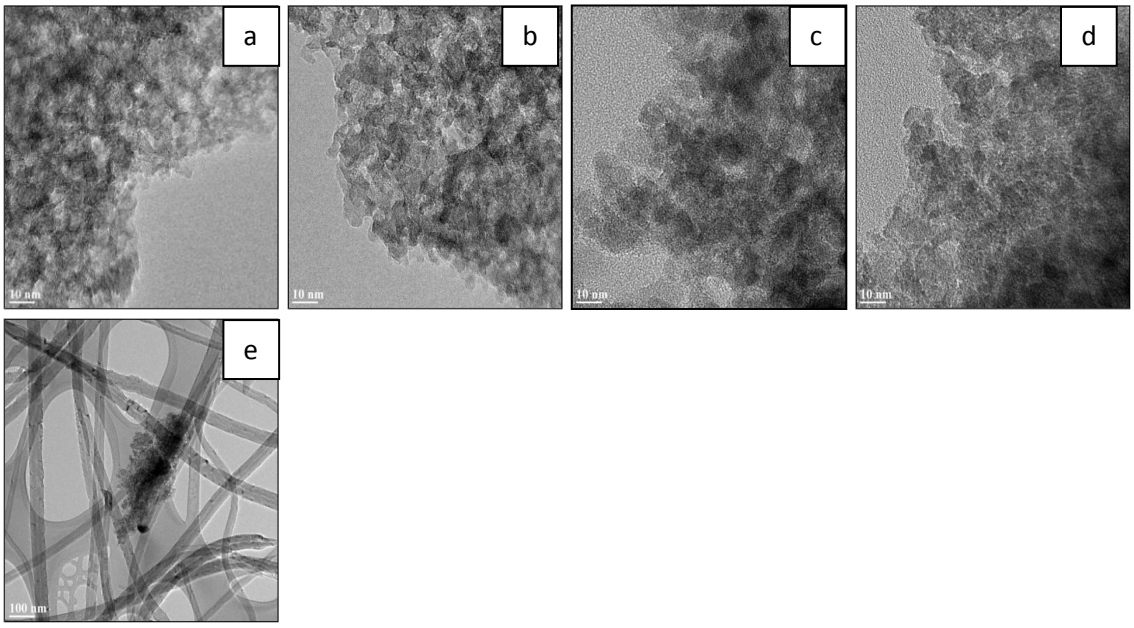

Table 2. SEM-EDAX analysis of fresh and used NCZA (1:1) catalysts.

NCZA	Element	wt%	Atomic%	Ce/Zr (atomic)
Fresh	O K	54.26	66.99	
	Al K	32.07	24.37	
	Ni K	8.09	4.23	
	Zr L	2.48	2.20	
	Ce L	3.10	2.19	0.99
Used 5h	O K	46.84	60.41	
	Al K	35.36	28.16	
	Ni K	9.99	5.49	
	Zr L	3.63	3.02	
	Ce L	4.20	2.94	0.97
Used 50h	C K	2.29	4.06	
	O K	44.89	59.88	
	Al K	41.16	32.55	
	Ni K	7.63	2.76	
	Zr L	1.55	0.36	
	Ce L	2.49	0.38	1.05

III.H.3 XPS study

Figure 17. C1s peaks on the NCZA fresh and used catalysts

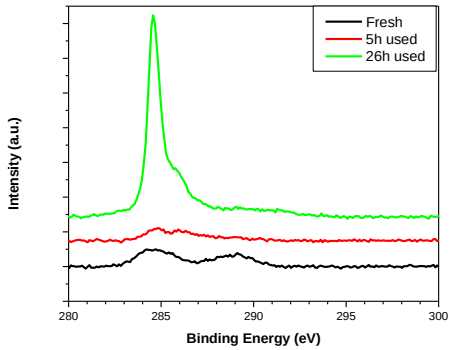

XPS study was carried out on fresh and used catalysts and the results are presented in figure 17 and 18. In Figure 17, C1s peak of fresh and used NCZA catalysts are presented. The fresh catalyst displays two peaks at 284.6 and 289.12, respectively. The peak at 284.6 is the standard carbon peak and the one at 289.12 is adventitious carbon which may have originated from the atmosphere, sample handling or contamination from XPS instrument itself[19]. This adventitious carbon peak is not observed in either of the used catalysts, hence it may have come from the atmosphere or handling. The catalyst used for 5 hours displays only standard carbon, which indicates that there is no carbon formation on the surface of the catalyst after 5h-reaction. On the other hand, at 26 hours (O/C= 0.1) the catalyst surface shows a large peak at 284.57 along with a shoulder peak at 285.6. The large peak represents carbon nanotubes formed on the surface with C-C bond and the shoulder represents C-H bond formation. Also, there is

another broad peak present at 289.6, which is almost at the level of noise, representing hydrogenated carbon as ketone or carboxyl groups[20,21].

Figure 18. Ni2p and Ce3d peaks of NCZA a) Fresh, b) 5h-used and c) 26h-used catalysts.

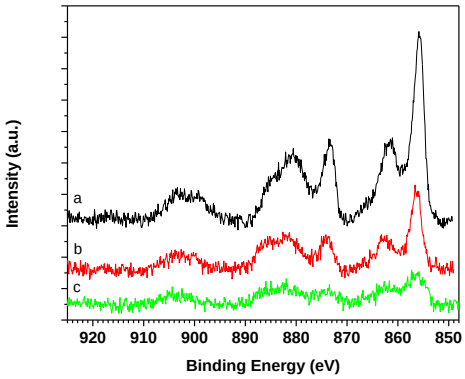

In Figure 18, XPS analysis of fresh and used NCZA catalysts for Ce 3d and Ni 2p peaks is presented. The intensity of these peaks on the fresh catalyst is higher than that on the used catalysts, because of the carbon formation and the possible presence of foreign particles like quartz wool on the latter (XPS is a surface technology which can penetrate into the sample only up to 10nm). But all the features of the Ce and Ni peaks remain intact. From the XPS analysis, we can observe the peaks of Ce^{+3}(880.5, 884.6, 903.3) and Ce^{+4}(882, 899.4, 900.3, 916.2) but Ce is present mostly in +3 state in all the catalysts[22,23]. Ni 2p spectra in fresh catalyst show nickel in the +2 state with a binding energy 855.8 eV. After the reaction, the used catalysts show slightly higher binding energy at around 856 eV, which indicates interaction of Ni with other metal oxides.

III.H.4. XRD study:

Figure 19. XRD peaks of NCZA a) Fresh, b) used for 5 hours and c) used for 50 hours.

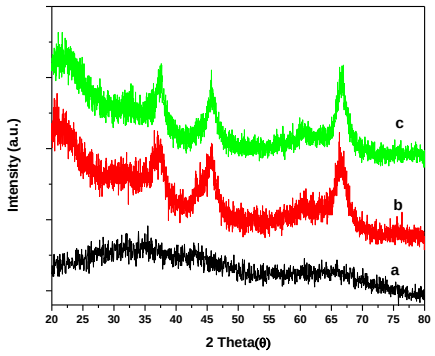

In figure 19, XRD patterns of fresh and used NCZA catalysts are presented. In fresh NCZA catalyst, there are no crystalline peaks. This means that all the metal oxides are amorphous in nature, and they are dispersed well in the solid matrix. Both used catalysts exhibit some crystalline structure with very low intensity. This proves that the particle size of the catalysts did not increase appreciably compared to the fresh catalysts. This supports the results from SEM and TEM analysis. The three peaks appearing at 2θ values represent NiO interacting with alumina (37.5) and γ-Al_2O_3 (45.7 and 66.6)[24,25].

III.H.5. Temperature programmed oxidation (TPO)

Temperature Programmed oxidation (TPO) experiments were performed on used NCZA catalysts to investigate the types of carbon deposited on the surface of the catalyst and the extent of carbon formation during the ATR reaction of n-Dodecane. TPO was carried out in the same system as described for TPR. In a typical experiment, ca. 20 mg of used sample was mounted on a quartz wool plug and placed in a U-shaped quartz sample tube. The sample was heated up to 1000 ^{0}C with 10 ^{0}C/min under 3%O_2/He flow with a flow rate of 50 ml/min. The desorbed CO_2 was detected using a TCD detector. Amount of carbon deposited on the surface of the catalyst was calculated by assuming that the carbon on the surface reacted to form only CO_2.

In figure 20, TPO results of used NCZA catalysts are presented. In literature, TPO peaks are classified as high temperature and low temperature carbon peaks, which represent nonreactive and reactive carbon species[25-27]. Low temperature carbon peaks represent adsorbed carbon species; and high temperature carbon peaks are due to graphitic and whisker and/or filamentous formation. Reforming over Ni catalysts primarily forms adsorbed carbon in the form of carbide which is reactive, but then polymerizes on the support and active metal surface, forming filaments and whiskers which ultimately take the nonreactive graphite form. Until the carbon deposit turns to whisker and graphitic form, it is in reactive state; once it attains the graphitic form, it is very stable and causes catalyst deactivation[28,29]. A carbon deposit in reactive form still participates in the reaction and may convert to CO and CO_2, and hence, the catalyst will not deactivate. This reactive carbon deposit may be in the form of C-H, C-C, Ni-C and C-O (intermediate ketone and carboxyl group). In our TPO results, NCZA catalyst with 5 hour and 50 hour use (O/C=0.35) exhibit only low temperature carbon peaks. Even though both 5h- and 50h-NCZA catalysts show low temperature peaks, their TPO patterns indicate different types of coke formation on the catalyst surface. In the 5h-NCZA catalyst, TPO pattern has one broad peak centered at 235 ^{0}C and a small hump at 388 ^{0}C with a total amount of deposited carbon of 15.6 mg/g catalyst (i.e., 1.5% C in 5h). These low temperature peaks represent adsorbed acidic coke on the support (Ce-Zr-Al-O) and the onset of polymeric carbon species, respectively. In 50h-NCZA catalyst TPO, one broad peak with T_{max} at three areas i.e., 121, 230 and 387 ^{0}C was observed. These peaks represent adsorbed carbon, acidic coke deposition and polymeric carbon deposits. Polymeric carbon growth is higher and adsorbed and acidic coke are less on this catalyst compared to the NCZA5h catalyst. This means that the deposited coke transforms from one phase to the other. 50h-NCZA catalyst has a total carbon deposit of 13.3 mg/g catalyst (i.e. 1.3% C in 50h) which is slightly lower than that on the 5h-NCZA catalyst; this is due to the in-situ redox conditions of the reaction atmosphere, improving, with time-on-stream the oxygen mobility of the Ce-Zr solid solution on the surface of the catalyst. 26h-NCZA (O/C=0.1) catalyst has two types of carbon species, one with low temperature and the other with high temperature carbon species. The low temperature coke deposits are found at 161 ^{0}C with two small humps with T_{max} at 265 and 417 ^{0}C, and a high temperature peak appears at 693 ^{0}C. The low temperature peaks represent physically adsorbed amorphous carbon, acidic coke and polymeric coke deposits, respectively; and the high temperature peak corresponds to filamentous carbon species. TEM and SEM studies, also, showed filamentous carbon in the 26h-run, supporting our interpretation of the TPO results. The low temperature peaks at 161 and 417^{0}C represent adsorbed carbon in the form of various types of coke like C-C, C-H or C-O, and this deduction is supported by the XPS data on the C1s peak.

Figure 20. TPO profiles of NCZA catalysts a) NCZA5h (O/C=0.35), b) NCZA50h (O/C=0.35) and c) NCZA26h (O/C=0.1)

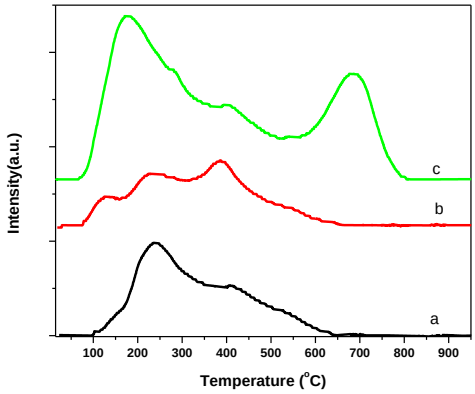

Table 3. Carbon deposit on used NCZA and RNCZA catalysts

	Carbon amount	
	µmol/g.cat	mg/g catalyst
NCZA5h (O/C=0.35)	1300.06	15.60
NCZA50h (O/C=0.35)	1109.06	13.30
NCZA26h (O/C=0.1)	3339.65	40.07
RNCZA5h (O/C=0.35)	2048.94	24.58
RNCZA25h (O/C=0.35)	1254.93	15.05

IV. Autothermal Reforming of Isobutanol on Nickel Catalysts– Results and Discussion

Based on Dr. Ivan Lee's and Dr. Mantz's suggestion, we performed an extensive study on the autothermal reforming of isobutanol; the results are presented below.

IV.A. Primary Screening

In primary screening, all prepared catalysts and a blank test were evaluated at a standard condition (obtained from previous results from ATR of dodecane), i.e. at 750 ^{0}C, catalyst amount of 75 mg, O/C=0.35 and H_2O/C=2 for Autothermal Reforming (ATR) of isobutanol. The results are presented in Figure 21. The main reaction products were H_2, CO, CO_2, CH_4 and other hydrocarbons (C2-C4). Very low methane and no C2-C4 by-products were detected on the RNCZA catalyst compared to the NA and NCZA catalysts. Higher hydrogen production over RNCZA catalyst is mainly due to the promotion effect by Ru which enhances the water gas shift activity. A blank test was conducted to study the combustion effect at the temperature used and for the extent of ATR reaction in the absence of a catalyst; very low hydrogen and CO_2, and higher CO and C1-C4 production occurred. Complete conversion of isobutanol was observed in all the Ni-loaded catalysts. Fractional conversion of isobutanol resulting from reforming, and the hydrogen yield over the NA catalyst are 0.6 and 1.06, respectively. The incorporation of Ce and Zr in the NA catalyst resulted in a positive effect on the reforming reaction, not only by increasing these

variables to 0.71 and 1.12, respectively, but also, there was no visible coke formation on the catalyst. In the NCZA catalyst, Ce and Zr formed a solid solution and weakened the interaction between Ni and Al by preventing the formation of $NiAl_2O_4$, thus, making the nickel species available for the reaction. There is evidence in literature on this positive effect of Ce and Zr as supports for reforming catalysts by forming a Ce-Zr solid solution in the structure of the catalyst and providing abundant oxygen storage and mobility to the surface[12,14-15]. These effects result in the reduction of coke formation on the surface during the ATR reaction, and increase the life of the catalyst. In the RNCZA catalyst, along with the above effects, Ru promotion increases the ATR activity tremendously, increasing the yield of hydrogen and extent of reforming to 1.49 and 0.83, respectively. Hence, RNCZA catalyst was selected as the catalyst for autothermal reforming reaction of isobutanol.

Figure 21. Extent of reforming and product yields during the autothermal reforming of isobutanol. (Catalyst reduction at 600 ^{0}C for 2 h; reaction conditions: temp: 750 ^{0}C; GHSV: 217000 h^{-1}; H_2O/C: 2.0; O/C: 0.35)

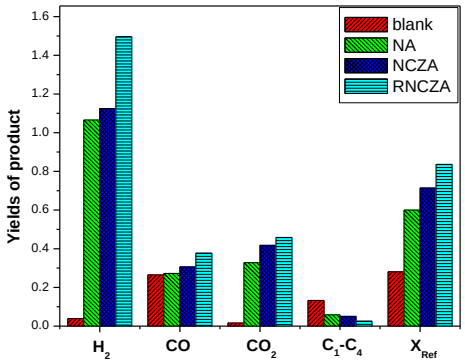

IV.B. Temperature effect

To identify the optimum temperature for the ATR of isobutanol over RNCZA catalyst, the effect of temperature was studied in the range of 600 to 750 ^{0}C, and the results are presented in figure 22. In all cases, complete conversion of isobutanol was observed. Increasing the temperature from 600 to 750 ^{0}C resulted first in an increase and then a decrease in the yield of H_2. This is due to the enhancement of reforming rate with increasing temperature; however, it causes the unfavorable equilibrium for the WGS reaction[17]. Our data on CO and CO_2 production support this explanation. At the low temperature of 600 ^{0}C, steam reforming and lower hydrogen production was due to insufficient energy supply, so that the hydrocarbon fragments did not convert to end products, resulting in the increased production of C1-C4 and other unidentified products. Thus, 700 ^{0}C was selected as the optimum temperature of operation to realize the objective of maximizing the hydrogen production.

Figure 22. Extent of reforming and product yields during the autothermal reforming of isobutanol on RNCZA catalyst at different temperatures. (Catalyst reduction at 600 ^{0}C for 2 h; reaction conditions: GHSV: 217000 h^{-1}; H_2O/C: 2.0; O/C: 0.35)

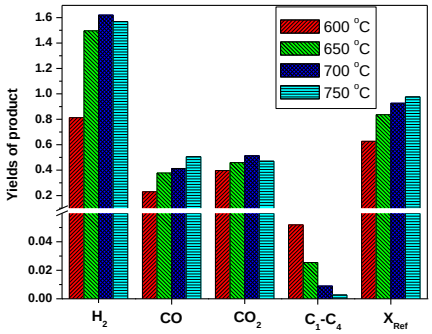

IV.C. Effect of Space velocity

Figure 23. Extent of reforming and product yields during the autothermal reforming of isobutanol on RNCZA catalyst at various GHSVs. (Catalyst reduction at 600 ^{0}C for 2 h; reaction conditions: Temp: 700 ^{0}C; H_2O/C: 2.0; O/C: 0.35)

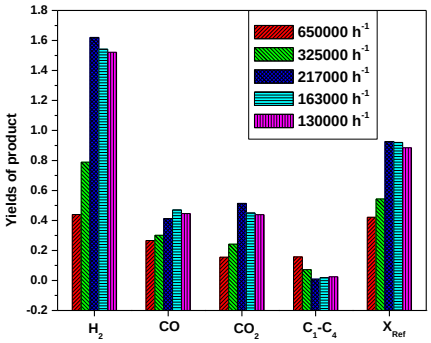

To determine the optimum space velocity for ATR of isobutanol over RNCZA catalyst, we studied gas hourly space velocities (GHSV) in the range of 130000-650000 h^{-1}, and the results are presented in figure 23. At the higher space velocities i.e., 650000 and 325000 h^{-1}, the yield of H_2 as well as X_{Ref} were low compared to those at lower space velocities. This is mainly due to insufficient number of active sites and residence time on the catalyst bed to convert all of the isobutanol into end products. This is evidenced by the reaction products containing a larger amount of lower hydrocarbons (C1-C4) at these space velocities. ATR activity increased at lower space velocities. At a space velocity of 217000 h^{-1}, ATR of isobutanol reached its highest H_2 production and reforming levels. At the lower space velocities (from 163000 to 130000 h^{-1}), the hydrogen yield decreased slightly and C1-C4 products increased slightly due to methanation over the catalyst surface (Figure 23)[16]. Yield of CO increased from 650000 to 163000 h^{-1} and then decreased indicating that methanation reaction is occurring at lower space velocities; the CO and CO_2 yields are dependent on the equilibrium between the water gas shift and reverse water gas shift reactions. Therefore, a space velocity of 217000 h^{-1} is the optimum for the reforming reactions of isobutanol on the RNCZA catalysts for higher hydrogen production and lower hydrocarbon and coke formation.

IV.D. Effect of Water

The effect of H_2O/C mole ratio on ATR of isobutanol over RNCZA catalyst was investigated in the range of 0-4 and the results are depicted in figure 24. With no water, i.e. partial oxidation, complete conversion of isobutanol and a low yield of hydrogen were observed. Also, CO yield was higher compared to the yield of CO_2, and the production of lower hydrocarbons was more pronounced. All these observations are due to the enhancement of cracking and oxidation reactions. At water to carbon ratio of 1, the extent of reforming and hydrogen yield drastically increased compared to those when no water was present. Appreciably higher CO yield compared to the yield of CO_2 is due to the predominant reverse water gas shift reaction. The formation of lower hydrocarbons (C1-C4) decreased due to the increased rate of the steam reforming reaction. With increasing H_2O/C ratio from 1 to 3, the extent of reforming increased; with a further increase in the ratio, the extent of reforming decreased. At higher water to carbon ratio (4), even though the initial H_2 yield was high, the time-on-stream catalyst activity decreased significantly. This may be due to the high dilution of the hydrocarbon with steam, causing oxidation of the active metal with prolonged time. The color of the catalyst after the reaction indicates that it underwent oxidation. In partial oxidation, appreciable amounts of coke were formed on the catalyst. With the introduction of higher amounts of water, the coke formation decreased drastically. At and above the H_2O/C ratio of 2, there was no visible carbon formation on the catalyst or on the walls of the reactor. Even though, high hydrogen yield and reforming activity were observed at H_2O/C ratio at 3, we did not consider it as the optimum because of energy considerations at the industrial scale. Thus, a water to carbon ratio of 2 is selected as the optimum for obtaining a high hydrogen yield and low coke formation.

Figure 24. Extent of reforming and product yields during the autothermal reforming of isobutanol on RNCZA catalyst at different H_2O/C ratios. (Catalyst reduction at 600 ^{0}C for 2 h; reaction conditions: Temp: 700 ^{0}C; GHSV: 217000 h^{-1}; O/C: 0.35)

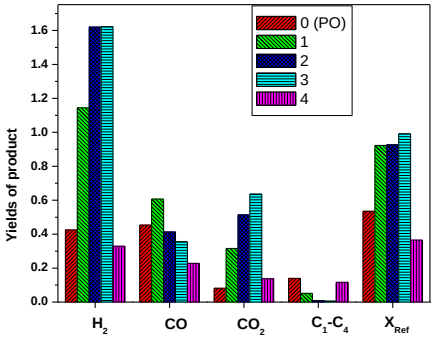

IV.E. Oxygen effect

The effect of oxygen to carbon mole ratio on the ATR of isobutanol over RNCZA catalyst was investigated in the range of 0-1, and the results are presented in figure 25. As the O/C ratio is increased from 0 to 1, hydrogen and CO yields decreased. From 0 to 0.35, the CO_2 yield increased and from 0.5-1 it decreased. At 0.5-1 ratios, the extent of reforming decreased drastically, and more water was produced by the reactions than that introduced to the reactor with the reactants and more coke formation was observed. These results indicate that at 0-0.35 ratio, the steam reforming and water gas shift reactions are dominant, while at ratios of 0.5-1, partial oxidation, methanation and cracking products and hydrogen oxidation reactions are dominant. These are the main reasons for the lower hydrogen production at this ratio. Hence, we used an O/C ratio of 0.35 as the optimum for this reaction.

Figure 25. Extent of reforming and product yields during the autothermal reforming of Isobutanol on RNCZA catalyst at different O/C ratios. (Catalyst reduction at 600 ^{0}C for 2 h; reaction conditions: Temp: 700 ^{0}C; GHSV: 217000 h^{-1}; H_2O/C: 2)

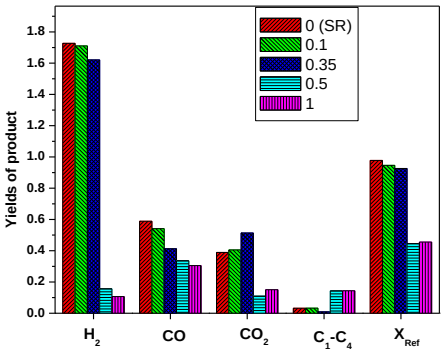

IV.F. Stability test

Figure 26. Extent of reforming and product yields during the autothermal reforming of isobutanol on RNCZA catalyst for long run. (Catalyst reduction at 600 ^{0}C for 2 h; reaction conditions: Temp: 700 ^{0}C; GHSV: 217000 h^{-1}; H_2O/C: 2; O/C: 0.1)

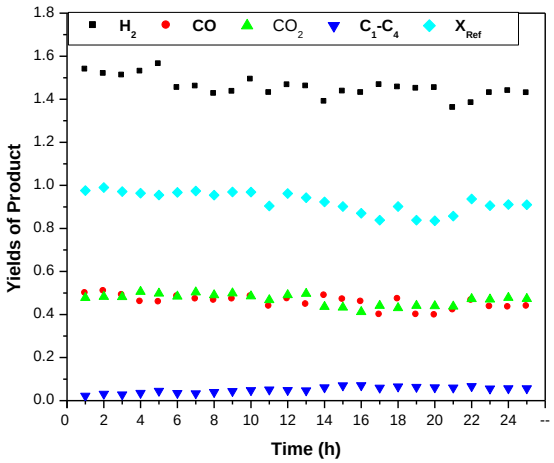

To determine the stability of the catalyst for ATR of isobutanol, a test was conducted for 25 hours at the optimized conditions, and the result is presented in Fig. 26. The run was carried out by stopping and restarting at regular intervals every day, and also, for refilling the feed pumps. The catalyst retained its activity for 25 hours. After 25 hours of testing with time-on-stream, the hydrogen yield decreased from 1.53 to 1.4, the extent of reforming decreases slowly and lower hydrocarbon products reached to 0.07. There was very low carbon formation on the catalyst. Overall, RNCZA catalyst showed stability towards isobutanol autothermal reforming under the optimized conditions.

IV.G. Post- reaction analysis of RNCZA catalysts for ATR of Isobutanol

IV.G.1. XRD study

Figure 27. XRD peaks of RNCZA a) Fresh, b) 5h-used and c) 25h-used catalysts.

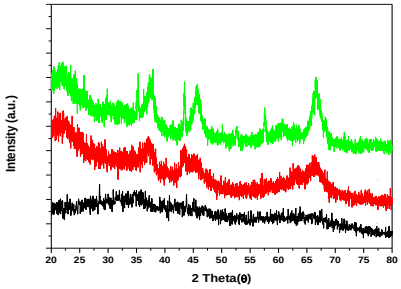

In figure 27, XRD patterns of fresh and used RNCZA catalysts are presented. In fresh RNCZA catalyst, no crystalline peaks appeared, i.e. all the metal oxides are well-dispersed in the support matrix and are amorphous in nature. In used catalysts, both show increases in crystallinity, and this increased with time from 5 to 25 hours. Even though both catalysts are crystalline in nature, the peak intensity is not high. This indicates that the particle sizes on the catalysts did not increase appreciably compared to the fresh catalysts. In RNCZA5h catalyst, 2θ values at 37.5 and 45.4 are due to NiO interacting with alumina, 43.9 due to Ni^0 and 66.4 due to γ-Al_2O_3[24,25]. The 2θ value of the peak observed at 45.4 on this catalyst compared to the one on the used NCZA catalyst at 45.7 (Figure 19) indicates that the interaction between NiO and alumina is stronger on the used RNCZA catalyst. In RNCZA-25h catalyst, additional to the peaks mentioned above, a peak at 35.2 represents $NiAl_2O_3$. This explains the minor decrease in activity of the catalyst in the 25-hour run.

IV.G.2. SEM-TEM–EDAX

Figure 28. SEM photographs of RNCZA a) Fresh, b) 5h-used and c) 25h-used catalysts

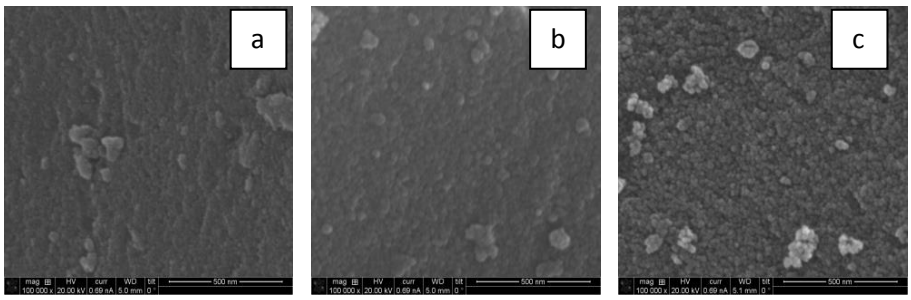

High resolution SEM photographs of fresh and used RNCZA catalysts are presented in figure 28. These figures show that there is no carbon formation on the surface of the catalyst with time-on-stream. The morphology of the catalysts has not changed appreciably on the 5h- and 25h-used RNCZA catalysts. It is observed that on fresh, RNCZA 5h- and RNCZA 25h-used catalysts, the particle size is below 10nm; 10 nm; and 10-15 nm, respectively. To explain these changes, TEM analysis of fresh and used catalysts was performed and the photographs are presented in figure 29. The TEM photographs show that the particle size in fresh, RNCZA5h-, RNCZA25h-used catalyst are 5-6nm, 6-8nm and 10-13 nm, respectively. It is, also, observed that the particle size increased with time-on-stream during the

autothermal reforming of isobutanol. No filamentous carbon or whiskers were observed on any of the photographs.

Figure 29. TEM photographs of RNCZA a) Fresh, b) 5h-used and c) 25h-used catalysts

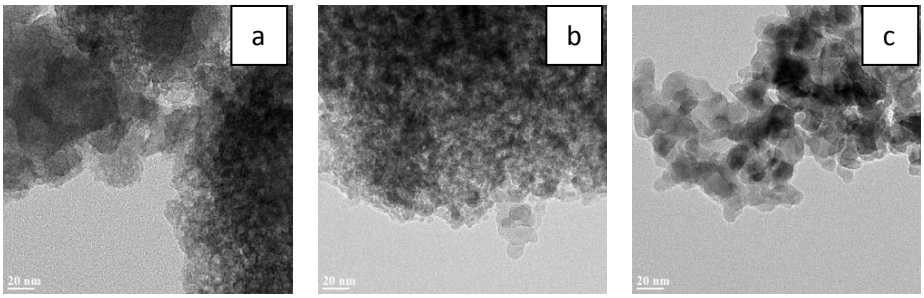

SEM-EDAX analysis was, also, performed on these fresh and used catalysts to study the changes in the surface composition, as well as carbon content on the surface. SEM-EDAX results are presented in table 4, which shows the presence of carbon in all the catalysts. There is 1.7 and 3.4 wt% carbon on the surface of RNCZA5h and RNCZA25h catalysts, indicating that the catalyst surface composition is changing during the course of the reaction.

Table 4. SEM-EDAX analysis of fresh and used RNCZA catalysts.

RNCZA	**Element**	**Weight%**	**Atomic%**
Fresh	C K	0.20	0.34
	O K	51.43	67.85
	Al K	37.21	29.1
	Ni K	7.10	2.68
	Ru K	0.19	0.06
	Ce L	2.31	0.53
	Zr L	2.05	0.31
5h used	C K	1.77	3.042
	O K	48.39	63.73
	Al K	37.72	29.53
	Ni K	7.58	2.732
	Ru K	0.21	0.15
	Ce L	1.98	0.46
	Zr L	2.35	0.36
25h used	C K	3.44	5.86
	O K	46.36	60.7
	Al K	37.97	29.7
	Ni K	7.37	2.79
	Ru K	0.26	0.08
	Ce L	2.3	0.53
	Zr L	2.3	0.35

IV.G.3. Visible Carbon analysis

In figure 30, the photographs of ATR of isobutanol post-reaction reactors are presented to make deductions on the carbon formation by visible examination. In SR post-reaction reactor, there is visible coke formation on the reactor walls and the catalyst bed. In PO post-reaction reactor, there is visible coke formation on the reactor walls as well as the catalyst bed in the reactor and coke formation was observed on the catalyst powder during both SR and PO. But in the ATR post-reaction reactor, there is no visible coke formation on the reactor walls and the catalyst bed. After 25 hours of reaction under the same ATR conditions, a slight darkening of the catalyst was observed; however, the extent looks similar to the ATR 5h-run. These results are amenable to the conclusion that during the ATR on this catalyst, there is much less carbon formation than during the SR and PO reactions.

Figure 30. Post reaction profiles of RNCZA catalysts with reactors for visible inspection a) Steam reforming after 5h, b)Partial Oxidation after 5h, c) Autothermal reforming after 5h and d) Autothermal reforming after 25h (Catalyst reduction at 600 ^{0}C for 2 h; reaction conditions: Temp: 700 ^{0}C; GHSV: 217000 h^{-1}; H_2O/C: 2; O/C=0.35)

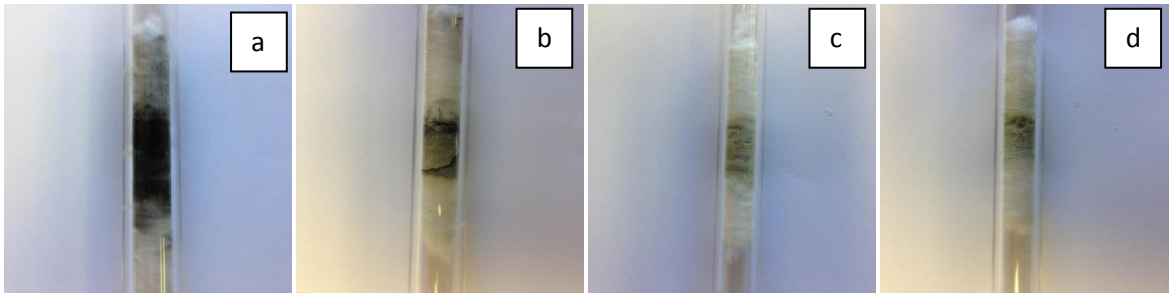

IV.G.4. TPO results for coke formation

Temperature Programmed oxidation (TPO) experiments were performed on used RNCZA catalysts to study the types of carbon deposited on the surface of the catalyst and the extent of carbon formation during the ATR reaction of isobutanol. TPO was carried out in the same system and the same procedure was used as discussed earlier.

Figure 31. TPO profiles of RNCZA catalysts a) RNCZA5h and b) RNCZA25h

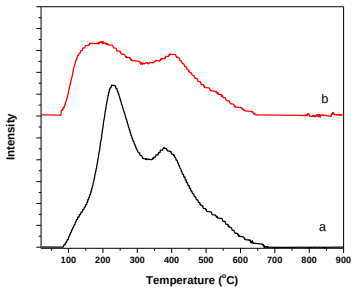

TPO results of the used RNCZA catalysts are presented in figure 31. In the TPO results, in RNCZA catalyst with 5h and 25h-use, there are only low-temperature carbon peaks, which correspond to different types of coke formation on the catalyst surface indicated by their TPO patterns. In RNCZA-5h catalyst, TPO pattern has one broad peak centered at 227 ^{0}C and a small hump at 377 ^{0}C with total carbon deposited being 24.6 mg/g catalyst (i.e., 2.4% in 5h). These low temperature peaks represent adsorbed

acidic coke on the support (Ce-Zr-Al-O), and onset of the polymeric carbon species, respectively. In RNCZA-25h catalyst TPO, one broad peak with T_{max} at 126-199 and a hump with T_{max} at 395 ^{0}C are observed, representing adsorbed carbon, acidic coke deposition and polymeric carbon deposits. The TPO pattern indicates that the adsorbed carbon and acidic coke formation are higher than the formation of polymeric carbon. In the 5h-run, acidic and polymeric coke formation are more. Carbon deposition during the 5h-run is higher compared to the 25h-run due to in-situ reduction and oxidation increasing the redox capability of metal oxides, which in turn increases the oxygen mobility on the surface of the catalyst. Therefore, the formation of the first type of carbon is enhanced resulting in a decrease in the carbon formation on the RNCZA-25h catalyst to 15 mg/g of catalyst (i.e. 1.5% in 25h). Our SEM, TEM and XRD results support these deductions. All these observations clearly indicate the formation of amorphous adsorbed carbon the surface of the catalysts.

V. Cobalt-Based catalysts

V.A. Preparation of Co-based Catalysts

The preparation of Co-based catalysts for the evaluation of the ATR of n-Dodecane was also undertaken. The typical procedure follows as described below.

a) For 10wt% Co/Al_2O_3 (CoA): A known amount of ATSB was dissolved in warm ethanol at 70 ^{0}C with vigorous stirring. For the partial hydrolysis of the aluminum precursor, small amounts of nitric acid and distilled water (40% nitric acid) solution, which had been mixed with ethanol, were slowly added to the solution containing the aluminum precursor, and stirred for 10 min at room temperature; the mixture was, then, transferred to a flat bottom 250 mL flask. Then, the desired amount of cobaltous acetate was added slowly into the solution containing the aluminum precursor, and stirred for 30 min at room temperature. Subsequently, the temperature was raised to 80 ^{0}C and kept there for 2 h under vigorous stirring. The resulting clear solution was then cooled to room temperature with vigorous stirring. A transparent gel was formed after a few minutes by adding a few drops of water diluted with ethanol to the solution. After aging the gel for 2 days with covering and 2 days as exposed to air, it was dried in an oven at 50 ^{0}C by mixing it at regular intervals to form a powder. The resulting xerogel was calcined step by step, i.e. at 150 ^{0}C for 30 min, at 300 ^{0}C for 30 min, and finally at 500 ^{0}C for 5 hours in air.

b) For 10wt% Co/3wt% CeO_2/Al_2O_3(CoCA): A known amount of ATSB was dissolved in warm ethanol at 70 ^{0}C with vigorous stirring. For the partial hydrolysis of the aluminum precursor, small amounts of nitric acid and distilled water (40% nitric acid) solution, which had been mixed with ethanol, were slowly added to the solution containing the aluminum precursor, and stirred for 10 min at room temperature; the mixture was, then, transferred to a flat bottom 250 mL flask. Then, the desired amounts of cerium ammonium nitrate and cobaltous acetate were added sequentially into the solution containing the aluminum precursor, and stirred for 30 min at room temperature. Subsequently, the temperature was raised to 80 ^{0}C and kept there for 2 h under vigorous stirring. The resulting clear solution was then cooled to room temperature with vigorous stirring. A transparent gel was formed after a few minutes by adding a few drops of water diluted with ethanol to the solution. After aging the gel for 2 days with covering and 2 days as exposed to air, it was dried in an oven at 50 ^{0}C by mixing it at regular intervals to form a powder. The resulting xerogel was calcined step by step, i.e. at 150 ^{0}C for 30 min, at 300 ^{0}C for 30 min, and finally at 500 ^{0}C for 5 hours in air.

c) For 10wt% Co/ZrO_2/Al_2O_3(CoZA): A known amount of ATSB was dissolved in warm ethanol at 70 ^{0}C with vigorous stirring. For the partial hydrolysis of the aluminum precursor, small amounts of nitric acid and distilled water (40% nitric acid) solution, which had been mixed with ethanol, were slowly added to the solution containing the aluminum precursor, and stirred for 10 min at room temperature Then, the desired amounts of zirconium (IV) butoxide (atomic ratio equivalent to cerium in CoCZA catalyst) and cobaltous acetate were added into the solution containing the aluminum precursor, and stirred for 30 min at room temperature. Subsequently, the temperature was raised to 80 ^{0}C and kept there for 2 h under vigorous stirring. The resulting clear solution was then cooled to room temperature with vigorous stirring. A transparent gel was formed after a few minutes by adding a few drops of water diluted with ethanol to the solution. After aging the gel for 2 days with covering and 2 days as exposed to air, it was dried in an oven at 50 ^{0}C by mixing it at regular intervals to form a powder. The resulting xerogel was calcined step by step, i.e. at 150 ^{0}C for 30 min, at 300 ^{0}C for 30 min, and finally at 500 ^{0}C for 5 hours in air.

d) For 10wt% Co/Ce(3wt%)O_2/ZrO_2/Al_2O_3(CoCZA): A known amount of ATSB was dissolved in warm ethanol at 70 ^{0}C with vigorous stirring. For the partial hydrolysis of the aluminum precursor, small amounts of nitric acid and distilled water (40% nitric acid) solution, which had been mixed with ethanol, were slowly added to the solution containing the aluminum precursor, and stirred for 10 min at room temperature; the mixture was, then, transferred to a flat bottom 250 mL flask. Then, the desired amounts of zirconium (IV) butoxide (atomic ratio of cerium to zirconium is kept at 1), cerium ammonium nitrate and cobaltous acetate were added sequentially into the solution containing the aluminum precursor and stirred for 30 min at room temperature. Subsequently, the temperature was raised to 80 ^{0}C and kept there for 2 h under vigorous stirring. The resulting clear solution was then cooled to room temperature with vigorous stirring. A transparent gel was formed after a few minutes by adding a few drops of water diluted with ethanol to the solution. After aging the gel for 2 days with covering and 2 days as exposed to air, it was dried in an oven at 50 ^{0}C by mixing it at regular intervals to form a powder. The resulting xerogel was calcined step by step, i.e. at 150 ^{0}C for 30 min, at 300 ^{0}C for 30 min, and finally at 500 ^{0}C for 5 hours in air.

e) For 0.3wt% Ru/10wt% Ni/Ce(3wt%)O_2/ZrO_2/Al_2O_3(RCoCZA): A known amount of ATSB was dissolved in warm ethanol at 70 ^{0}C with vigorous stirring. For the partial hydrolysis of the aluminum precursor, small amounts of nitric acid and distilled water (40% nitric acid) solution, which had been mixed with ethanol, were slowly added to the solution containing the aluminum precursor, and stirred for 10 min at room temperature; the mixture was, then, transferred to a flat bottom 250 mL flask. Then, the desired amounts of zirconium (IV) butoxide (atomic ratio of cerium to zirconium is kept at 1), cerium ammonium nitrate, cobaltous acetate and ruthenium chloride were added sequentially into the solution containing the aluminum precursor and stirred for 30 min at room temperature. Subsequently, the temperature was raised to 80 ^{0}C and kept there for 2 h under vigorous stirring. The resulting clear solution was then cooled to room temperature with vigorous stirring. A transparent gel was formed after a few minutes by adding a few drops of water diluted with ethanol to the solution. After aging the gel for 2 days with covering and 2 days as exposed to air, it was dried in an oven at 50 ^{0}C by mixing it at regular intervals to form a powder. The resulting xerogel was calcined step by step, i.e. at 150 ^{0}C for 30 min, at 300 ^{0}C for 30 min, and finally at 500 ^{0}C for 5 hours in air.

V.B. Surface area

Measurements of the surface area of cobalt(Co)-based catalysts were carried out in the Chembet Pulsar instrument and the results are presented in table 5. The CoA catalyst has higher surface area compared to the other xerogel catalysts. The surface areas decreased from CoCA to RCoCZA, respectively, due to the addition of metal precursors in the catalyst matrix. This might be due to crystallite growth process being accelerated by the incorporation of Ce, Zr, and Ru ions into the mixed oxide catalysts; and also, the rearrangement of Ce due to its interaction with the other precursors, affecting the dispersion of the active metal.

Table 5. Surface areas of Co-based catalysts

Catalyst	**BET Surface area (m^2/g)**
CoA	445.2
CoCA	400.45
CoZA	402.72
CoCZA	365.28
RCoCZA	358.4

V.C. Primary Screening

In primary screening, we tested the CoA and RCoCZA catalysts at a standard condition (same as those obtained from the previous results from the ATR of dodecane), i.e. at 750 ^{0}C, catalyst amount of 75 mg, O/C=0.35 and H_2O/C=2. The results are presented in Figure 32. The main reaction products obtained were H_2, CO, CO_2, CH_4 and other hydrocarbons (C2-C4). CoA catalysts showed no activity as in the case of the blank test. RCoCZA catalysts initially showed low activity, but time-on-stream yield of H_2 and extent of reforming increased eventually to 0.85 and 0.63, respectively. This indicates that in-situ reduction of the RCoCZA catalyst occurred with time-on-stream, resulting in the increase in ATR activity with time-on-stream. These observations indicated that the reduction procedure used during the preparation of the cobalt catalysts was not sufficient; therefore, the reduction temperature and time were varied, i.e. 400 ^{0}C for 5h; 600 ^{0}C for 2h; 400 ^{0}C for 10h; and 600 ^{0}C for 5h. These attempts did not result in an increased activity in the CoA catalysts. For the RCoCZA catalyst, the prolonged reduction time (i.e., 600 ^{0}C for 5h) resulted in higher initial hydrogen yield and extent of reforming as 1 and 0.8, respectively; but with time-on-stream after 5 hours, these values decreased to 0.48 and 0.43, respectively. These observations may be interpreted that the activity of these cobalt catalysts is due only to the promotion by Ru, because Co atoms are dispersed very well in the support matrix, and therefore, are not completely available for reduction, thus, mostly remaining inactive for the reforming reaction. It is well-known that cobalt is difficult to reduce and a promoter, like ruthenium, is needed to facilitate its reduction. Therefore, especially with the sol-gel method of preparation used in this project, it may be needed to increase the content of ruthenium in these cobalt catalysts.

Figure 32. Extent of reforming and product yields during the autothermal reforming of n-Dodecane. (Catalyst reduction at 600 ^{0}C for 2 h; reaction conditions: temp: 750 ^{0}C; GHSV: 220000 h^{-1}; H_2O/C: 2.0; O/C: 0.35)

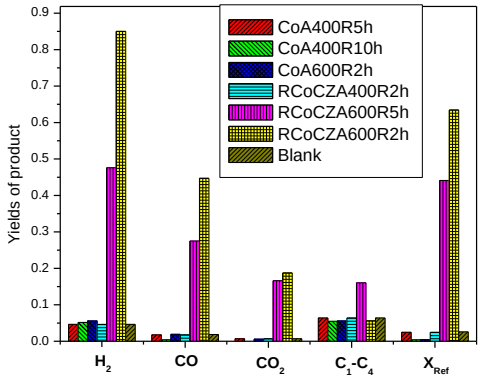

VI. Autothermal Reforming of JP-8 on Nickel Catalysts – Results and Discussion

Autothermal reforming of JP-8 over NCZA and RNCZA catalysts was undertaken at the operating conditions that were obtained from the optimization of n-Dodecane ATR reaction. The results are presented in figure 33. One reason for the low hydrogen yield must be sulfur poisoning. With 0.3wt% Ru promotion, the initial H_2 yield is higher (0.2) than that on the NCZA catalyst (0.15) and the blank test (0.06). With time-on-stream, i.e. after 5 hours of reaction, hydrogen yield decreased to 0.06, 0.11 and 0.09 for blank, NCZA and RNCZA catalysts, respectively. The CO yields were high on the two catalysts and the blank test; but CO_2 yield increased on both the RNCZA and NCZA catalysts due to oxygen mobility on the support (Ce-Zr-O) compared to the blank test. On the RNCZA catalyst, methanation products are high because of methanation being promoted by ruthenium. NCZA catalyst exhibited better stable activity for ATR of JP-8 compared to the RNCZA catalyst. Naomi et. al., with 125 ppm of sulfur in JP8 with Pt /Rh monolith catalysts achieved similar results[30].

In the post-reaction analysis of RNCZA and NCZA catalysts, reactors are presented in figure 34. It may be observed from the figure that appreciable coke formation took place on the RNCZA catalyst compared to the NCZA due to better oxygen mobility of the support in the latter catalyst. Also, cracking of the polymeric products were observed at the exit end of the reactor.

Figure 33. Extent of reforming and product yields during the autothermal reforming of JP-8. (For NCZA and Blank- Catalyst reduction at 600 ^{0}C for 2 h; reaction conditions: temp: 750 ^{0}C; GHSV: 220000 h^{-1}; H_2O/C: 2.0; O/C: 0.35; For RNCZA- Catalyst reduction at 600 ^{0}C for 2 h; reaction conditions: temp: 700 ^{0}C; GHSV: 220000 h^{-1}; H_2O/C: 2.0; O/C: 0.35)

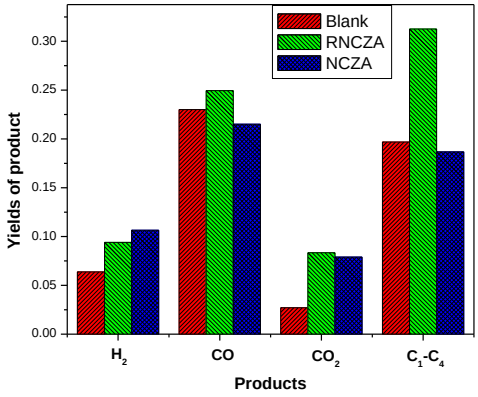

Figure 34. ATR reactors of JP-8 after 5h duration a) NCZA b)RNCZA

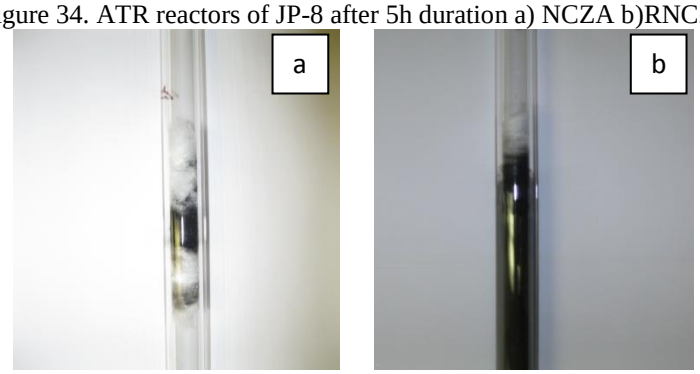

VII. Contribution to Undergraduate Engineering Education

One of the goals of this project is integration of research into education. To fulfill this goal, five minority undergraduate engineering students worked on the project. They were taught to prepare catalysts by the sol-gel process, to operate instruments for characterization of the catalysts and to perform the ATR experiments.

In the first year of the project, Ms. Rhonda Jack, a chemical engineering senior; Ms. Brittany Henderson, a chemical engineering sophomore; and Ms. Dinah Holland, a chemical engineering sophomore, worked on the project. They prepared Ni/Silica catalysts based on a 2^3 factorial experimental design; and repeated the experiments to enable statistical analysis of the results. They evaluated the effect of the preparation variables, namely, water/TEOS ratio, alcohol/TEOS ratio, and temperature on the BET surface area of the catalysts. Based on the results of this work, Ms. Rhonda Jack made a presentation at the NOBCChE (The National Organization for the Professional Advancement of Black Chemists and Chemical Engineers) 38th National Conference held in Houston, TX on April 19-22, 2011. The paper was entitled 'Synthesis and Characterization of Nickel-Silica Aerogels Using Sub-Critical Drying'. The co-authors of the paper were Brittany Henderson, Dinah Holland (both chemical engineering sophomores), Jale Akyurtlu and V.P.K. Mangalampalli. Ms. Jack graduated in May 2011, and is a graduate student at

the University of Michigan working towards a Ph.D. degree in chemical engineering. Ms. Henderson and Ms. Holland graduated in May 2013.

Since fall 2011, Mr. Julian Braithwaite, and Mr. Joshua Gopeesingh, both chemical engineering undergraduates, are working on the project. They continued with the work started by the three undergraduates during the previous year. They also participated in the ATR experiments and measurements of surface area on the Quantachrome ChemBETPulsar equipment, and of porosity on the Micromeritics 2020 equipment.

Mr. Gopeesingh participated in the MSRP program at MIT during Summer 2012 as a research student; he presented a poster entitled "Modeling of an Industrial Hydrotreating Process for Diesel Production under Uncertainty" based on the research he worked on at MIT. Mr. Brathwaite worked as a summer undergraduate researcher in Columbia University in Summer 2012. In Summer 2013, Mr. Gopeesingh was an undergraduate researcher at the Syracuse University and Mr. Brathwaite at MIT. They will graduate in May 2014; and are applying to graduate schools to obtain their Ph.D. degrees in chemical engineering. They are continuing to work on the measurement of the surface areas of their catalysts. They will make a presentation on their results at the 2014 AIChE Mid-Atlantic Regional Conference to be held at the University of Virginia on March 28-30, 2014. Then, we plan to publish it in the journal 'Chemical Engineering Education'.

Figure 35. (a)Mr. Brathwaite operating the Micromeritics 2020 porosimeter; (b)Mr. Gopeesingh operating the Quantachrome ChemBETPulsar Surface Analyzer; (c) Mr. Gopeesingh operating the ATR setup

(a)

(b)

(c)

VIII. Technology Transfer

There was interaction with Dr. Ivan Lee at the Army Research Laboratory. Dr. Lee's expertise includes fuel reformation, fuel chemistry, nanomaterials, catalysis and surface science. These are areas common to this project. Upon his recommendation, we tested our catalysts extensively for the reforming of isobutanol. He visited our laboratories and gave a seminar entitled 'Portable Power Sources with Biofuel: Catalytic Conversion of Butanol' on September 30, 2011 at Hampton University. During the visit, we discussed the areas of further cooperation.

Based on this discussion, we dip-coated NCA, NCZA and RNCZA sols on the alumina monoliths that Dr. Ivan Lee sent us. The sols were prepared as described in section I.A. He will use them as

catalysts for the ATR reforming of JP-8 at the Army Research Laboratory. The experimentation was delayed at ARL due to some equipment failure. It is planned to make a publication based on that study.

IX. Conclusions

Ni-based catalysts are prepared by using the Sol-Gel method, resulting in all the metal precursors being well-dispersed in the catalyst matrix. All the catalysts have high BET surface area and mesoporous pore size. XRD patterns indicate an amorphous nature of the fresh catalysts. Addition of metal oxides in the catalyst matrix reduced the reduction temperature of the catalyst appreciably. SEM and TEM images exhibit the uniform distribution of the metal oxides in the solid matrix and their nano-size nature. Active metal (Ni) dispersion and metal area increased with the addition of metal oxides in the matrix, increasing the availability of active Ni atoms for the reaction. Among the prepared Ni-based catalysts, NCZA catalyst produced higher hydrogen yield and less methanation products for the ATR of n-Dodecane, a surrogate of JP8 fuel. NCZA catalyst was active during a 50h run, and low coke formation indicated that this catalyst is highly stable and has a long life under the optimized operating conditions, namely, a temperature of $750^{O}C$, a space velocity of $220000h^{-1}$, an O/C ratio of 0.35 and a H_2O/C ratio of 2. Used catalysts are characterized extensively to support the results from the ATR, SR and POx reactions. The results from characterization confirm that coke formation is appreciable in SR and POx of n-dodecane, while it is very low in the case of ATR of n-dodecane. XRD, SEM and TEM patterns of the used catalysts indicate that the morphological features of the catalysts have not changed appreciably, supporting the previous observation that the catalysts are very stable and remained active during 50 hours of operation.

RNCZA catalyst was found to be the best compared to the other Ni-based catalysts for the ATR of isobutanol. The optimum conditions for the autothermal reforming of isobutanol are a temperature of $700\ ^{O}C$, a space velocity of $217000h^{-1}$, an O/C ratio of 0.35 and a H_2O/C ratio of 2. The catalyst was stable during a 25h-run with low coke formation. After the long run, the morphology and features of the catalyst did not change appreciably.

Co-based catalysts were also prepared by the sol-gel method. They were found to be very hard to reduce, mainly, since the sol-gel method used for preparation results in Co being dispersed very homogeneously within the support matrix. However, Co catalysts exhibited very high BET surface areas. RNCZA and NCZA catalysts were tested for the ATR of JP-8, but due to the high sulfur content of JP-8, the catalysts deactivated within 3 hours. Among the developed catalysts, NCZA catalyst was proven to undergo less coking and to exhibit high stability for the ATR of n-Dodecane and JP-8.

The autothermal reforming of n-dodecane was studied in great detail during the project. Also, based on the recommendation of Dr. Ivan Lee of the US Army Research Laboratory, these catalysts were studied extensively for the ATR of isobutanol, which is regarded as a promising raw material for hydrogen production for fuel cells. This put time constraints on the section of the project when cobalt catalysts and the ATR of JP8 were investigated. Therefore, our recommendation to complete a study on cobalt catalysts and make them operable for ATR of dodecane is to undertake a comprehensive systematic study by varying several variables, such as the calcination temperature, ruthenium content, several preparation variables, and reduction temperature and time. With respect to the ATR of JP8, our observations may be explained with a systematic study on the effects of sulfur, aromatics and a consortium of higher hydrocarbons on the ATR along with dodecane over these catalysts.

X. Outcomes of the project

- 3 paper presentations at Annual AICHE conferences; one presentation at 23rd NAM
- One publication in a refereed journal
- Will submit two research articles to refereed journals
- Will apply for a patent on NCZA catalyst for the ATR of n-Dodecane.

X.A. Papers and Presentations:

1. G. Vidya Sagar, M.V. Phanikrishna Sharma, J. F. Akyurtlu, A. Akyurtlu, H_2 production by autothermal reforming of n-dodecane over highly active Ru−Ni−Ce−Al_2O_3 catalyst, Industrial & Engineering Chemistry Research, 52 (2013) 338−345.
2. R. Jack, B. Henderson, D. Holland, J. Akyurtlu and M.V. Phanikrishna Sharma, 'Synthesis and Characterization of Nickel-Silica Aerogels Using Sub-Critical Drying', presented at the NOBCChE (The National Organization for the Professional Advancement of Black Chemists and Chemical Engineers) 38th National Conference held in Houston, TX on April 19-22, 2011.
3. M.V. Phanikrishna Sharma, Jale Akyurtlu, Ates Akyurtlu, 'Autothermal Reforming of n-Dodecane over Promoted Nickel Xerogel Catalysts', accepted for presentation at the 2011 AIChE Annual Meeting at Minneapolis, MN, October 16-21, 2011.
4. M.V. Phanikrishna Sharma, Jale Akyurtlu, Ates Akyurtlu, Autothermal Reforming of Dodecane Over Ni-Based Sol-Gel Catalysts, presented at the 2012 AIChE Annual Meeting at Pittsburg, PA, October 28-November 2, 2012.
5. M.V. Phanikrishna Sharma, Jale Akyurtlu, Ates Akyurtlu, Autothermal Reforming of n-Dodecane for Fuel-Cell Applications – Nickel Based Xerogel Catalysts for Activity, Stability and Coking Studies, accepted for presentation at 23rd NAM (North American Catalysis Society) meeting at Louisville, Kentucky, June 2-7, 2013.
6. M.V. Phanikrishna Sharma, Jale Akyurtlu, Ates Akyurtlu, Oxidative Steam Reforming of Iso-Butanol Over Promoted Nickel Xerogel Catalysts, accepted for presentation at the 2013 AIChE Annual Meeting at San Francisco, CA, November 3-8, 2013.
7. M.V. Phanikrishna Sharma, Jale Akyurtlu, Ates Akyurtlu, Autothermal reforming of n-dodecane over alumina, ceria, zirconia-supported nickel catalysts for the hydrogen production for fuel cell applications, International Journal of Hydrogen energy (to be submitted) 2013.
8. M.V. Phanikrishna Sharma, Jale Akyurtlu, Ates Akyurtlu, Autothermal reforming of isobutanol over ruthenium-promoted nickel catalysts, International Journal of Hydrogen energy (to be submitted) 2014.

X.B. Patent:

Sol-Gel mediated Ce-Zr-Al-supported Ni catalyst for dodecane autothermal reforming for clean hydrogen production, to prevent coking, US patent to be applied in 2014.

D. REFERENCES

1. M.V. P. Sharma, V. Durga Kumari and M. Subrahmanyam, TiO_2 supported over porous silica photocatalysts for pesticide degradation using solar light: Part 2. Silica prepared using acrylic acid emulsion, J. Hazard. Mater., 175 (2010) 1101-1105.
2. A.Cabañas, E. Enciso, M.C. Carbajo, M.J. Torralvo, C. Pando and J.A.R. Renuncio, Synthesis of ordered macroporous SiO2 in supercritical CO2 using 3D-latex array templates, Chem. Commun.20 (2005), pp. 2618–2620.
3. J.F.S. Bitencourt, A. Ventieri, K.A. Gonçalves, E.L. Pires, J.C. Mittani and S.H. Tatumi, A comparison between neodymium doped alumina samples obtained by Pechini and sol–gel methods using thermo-stimulated luminescence and SEM, J. Non-Crystal. Sol.356 (2010) 2956-2959.
4. H-S. Roh, K-W. Jun, W-S. Dong, J-S. Chang, S-E. Park, Y-I. Joe, Highly active and stable Ni/Ce–ZrO_2 catalyst for H_2 production from methane, J. Mol. Catal A: Chem., 181(2002) 137–142.
5. J. Ashok, G. Raju, P. S. Reddy, M. Subrahmanyam and A. Venugopal, Catalytic decomposition of CH_4 over NiO–Al_2O_3–SiO_2 catalysts: Influence of catalyst preparation conditions on the production of H_2, Int. J. Hydrogen Energy, 33 (2008) 4809-4818.
6. A. Valentini, N.L.V. Carreno, L.F.D. Probst, A. Barison, A.G. Ferreira, E.R. Leite, E. Longo, Ni:CeO_2 nanocomposite catalysts prepared by polymeric precursor method, Appl. Catal. A: Gen., 310 (2006) 174–182.
7. S.J. Hana, Y. Bang, J.G. Seo, J. Yoo , I.K. Song, Hydrogen production by steam reforming of ethanol over mesoporous Ni/Al_2O_3/ZrO_2 xerogel catalysts: Effect of Zr/Al molar ratio, Int. J. Hydrogen Energy, 38 (2013) 1376-1383.
8. V.Modafferi, G. Panzera, V. Baglio, F. Frusteri and P. L. Antonucci, Propane reforming on Ni-Ru/GDS catalyst: H2 production for IT-SOFCs under SR and ATR conditions, Appl. Catal. A: Gen., 334 (2008) 1– 9.
9. G. Vidya Sagar, J. Akyurtlu, A. Akyurtlu and I. Blankson, Steam Reforming of *n*-Dodecane over Ru−Ni-Based Catalysts, *Ind. Eng. Chem. Res.*,49 (2010) 8164–8173.
10. S. Nateskahawat, O. Oktar, U.S. Ozkan, Effect of Lanthanide Promotion on Catalytic Performance of Sol-Gel Ni/Al_2O_3 Catalysts in Steam Reforming of Propane, J. Mol. Catal., 241 (2005) 133.
11. C.H. Bartholomew, R.B. Pannell, Support and Crystallite Size Effects in CO hydrogenation on Nickel. J. Catal. 65 (1980) 335.
12. M.F. Garcıa, A.M. Arias, J.C. Hanson, J.A. Rodriguez, Nanostructured Oxides in Chemistry: Characterization and Properties, *Chem. Rev*. 104 (2004) 4063-4104.
13. L.F. Liotta, A. Longo, G. Pantaleo, G. Di Carlo, A. Martorana, S. Cimino, G. Russo and G. Deganello, Alumina supported Pt(1%)/$Ce_{0.6}Zr_{0.4}O_2$ monolith: Remarkable stabilization of ceria–zirconia solution towards $CeAlO_3$ formation operated by Pt under redox conditions, *Appl. Catal., B,* 90 (2009) 470–477.
14. T.F. Silva, J.A.C. Dias, C.G. Maciela, J.M. Assafa Ni/Al_2O_3 catalysts: effects of the promoters Ce, La and Zr on the methane steam and oxidative reforming reactions, *Catal. Sci. Technol.*, 3 (2013) 635-643.
15. H-S. Roh, I-H. Eum, D-W. Jeong, Low temperature steam reforming of methane over Ni-$Ce_{(1-x)}Zr_{(x)}O_2$ catalysts under severe conditions, *Renewable Energy*, 42 (2012) 212-216.

16. Z. Kowalczyk, K. Stołecki, W. R-Pilecka, E. Mis´kiewicz, E. Wilczkowska and Z. Karpinski, Supported ruthenium catalysts for selective methanation of carbon oxides at very low CO_x/H_2 ratios, *Appl. Catal. A: Gen.,* 342 (2008) 35–39.
17. B. D. Gould, X. Chen and J. W. Schwank, Dodecane reforming over nickel-based monolith catalysts, *J. Catal.*, 250 (2007) 209-221.
18. D.M. Walker, S.L. Pettit, J.T. Wolan, J.N. Kuhn, Synthesis gas production to desired hydrogen to carbon monoxide ratios by tri-reforming of methane using Ni–MgO–$(Ce,Zr)O_2$ catalysts, *Appl. Catal. A: Gen.* 445–446 (2012) 61–68.
19. T. L. Barr, S. Seal, Nature of the use of adventitious carbon as a binding energy standard, J. Vac. Sci. Technol. A. 13 (1995) 1239.
20. T.I.T. Okpalugo, P. Papakonstantinou, H. Murphy, J. McLaughlin, N.M.D. Brown, High resolution XPS characterization of chemical functionalized MWCNTs and SWCNTs, Carbon 43 (2005) 153–161.
21. A. Bratt, A. R. Barron, XPS of Carbon nanomaterials, Connexions module: m34549, http://cnx.org/content/m34549/1.2/
22. J. Z. Shyu, W. H. Weber, H. S. Gandhi, Surface Characterization of Alumina-Supported Ceria, J. Phys. Chem. 92 (1988) 4964.
23. F. Larachi, J. Pierre, A. Adnot, A. Bernis, Ce 3d XPS study of composite $Ce_xMn_{1\_x}O_{2\_y}$ wet oxidation catalysts, Applied Surface Science 195 (2002) 236
24. H. Li, J. Wang, Study on CO_2 reforming of methane to syngas overAl_2O_3–ZrO_2 supported Ni catalysts prepared via a direct sol–gel process, Chem. Eng. Science, 59 (2004) 4861 – 4867.
25. Y.Song, H. Liu, S. Liu, D. He, Partial Oxidation of Methane to Syngas over Ni/Al_2O_3 Catalysts Prepared by a Modified Sol-Gel Method, Energy & Fuels, 23 (2009) 1925–1930.
26. B.D. Gould, X. Chen, J.W. Schwank, n-Dodecane reforming over nickel-based monolith catalysts: Deactivation and carbon deposition, Appl. Catal. A: Gen. 334 (2008) 277–290.
27. K. Urasaki, Y. Sekine, S. Kawabe, E. Kikuchi, M. Matsukata, Catalytic activities and coking resistance of Ni/perovskites in steam reforming of methane, Appl. Catal. A: Gen. 286 (2005) 23–29.
28. M.C. Seemann, T.J. Schildhauer, S.M.A. Biollaz, S. Stucki, A. Wokaun, The regenerative effect of catalyst fluidization under methanation conditions, Appl. Catal. A: Gen. 313 (2006) 14–21.
29. C.H. Bartholomew, Mechanisms of catalyst deactivation, Appl. Catal. A: Gen. 212 (2001) 17–60.
30. N.B. Klinghoffer, F. Barrai, M.J. Castaldi, Autothermal reforming of JP8 on a Pt/Rh catalyst: Catalyst durability studies and effects of sulfur, J. Power Sources 196 (2011) 6374–6381
31. T.G. DuBois, S. Nieh, Selection and performance comparison of jet fuel surrogates for autothermal reforming, Fuel 90 (2011) 1439–1448.

E. APPENDIX

Table 1. Surface area, average pore diameter, cumulative pore volume, T_{max} of TPR peak, metal dispersion and active metal area of catalysts

Catalyst	Surface area (m^2/g)	Average Diameter (Å)	Cumulative pore volume (cm^3/g)	TPR-peak T_{max} (^0C)	H_2 desorbed (□mol/g)	Metal dispersion (Ni - %)	Active metal area (Ni-m^2/g)
NA	417.44	54.43	0.749	826.1	180.66	10.6	7.1
NCA	380.25	58.33	0.598	750.2	210.98	12.4	8.3
NZA	395.12	-	-	709.2	213.89	12.6	8.4
NCZA	375.06	47.15	0.583	695.8	226.12	13.3	8.8
RNCZA	364.94	49.79	0.567	574	236.94*	13.9*	9.3

*- cumulative Ni and Ru

Table 2. SEM-EDAX analysis of fresh and used NCZA (1:1) catalysts.

NCZA	Element	wt%	Atomic%	Ce/Zr (atomic)
Fresh	O K	54.26	66.99	
	Al K	32.07	24.37	
	Ni K	8.09	4.23	
	Zr L	2.48	2.20	
	Ce L	3.10	2.19	0.99
Used 5h	O K	46.84	60.41	
	Al K	35.36	28.16	
	Ni K	9.99	5.49	
	Zr L	3.63	3.02	
	Ce L	4.20	2.94	0.97
Used 50h	C K	2.29	4.06	
	O K	44.89	59.88	
	Al K	41.16	32.55	
	Ni K	7.63	2.76	
	Zr L	1.55	0.36	
	Ce L	2.49	0.38	1.05

Table 3. Carbon deposit on used NCZA and RNCZA catalysts

	Carbon amount	
	□mol/g.cat	mg/g. cat
NCZA5h (O/C=0.35)	1300.06	15.60
NCZA50h (O/C=0.35)	1109.06	13.30
NCZA26h (O/C=0.1)	3339.65	40.07
RNCZA5h (O/C=0.35)	2048.94	24.58
RNCZA25h (O/C=0.35)	1254.93	15.05

Table 4. SEM-EDAX analysis of fresh and used RNCZA catalysts.

RNCZA	Element	Weight%	Atomic%
Fresh	C K	0.20	0.34
	O K	51.43	67.85
	Al K	37.21	29.1
	Ni K	7.10	2.68
	Ru K	0.19	0.06
	Ce L	2.31	0.53
	Zr L	2.05	0.31
5h used	C K	1.77	3.042
	O K	48.39	63.73
	Al K	37.72	29.53
	Ni K	7.58	2.732
	Ru K	0.21	0.15
	Ce L	1.98	0.46
	Zr L	2.35	0.36
25h used	C K	3.44	5.86
	O K	46.36	60.7
	Al K	37.97	29.7
	Ni K	7.37	2.79
	Ru K	0.26	0.08
	Ce L	2.3	0.53
	Zr L	2.3	0.35

Table 5. Surface areas of Co-based catalysts

Catalyst	Surface area (m^2/g)
CoA	445.2
CoCA	400.45
CoZA	402.72
CoCZA	365.28
RCoCZA	358.4

Figure 1. Experimental Setup

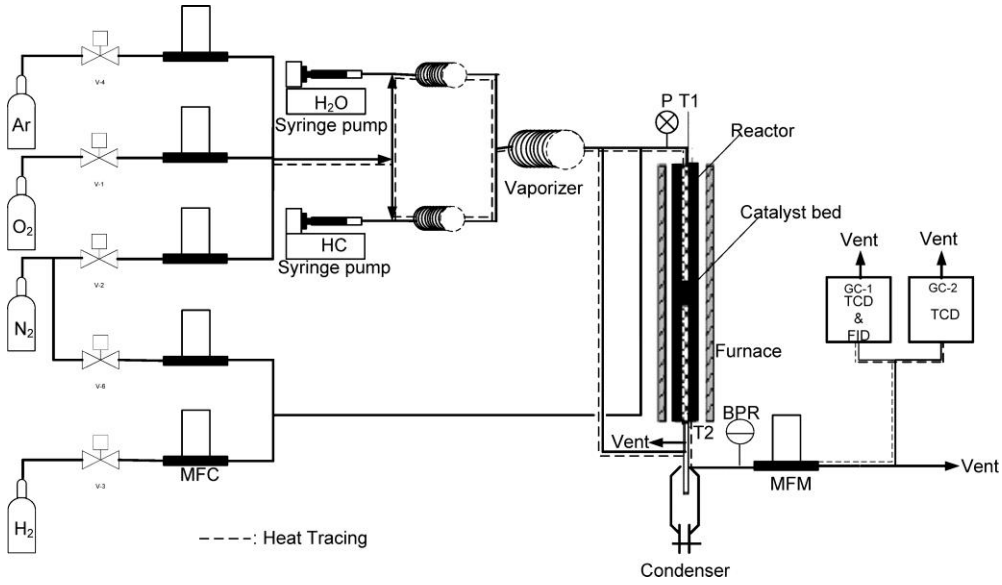

Figure 2. N_2 adsorption-desorption isotherms of Ni-based catalysts; inset: Pore size distribution curves

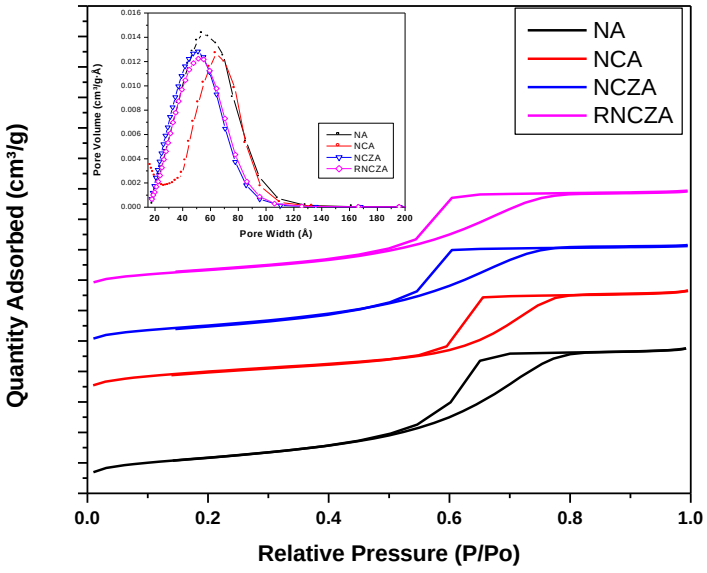

Figure 3. XRD patterns of Ni-based catalysts

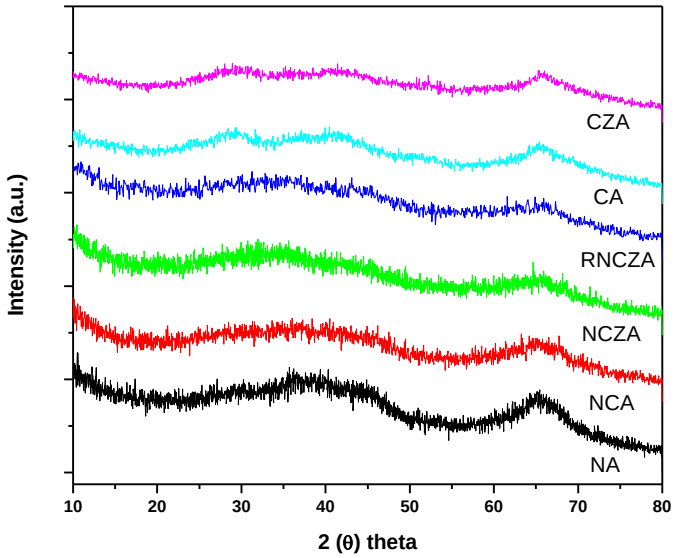

Figure 4. SEM photographs of a) NA b) NCA C) NZA d) NCZA and d) RNCZA

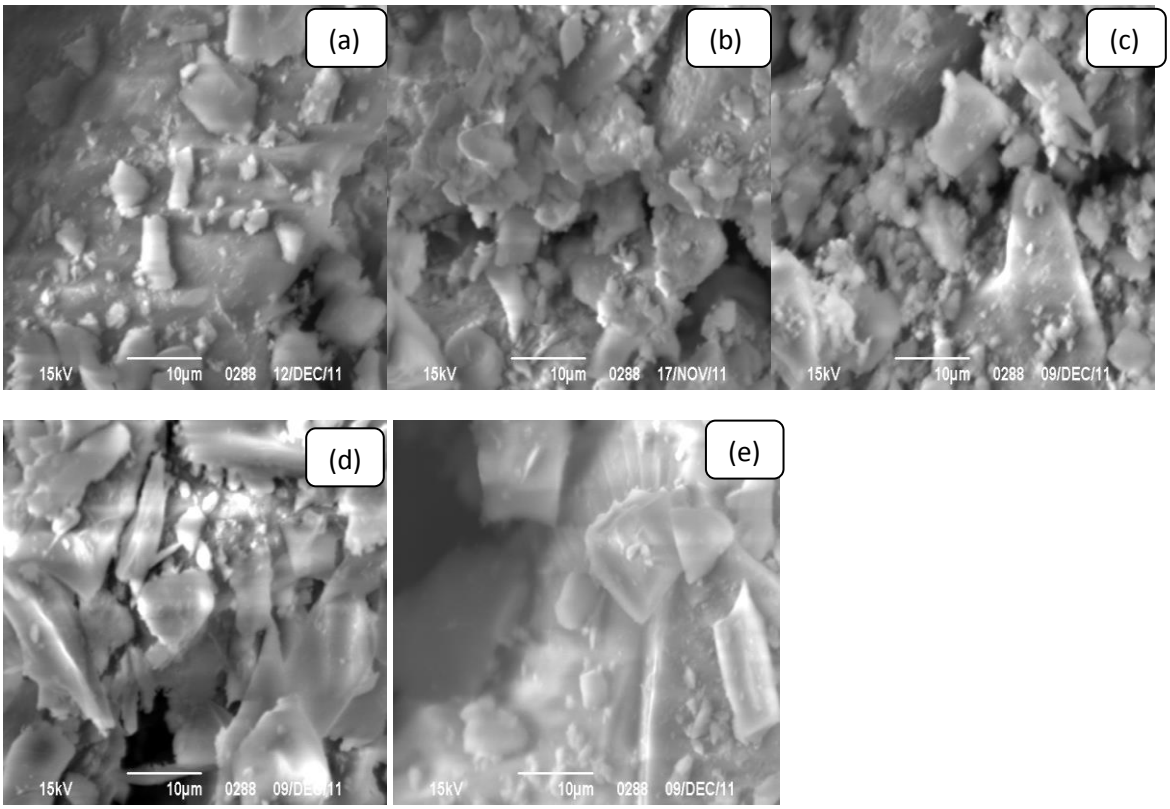

Figure 5. TPR profiles of Ni-based catalysts

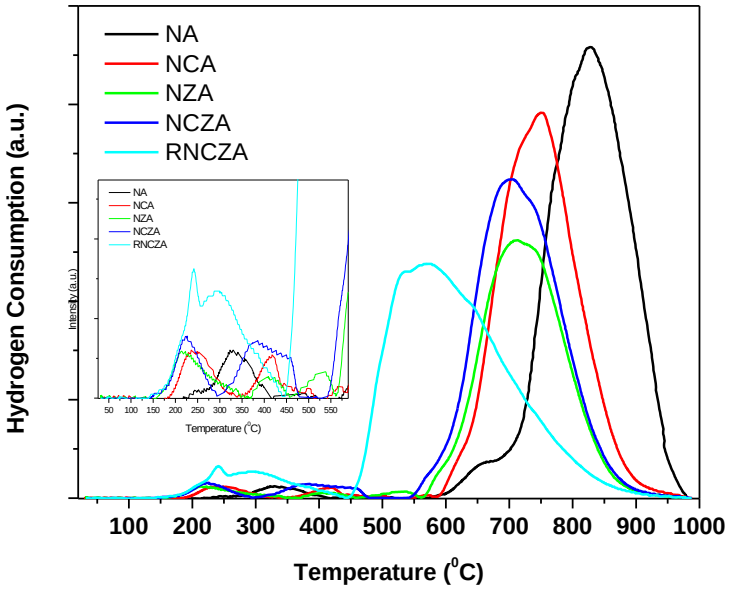

Figure 6. Extent of reforming and product yields during the autothermal reforming of n- dodecane over catalysts. (Catalyst reduction at 600 ^{0}C for 2 h; reaction conditions: temp: 800 ^{0}C; GHSV: 220000 h^{-1}; H_2O/C: 2.0; O/C: 0.35)

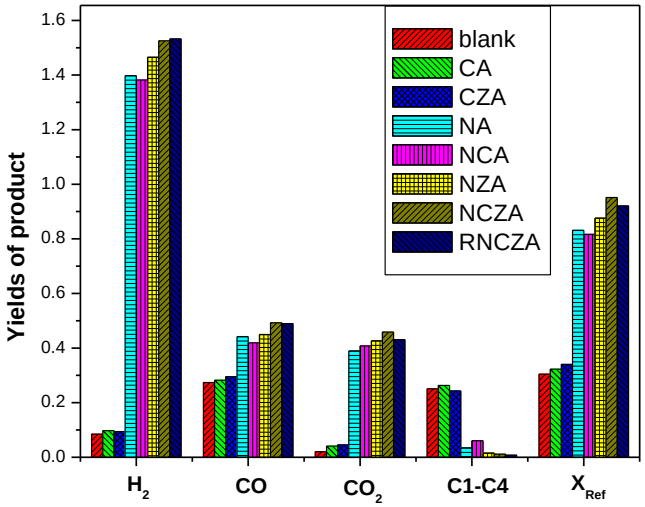

Figure 7. Extent of reforming and product yields during the autothermal reforming of n- dodecane on NCZA catalyst at different temperatures. (Catalyst reduction at 600 ^{0}C for 2 h; reaction conditions: GHSV: 220000 h^{-1}; H_2O/C: 2.0; O/C: 0.35)

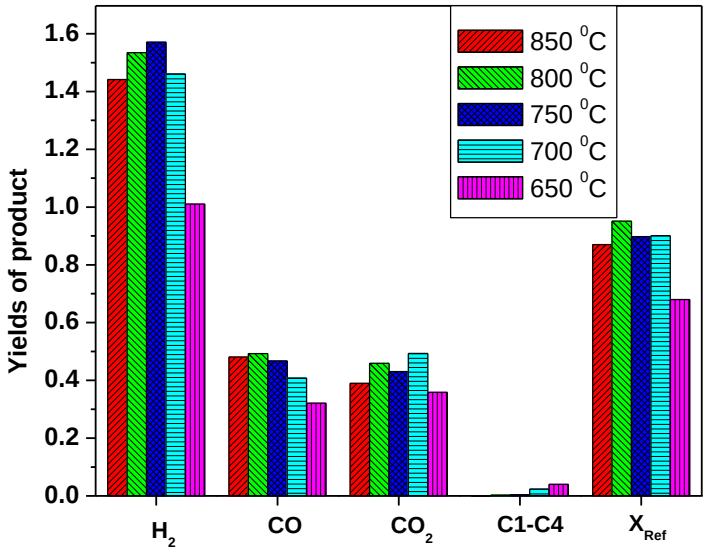

Figure 8. Extent of reforming and product yields during the autothermal reforming of n- dodecane on NCZA catalyst at different GHSVs. (Catalyst reduction at 600 ^{0}C for 2 h; reaction conditions: Temp: 750 ^{0}C; H_2O/C: 2.0; O/C: 0.35)

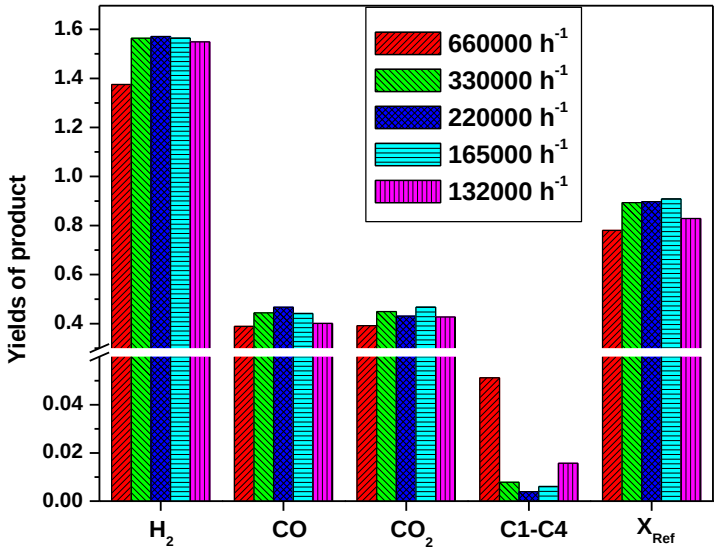

Figure 9. Extent of reforming and product yields during the autothermal reforming of n- dodecane on NCZA catalyst at different H_2O/C ratios. (Catalyst reduction at 600 ^{0}C for 2 h; reaction conditions: Temp: 750 ^{0}C; GHSV: 220000 h^{-1}; O/C: 0.35)

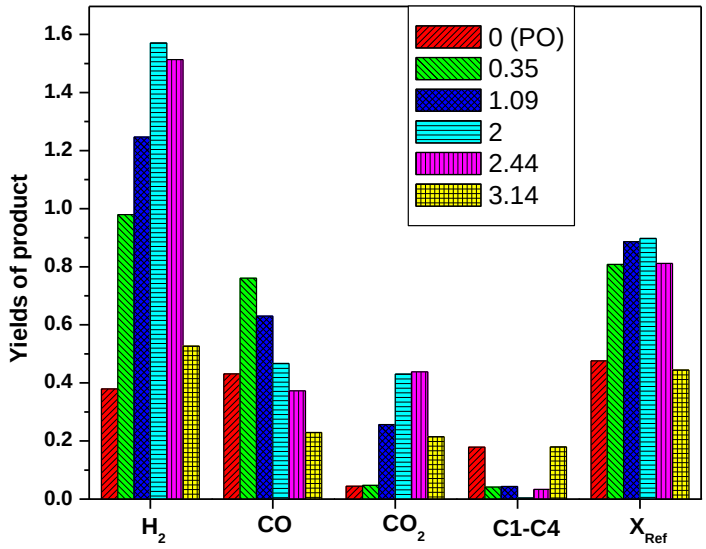

Figure 10. Extent of reforming and product yields during the autothermal reforming of n- dodecane on NCZA catalyst at different O/C ratios. (Catalyst reduction at 600 ^{0}C for 2 h; reaction conditions: Temp: 750 ^{0}C; GHSV: 220000 h^{-1}; H_2O/C: 2)

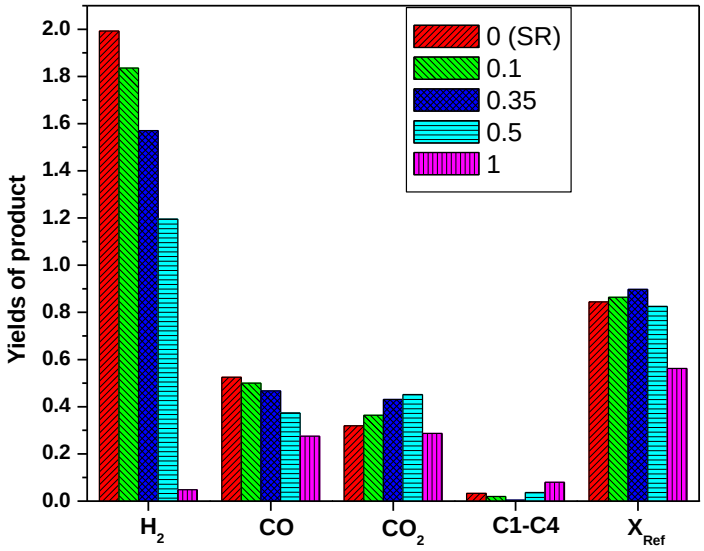

Figure 11. Extent of reforming and product yields during the auto thermal reforming of n- dodecane on NCZA catalyst at different Ce/Zr ratios. (Catalyst reduction at 600 ^{0}C for 2 h; reaction conditions: Temp: 750 ^{0}C; GHSV: 220000 h^{-1}; H_2O/C: 2; O/C : 0.35)

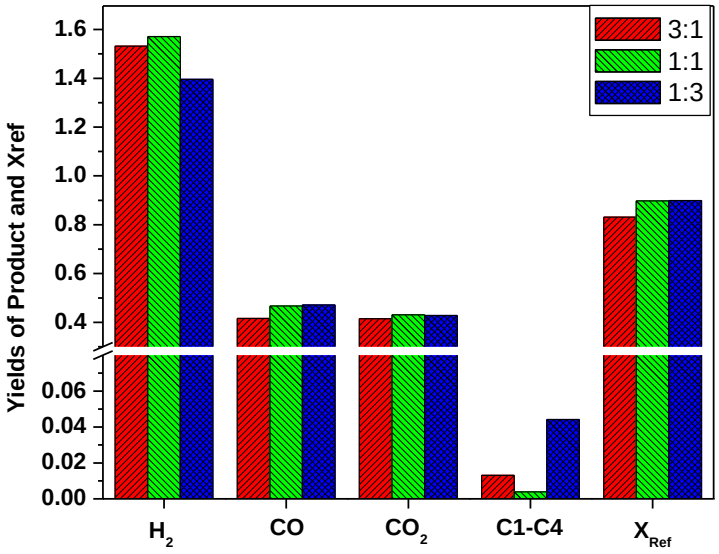

Figure 12. Extent of reforming and product yields during the autothermal reforming of n-dodecane on NCZA catalyst for long run. (Catalyst reduction at 600 ^{0}C for 2 h; reaction conditions: Temp: 750 ^{0}C; GHSV: 220000 h^{-1}; H_2O/C: 2; O/C: 0.1)

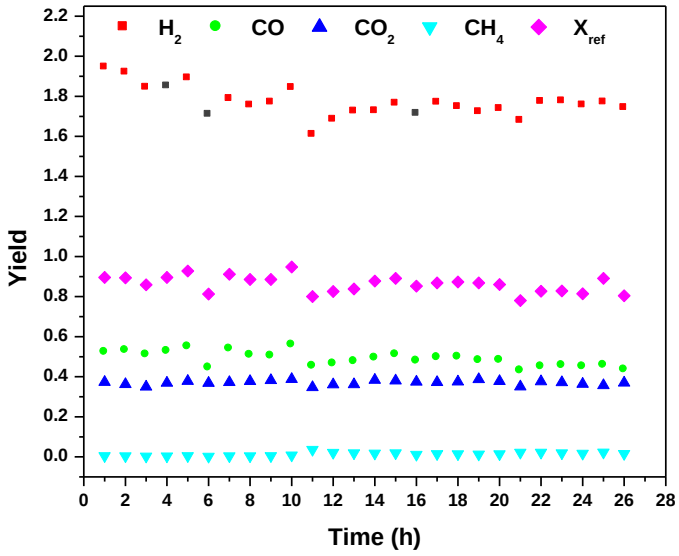

Figure 13. Extent of reforming and product yields during the autothermal reforming of n- dodecane on NCZA catalyst for long run. (Catalyst reduction at 600 ^{0}C for 2 h; reaction conditions: Temp: 750 ^{0}C; GHSV: 220000 h^{-1}; H_2O/C: 2; O/C: 0.35)

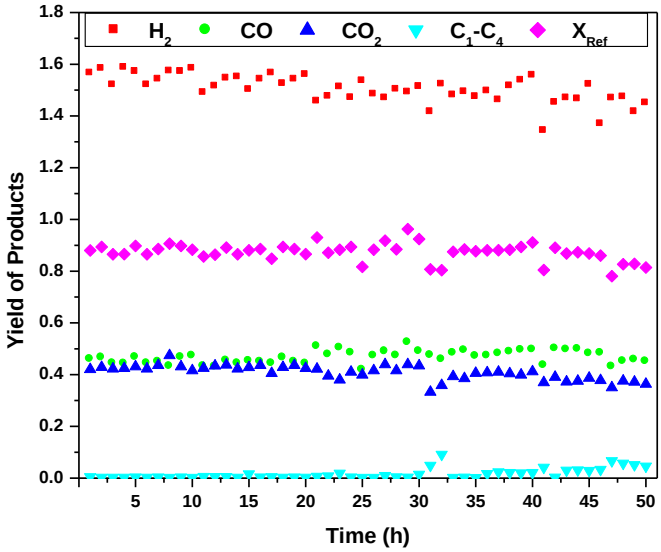

Figure 14. Post reaction profiles of NCZA (C/Z=1:1) catalysts, reactor and beads a) SR after 5h (Catalyst reduction at 600 ^{0}C for 2 h; reaction conditions: Temp: 750 ^{0}C; GHSV: 220000 h^{-1}; H_2O/C: 2); b) PO after 5h (Catalyst reduction at 600 ^{0}C for 2 h; reaction conditions: Temp: 750 ^{0}C; GHSV: 220000 h^{-1}; O/C: 0.35); c) ATR after 5h (Catalyst reduction at 600 ^{0}C for 2 h; reaction conditions: Temp: 750 ^{0}C; GHSV: 220000 h^{-1}; H_2O/C: 2; O/C: 0.35); d) O/C at 0.35 reactor after 50h (Catalyst reduction at 600 ^{0}C for 2 h; reaction conditions: Temp: 750 ^{0}C; GHSV: 220000 h^{-1}; H_2O/C: 2; O/C: 0.35); e) O/C at 0.1 reactor after 26h (Catalyst reduction at 600 ^{0}C for 2 h; reaction conditions: Temp: 750 ^{0}C; GHSV: 220000 h^{-1}; H_2O/C: 2; O/C: 0.1) and f) fresh NCZA catalyst

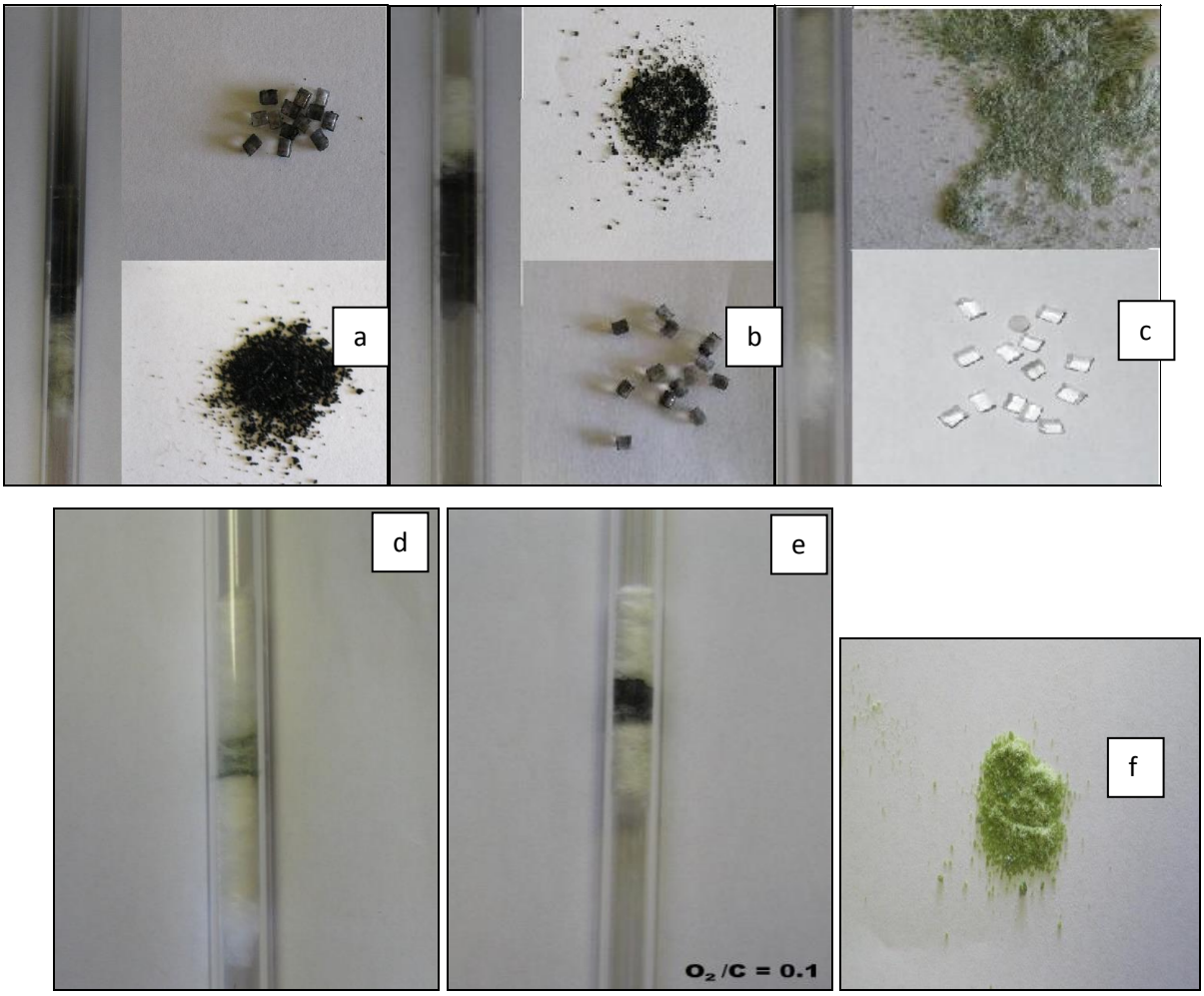

Figure 15. SEM photographs of NCZA catalysts a) fresh, b) used after 5h (Catalyst reduction at 600 ^{0}C for 2 h; reaction conditions: Temp: 750 ^{0}C; GHSV: 220000 h^{-1}; H_2O/C: 2; O/C: 0.35), c) used after 50h (Catalyst reduction at 600 ^{0}C for 2 h; reaction conditions: Temp: 750 ^{0}C; GHSV: 220000 h^{-1}; H_2O/C: 2; O/C: 0.35) and d) used after 26h (Catalyst reduction at 600 ^{0}C for 2 h; reaction conditions: Temp: 750 ^{0}C; GHSV: 220000 h^{-1}; H_2O/C: 2; O/C: 0.1)

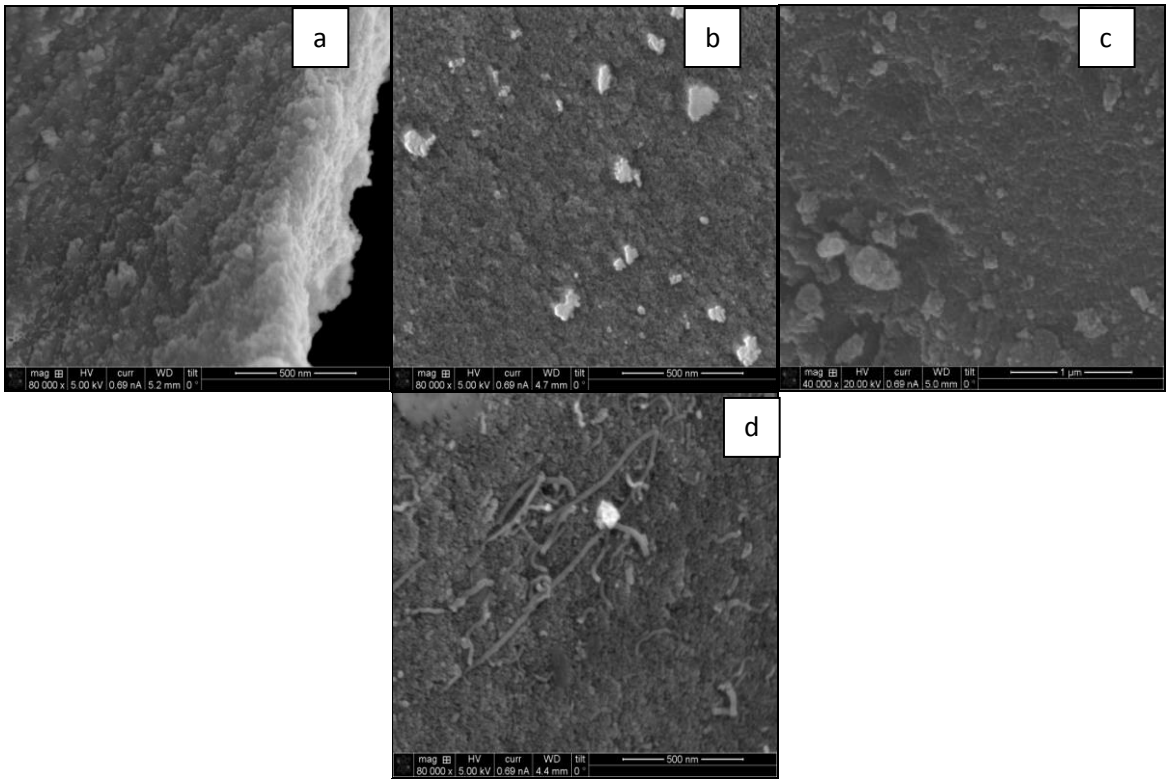

Figure 16. TEM photographs of NCZA catalysts a) fresh, b) used after 5h (Catalyst reduction at 600 ^{0}C for 2 h; reaction conditions: Temp: 750 ^{0}C; GHSV: 220000 h^{-1}; H_2O/C: 2; O/C: 0.35), c) used after 50h (Catalyst reduction at 600 ^{0}C for 2 h; reaction conditions: Temp: 750 ^{0}C; GHSV: 220000 h^{-1}; H_2O/C: 2; O/C: 0.35), d) used after 26h (Catalyst reduction at 600 ^{0}C for 2 h; reaction conditions: Temp: 750 ^{0}C; GHSV: 220000 h^{-1}; H_2O/C: 2; O/C: 0.1) and e) Carbon nanotubes formed in 26h run.

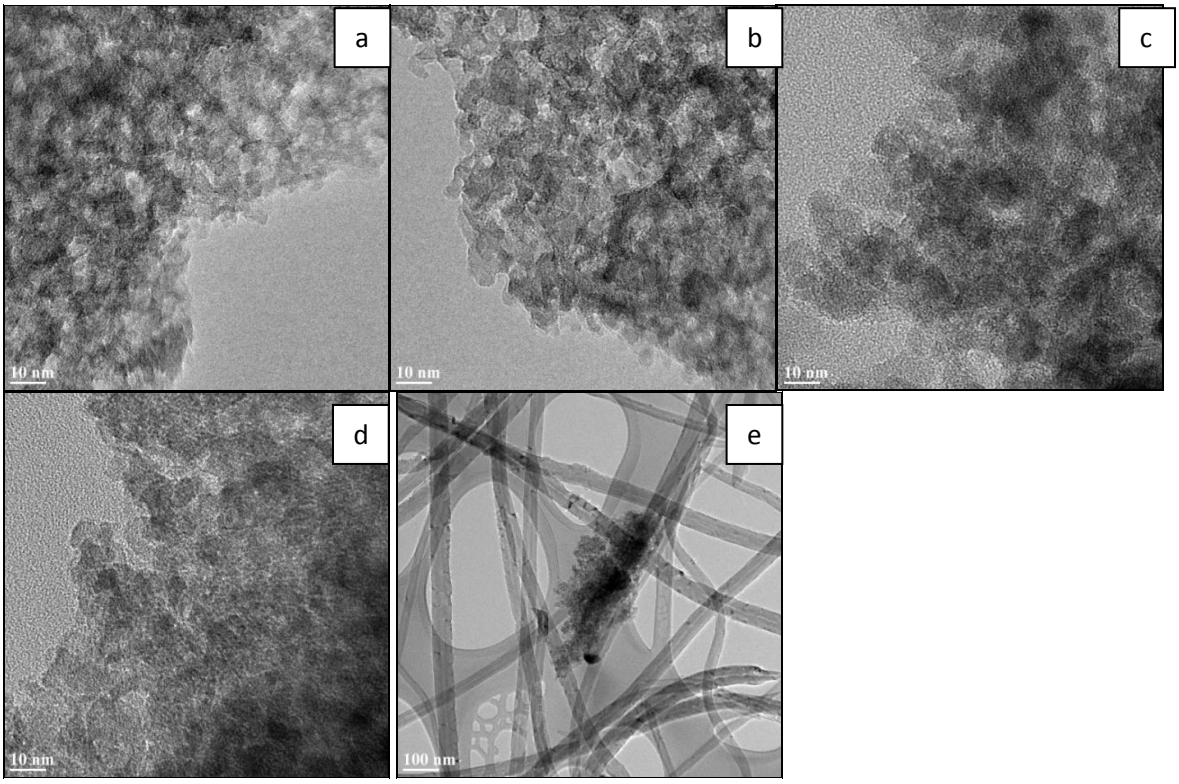

Figure 17. NCZA fresh and used catalysts C1s peaks

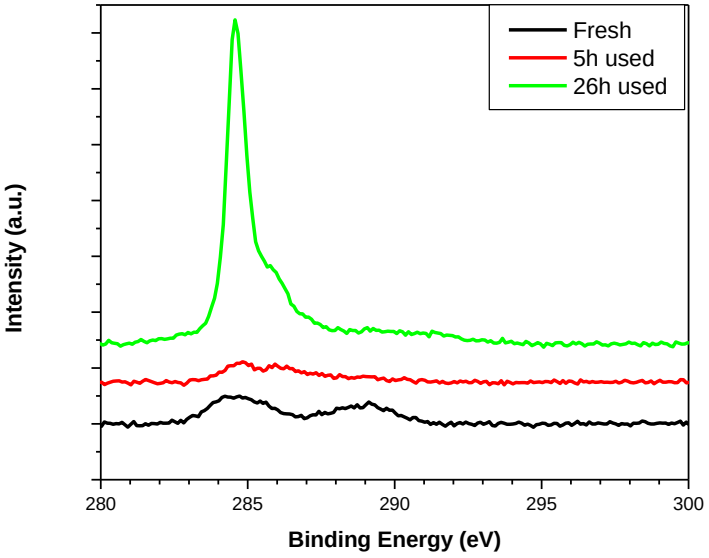

Figure 18. Ni2p and Ce3d peaks of NCZA a) Fresh, b) 5h-used and c) 26h-used catalysts.

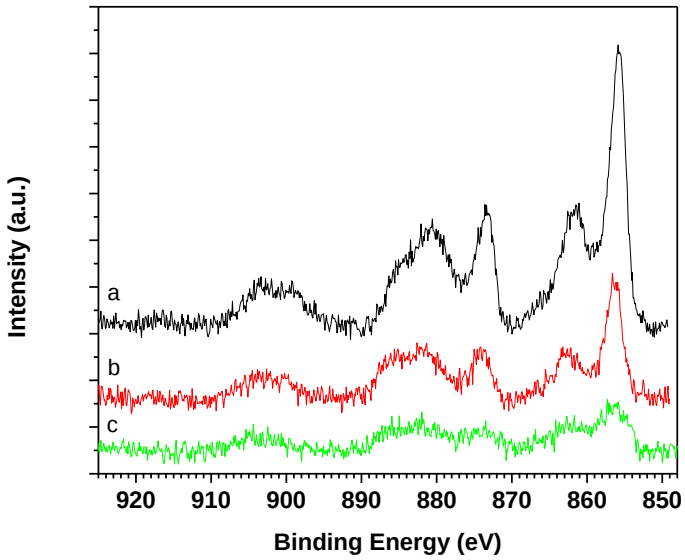

Figure 19. XRD peaks of NCZA a) Fresh, b) used for 5 hours and c) used for 50 hours.

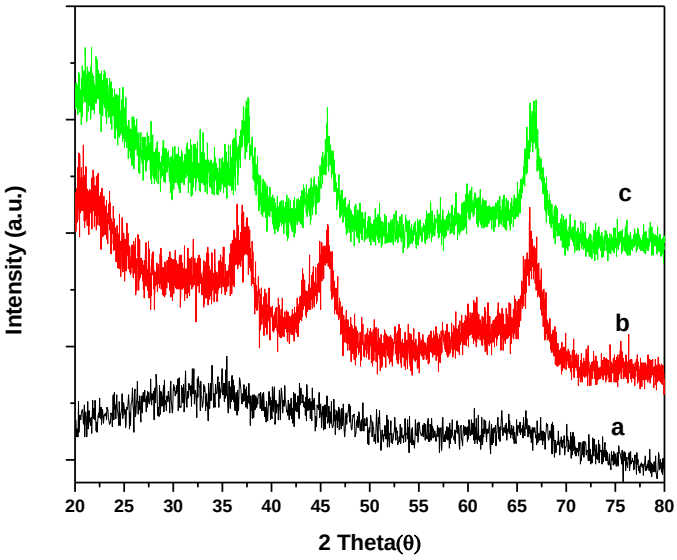

Figure 20. TPO profiles of NCZA catalysts a) NCZA5h (O/C=0.35), b) NCZA50h (O/C=0.35) and c) NCZA26h (O/C=0.1)

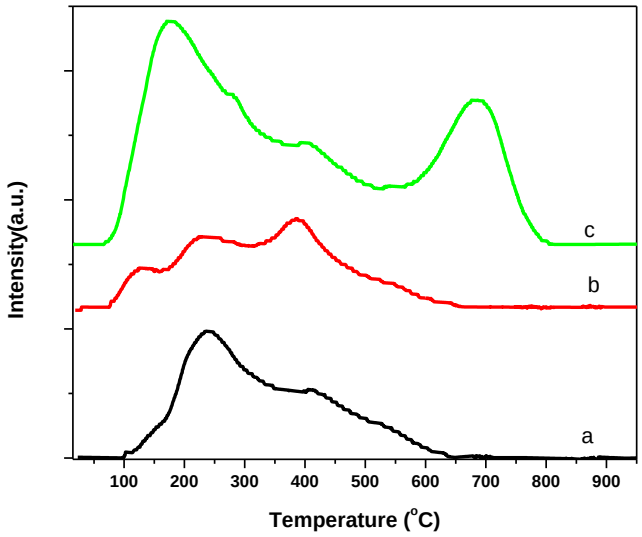

Figure 21. Extent of reforming and product yields during the autothermal reforming of isobutanol. (Catalyst reduction at 600 ^{0}C for 2 h; reaction conditions: temp: 750 ^{0}C; GHSV: 217000 h^{-1}; H_2O/C: 2.0; O/C: 0.35)

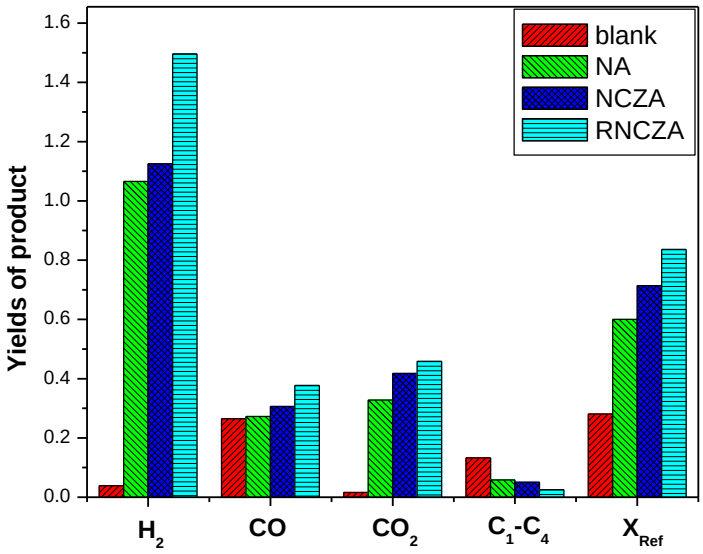

Figure 22. Extent of reforming and product yields during the autothermal reforming of isobutanol on RNCZA catalyst at different temperatures. (Catalyst reduction at 600 ^{0}C for 2 h; reaction conditions: GHSV: 217000 h^{-1}; H_2O/C: 2.0; O/C: 0.35)

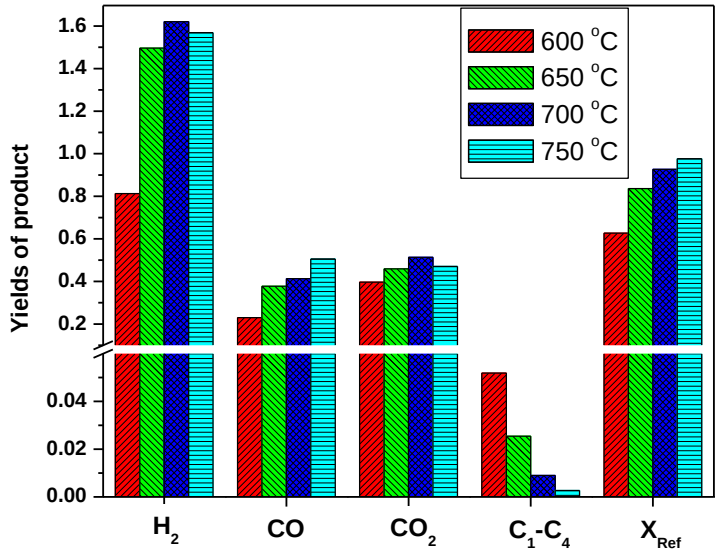

Figure 23. Extent of reforming and product yields during the autothermal reforming of isobutanol on RNCZA catalyst at various GHSVs. (Catalyst reduction at 600 ^{0}C for 2 h; reaction conditions: Temp: 700 ^{0}C; H_2O/C: 2.0; O/C: 0.35)

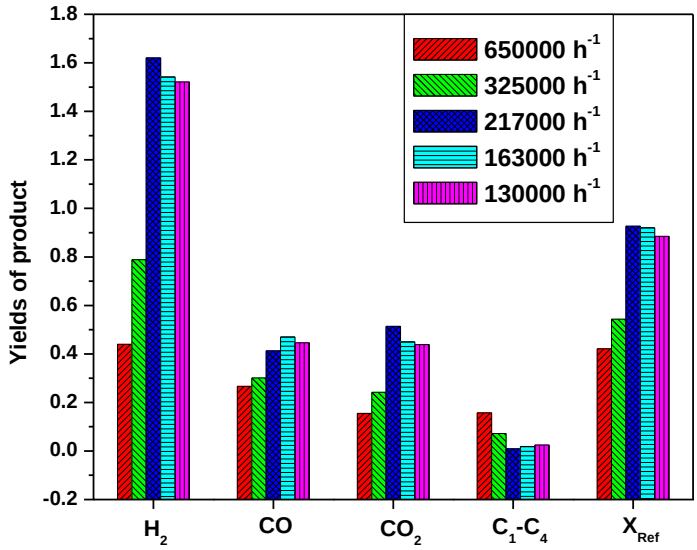

Figure 24. Extent of reforming and product yields during the autothermal reforming of isobutanol on RNCZA catalyst at different H_2O/C ratios. (Catalyst reduction at 600 ^{0}C for 2 h; reaction conditions: Temp: 700 ^{0}C; GHSV: 217000 h^{-1}; O/C: 0.35)

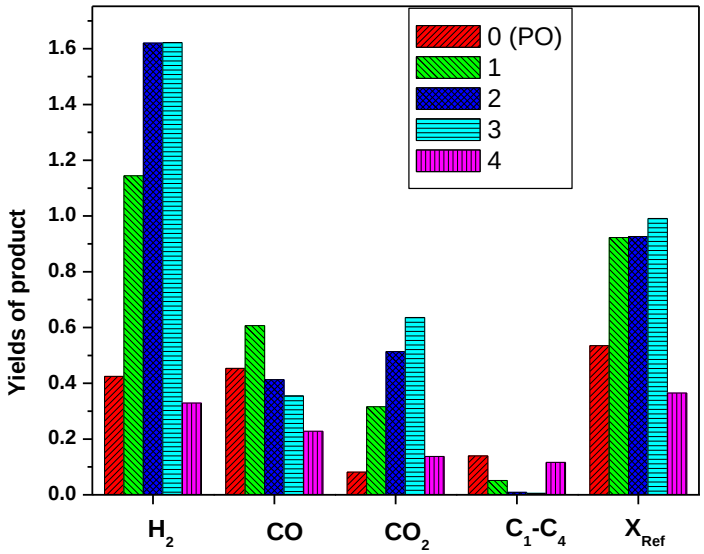

Figure 25. Extent of reforming and product yields during the autothermal reforming of Isobutanol on RNCZA catalyst at different O/C ratios. (Catalyst reduction at 600 ^{0}C for 2 h; reaction conditions: Temp: 700 ^{0}C; GHSV: 217000 h^{-1}; H_2O/C: 2)

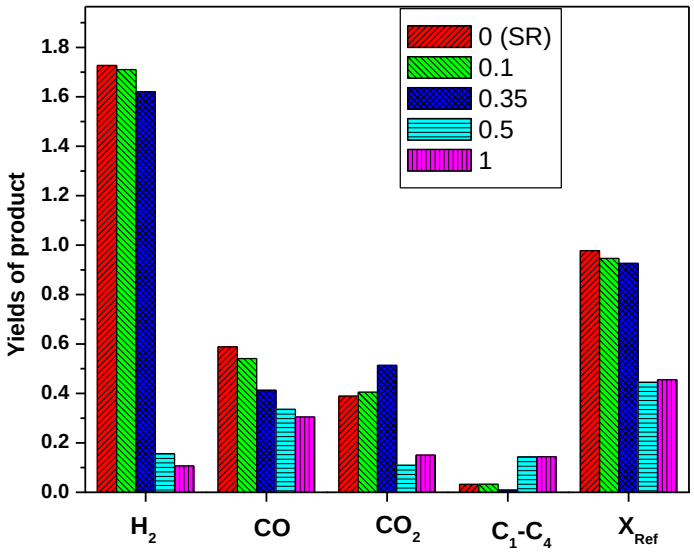

Figure 26. Extent of reforming and product yields during the autothermal reforming of isobutanol on RNCZA catalyst for long run. (Catalyst reduction at 600 ^{0}C for 2 h; reaction conditions: Temp: 700 ^{0}C; GHSV: 217000 h^{-1}; H_2O/C: 2; O/C: 0.1)

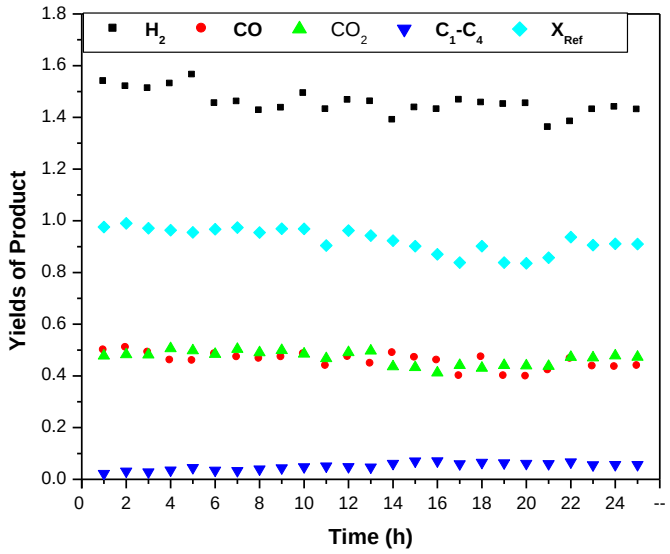

Figure 27. XRD peaks of RNCZA a) Fresh, b) used for 5 hours and c) used for 25 hours.

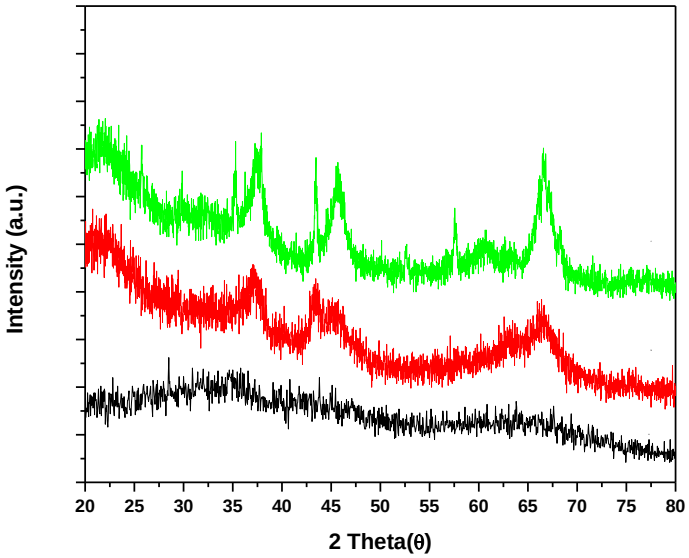

Figure 28. SEM photographs of RNCZA a) Fresh, b) 5h-used and c) 25h-used catalysts

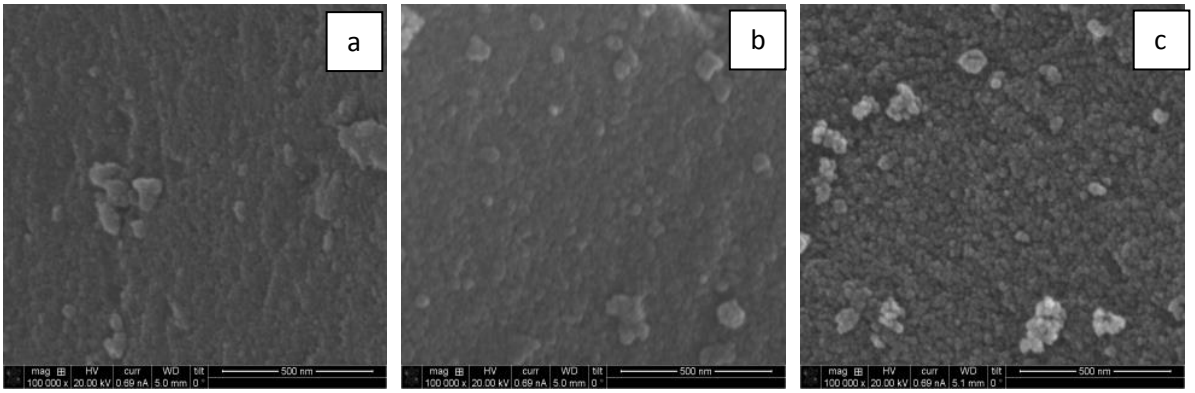

Figure 29. TEM photographs of RNCZA a) Fresh, b) 5h-used and c) 25h-used catalysts

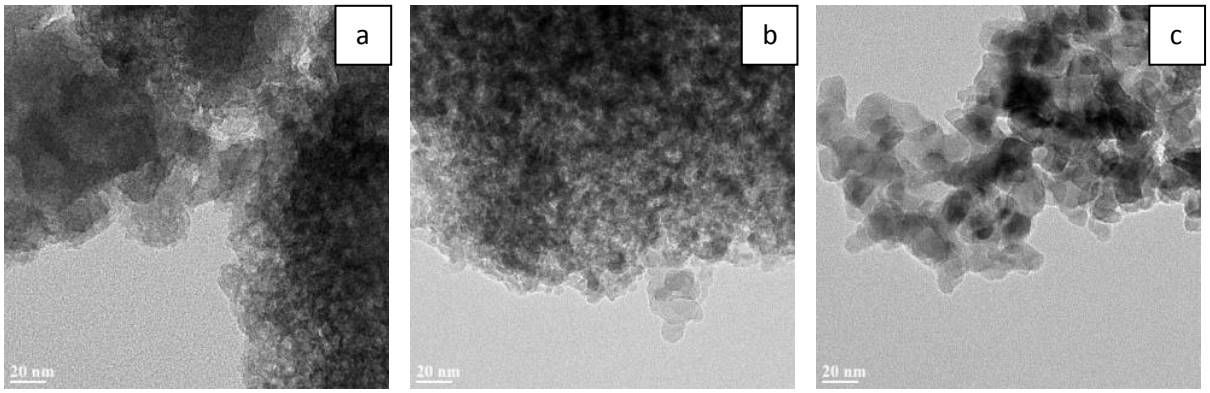

Figure 30. Post reaction profiles of RNCZA catalysts with reactors for visible inspection a) Steam reforming after 5h, b)Partial Oxidation after 5h, c) Autothermal reforming after 5h and d) Autothermal reforming after 25h (Catalyst reduction at 600 ^{0}C for 2 h; reaction conditions: Temp: 700 ^{0}C; GHSV: 217000 h^{-1}; H_2O/C: 2; O/C=0.35)

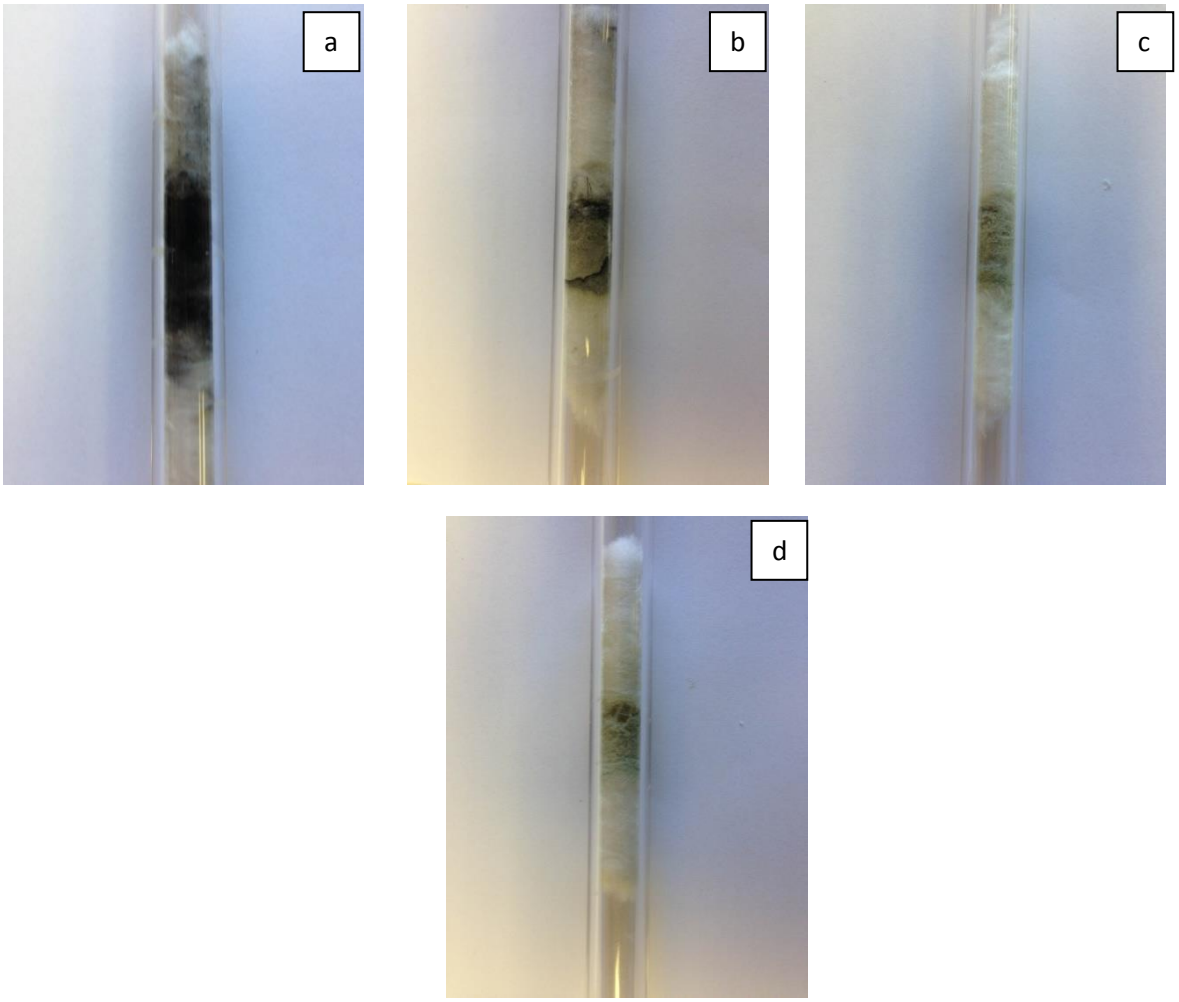

Figure 31. TPO profiles of RNCZA catalysts a) RNCZA5h and b) RNCZA25h

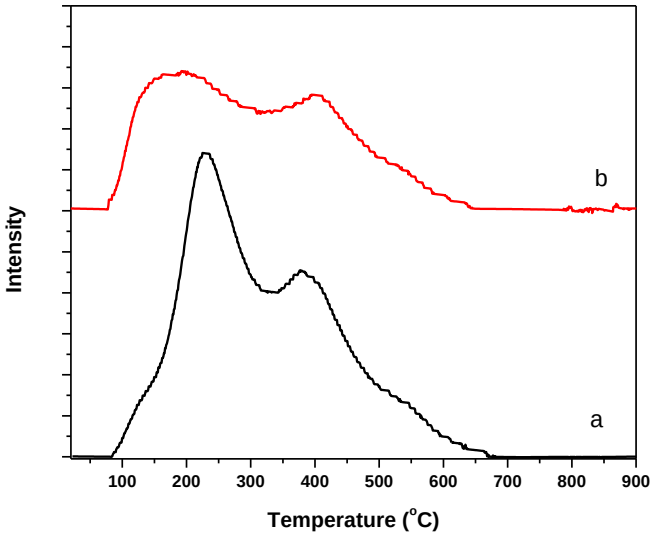

Figure 32. Extent of reforming and product yields during the autothermal reforming of n-dodecane. (Catalyst reduction at 600 ^{0}C for 2 h; reaction conditions: temp: 750 ^{0}C; GHSV: 220000 h^{-1}; H_2O/C: 2.0; O/C: 0.35)

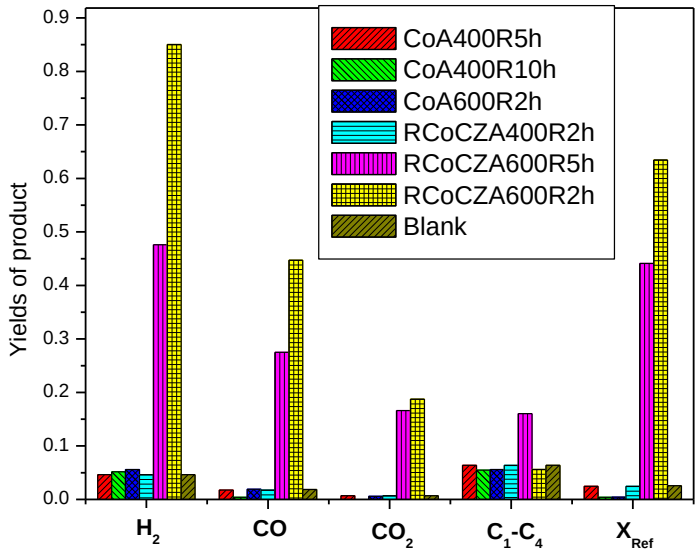

Figure 33. Extent of reforming and product yields during the autothermal reforming of JP-8. (For NCZA and Blank- Catalyst reduction at 600 ^{0}C for 2 h; reaction conditions: temp: 750 ^{0}C; GHSV: 220000 h^{-1}; H_2O/C: 2.0; O/C: 0.35; For RNCZA- Catalyst reduction at 600 ^{0}C for 2 h; reaction conditions: temp: 700 ^{0}C; GHSV: 220000 h^{-1}; H_2O/C: 2.0; O/C: 0.35)

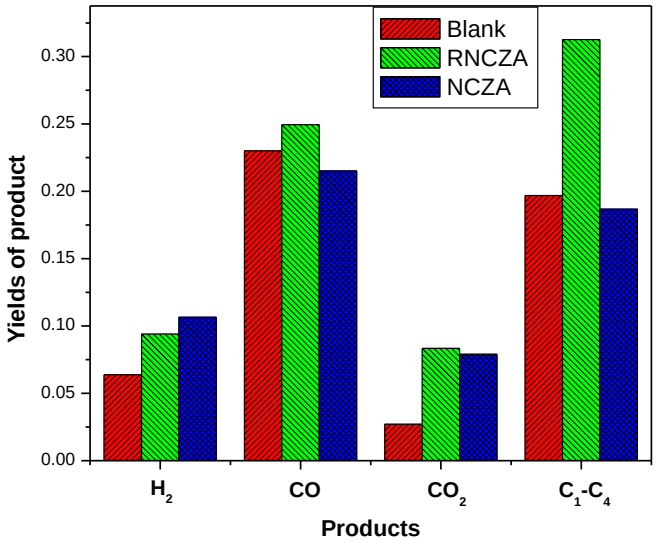

Figure 34. ATR reactors of J-P8 after 5h duration a) NCZA b)RNCZA

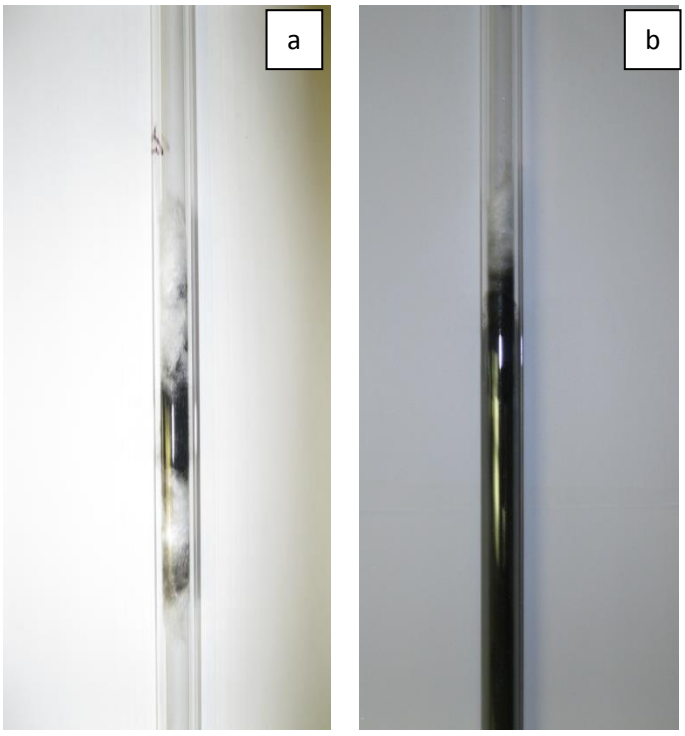

Figure 35. (a)Mr. Brathwaite operating the Micromeritics 2020 porosimeter; (b)Mr. Gopeesingh operating the Quantachrome ChemBETPulsar Surface Analyzer; (c) Mr. Gopeesingh operating the ATR setup

(a)

(b)

(c)